GENE AND PROTEIN EXPRESSION IN CANINE FOLLICULAR THYROID CARCINOMA

A DISSERTATION
SUBMITTED TO THE FACULTY OF THE GRADUATE SCHOOL
OF THE UNIVERSITY OF MINNESOTA
BY

Kristy Stacy Metivier

IN PARTIAL FULFILLMENT OF THE REQUIREMENTS
FOR THE DEGREE OF
DOCTOR OF PHILOSOPHY

Vicki Wilke (Co-advisor); Michael Conzemius (Co-advisor),

August 2011

ACKNOWLEDGEMENTS

I thank God for wisdom in the midst of challenges, hope surrounding despair, and understanding of the things and people that cannot be changed.

To Fulbright/Laspau, the College of Veterinary Medicine, and the International Student and Scholars Services, I extend gratitude for funding and academic support.

Special thanks are due to my academic committee; Vicki Wilke, Michael Conzemius, Amy Skubitz, and Catherine St. Hill for valuable input, time and expertise. Vicki, you are truly an inspiration and my life is richer for knowing you. Thank you for entrusting me with this project, for always demonstrating the right combination of authority, respect and compassion and for encouraging me to pursue my dream against all odds.

I thank the doctors and staff at Boynton and Fairview Health Services for working diligently to keep me healthy during many difficult times; Lisa Hubinger for always ensuring that I was safe and on the right path; and Gabriele Schmiegel for patience and valuable help.

Much of this research depended on recruiting cases and samples from dogs at our Veterinary Teaching Hospital as well as other independent clinics. I was blessed with many willing and able veterinarians and technicians, especially Amber Winter and Dr. Brian Husbands; and also all of the owners who agreed to have their dogs as part of the study. I could not have done this without you. Your generosity has made it possible to embark on research that could one day improve the quality of life for dogs affected with this condition.

Thank you to those who provided valuable experimental and academic support, particularly Dr. Jaime Modiano, Juan Abrahante, Mary Mauzy, Cheryl Dvorak, Josh Parker, Mike Ehrhart, John Wojcieszyn, Wayne Xu, Aaron Rendahl, Krysta Deitz and Anna Tchernatynskaia; to the Minnesota Supercomputing Institute (MSI) and the Biomedical Genomics Center (BMGC); to the American Kennel Club (AKC) Canine Health Foundation for providing microarray funding (grant 830-A) and the Animal Cancer Care and Research (ACCR) for immunohistochemistry funding.

To my family and friends, I can't say enough how much your presence, thoughts and prayers have kept me afloat and given me courage; my mother Jean Metivier who always knows the right words to say to me; my father and brothers for showing me the meaning of courage and hard work; my colleague Duane Robinson for always making me feel welcome; and my friends Amanda Beaudoin and Deepti Joshi for being there when I needed you most. DJ, you mean more to me than I can ever explain and you have shown me that true friendship still exists.

Most of all I am grateful for my entire experience over the past four years and the role it played in shaping my future and fostering an understanding of duty and purpose.

DEDICATION

For Barbara

My Name is Memory…

ABSTRACT

The major goal of this study was to investigate the molecular characteristics of canine follicular thyroid carcinoma (FTC). This is a rapidly growing and highly aggressive tumor in dogs, and many patients present with evidence of invasion or metastasis. Some smaller independent studies have attempted to evaluate the role of single molecules such as *p53* and thyroid transcription factor-1 in tumor development, often with inconclusive results. In the present study, a genome-wide approach was employed to achieve the first objective of determining the gene expression profile of FTC compared to normal thyroid tissue. Microarray analysis was performed in a pilot study using five FTC tissues and four normal thyroid gland tissues, and this showed 489 transcripts as differentially expressed between the two groups; 242 were down-regulated and 247 were up-regulated. Some important biological functions that were affected include regulation of cell shape, cell adhesion, regulation of MAP kinase activity, angiogenesis, and regulation of cell migration.

Osteopontin was a gene of interest as tumors consistently expressed it at high levels while it was expressed at low levels in all of the healthy samples. One of its up-stream regulators, VEGFA, was also differentially expressed but with a smaller fold change. The expression of osteopontin was validated by quantitative PCR using three groups: non-invasive FTC (tumors with capsular invasion only), invasive FTC (tumors with capsular and vascular invasion), and normal thyroid tissue. Both non-invasive FTC and invasive FTC had higher osteopontin gene expression than normal thyroid tissue but the two tumor groups were not different from each other. The second objective was to determine the protein expression of osteopontin and VEGFA in the same cases using semi-quantitative scoring of tissues stained by immunohistochemistry. The results were similar, with non-invasive and invasive FTC having higher osteopontin protein expression than normal thyroid tissue, but showing no difference from each other. With respect to VEGFA, there was no difference in gene or protein expression among the three groups.

The final objective was to determine the plasma concentration of VEGFA and osteopontin in dogs diagnosed with FTC compared to clinically healthy dogs using a commercially available canine-specific ELISA. In this case, both VEGFA and osteopontin had higher plasma concentrations in dogs with FTC compared to healthy dogs. A small number of FTC cases were also measured two weeks after surgical removal of the tumor. Some cases showed a post-surgical decrease in VEGFA and osteopontin while others either remained the same or increased; however, the sample size for this comparison was small. The consistent expression of osteopontin in both tissues and blood suggest that it is a promising marker for identification of canine FTC. As in human studies of osteopontin in aggressive carcinomas, it is also possible to investigate it as a means of monitoring response to therapy, recurrence, and clinical outcome.

TABLE OF CONTENTS

LIST OF TABLES

LIST OF FIGURES

Figure **Page**

LIST OF ABBREVIATIONS

Abbreviation	Definition
°C	degrees Celsius
ACCR	animal cancer care and research
ACTB	beta actin
AKC	American Kennel Club
Akt	v-akt murine thymoma viral oncogene homolog
ANOVA	analysis of variance
ATP	adenosine triphosphate
β-actin	beta actin
BH	Benjamini and Hochberg
bioB	biotin synthase
bioC	predicted methyltransferase, enzyme of biotin synthesis
bioD	dethiobiotin synthetase
BLAST	Basic local alignment search tool
BMGC	Biomedical Genomics Center
BRAF	V-raf murine sarcoma viral oncogene homolog B1
cAMP	cyclic adenosine monophosphate
C-cells	Clear cells
CCND2	cyclin D2
CD44	cluster of differentiation 44
cDNA	complementary deoxyribonucleic acid
CEACAM1	carcinoembryonic antigen-related cell adhesion molecule 1
60Co	Cobalt-60, Cobalt radioisotope
COX-2	cyclooxygenase 2
cre	cre recombinase (type 1 topoisomerase)
Ct	cycle threshold
CT	computed tomography
dap	death associated protein
DIO2	type II iodothyronine deiodinase
DNA	deoxyribonucleic acid
E. coli	Escherichia coli
EDR	error discovery rate
EDTA	ethylenediaminetetraacetic acid
EGFR	epidermal growth factor receptor

Abbreviation	Definition
ELISA	enzyme-linked immunosorbent assay
EMMPRIN	extracellular matrix metalloproteinase inducer
ERK	extracellular signal-regulated kinases (also referred to as MAPK)
fT4	free tetraiodothyronine
FGF	fibroblast growth factor
FGF2	fibroblast growth factor 2
FGFR	fibroblast growth factor receptor
FGFR1	fibroblast growth factor receptor-1
FGFR3	fibroblast growth factor receptor-3
FGFR4	fibroblast growth factor receptor-4
FMTC	familial medullary thyroid carcinoma
FNA	fine needle aspiration
FTC	follicular thyroid carcinoma
FVPTC	follicular variant of papillary thyroid carcinoma
GAPDH	glyceraldehyde 3-phosphate dehydrogenase
Gy	Gray
HaeII	Haemophilus aegyptius restriction enzyme
HT	Hashimoto's thyroiditis
IACUC	Institutional animal care and use committee
123I	Iodine-123, Iodine radioisotope
131I	Iodine-131, radioiodine
IGF-1	insulin-like growth factor-1
IHC	immunohistochemistry
IPC	incidental papillary carcinoma
LOH	loss of heterozygosity
lys	lysine
MAPK	mitogen-activated protein kinase
MEN	multiple endocrine neoplasia
MET	met proto-oncogene (hepatocyte growth factor receptor)
MIVAT	minimally-invasive video-assisted thyroidectomy
ml	milliliters
MRI	magnetic resonance imaging
mRNA	messenger ribonucleic acid
MTC	medullary thyroid carcinoma

Abbreviation	Definition
Na+/K+/ATPase	sodium-potassium ATPase pump
NSAID	non-steroidal anti-inflmmatory drug
NTC	no-template control
OPN	osteopontin
p53	protein 53
PCR	polymerase chain reaction
PCSK2	proprotein convertase subtilisin/kexin type 2
phe	phenylalanine
PI3K	phosphatidylinositol-3 kinase
PLAB	placental bone morphogenetic protein
PTC	papillary thyroid carcinoma
Pten	Phosphatase and tensin homolog
PV	dominant negative thyroid hormone receptor mutant
qPCR	quantitative polymerase chain reaction
R	programming language and statistical software
Ras	rat sarcoma viral oncogene
RET	rearranged during transfection
RLN	regional lymph nodes
RNA	ribonucleic acid
ROC	relative operating characteristic
rpm	revolutions per minute
SAPE	streptavidin-phycoerythrin
SAS	statistical analysis software
SCID	severe combined immunodeficient
SEER	surveillance, epidemiology and end results
SEM	standard error of the mean
SPP1	secreted phosphoprotein-1
T3	triiodothyronine
T4	tetraiodothyronine (thyroxine)
thr	threonine
TMB	tetramethylbenzidine
TNM	tumor, node, metastasis
TRH	thyrotropin releasing hormone
TSH	thyroid stimulating hormone, thyrotropin

Abbreviation	Definition
TSHR	thyroid stimulating hormone receptor
TTF-1	thyroid transcription factor-1
VEGF	vascular endothelial growth factor
VEGFA	vascular endothelial growth factor A
VMDB	Veterinary Medical Database
WHO	World Health Organization
Wnt	wingless-type MMTV integration site

CHAPTER 1

LITERATURE REVIEW

CANINE THYROID GLAND ANATOMY AND PHYSIOLOGY

The thyroid gland is one of the largest endocrine glands in the adult dog. It is an elongated structure consisting of two lobes, and is located on the proximal ventral surface of the trachea[1]. The right lobe, situated more cranially than the left, extends from the larynx to the fifth tracheal ring with its cranial surface adjoining the caudal surface of the cricoid cartilage. The left lobe spans the third to eighth tracheal rings. Muscles surrounding the gland include the sternohyoideus and sternocephalicus laterally and the sternothyroideus ventrally. Structures in close proximity to the right lobe include the common carotid artery, internal jugular vein, tracheal duct, and vagosympathetic trunk dorsolaterally; and the recurrent laryngeal nerve dorsally (Figure 1-1). The left lobe is bound dorsolaterally by the esophagus. Dorsal and medial to the gland are the caudal laryngeal nerve and trachea respectively.

The size of the thyroid gland varies according to breed, and in some dogs the lobes are connected via their caudoventral surface by an isthmus traversing the ventral surface of the trachea. It originates as the *isthmus glandularis*, comprises glandular parenchyma, and is more common in brachycephalic breeds. During development, it gradually narrows and may become a connecting fibrous band. Another possible event during development is the emergence of accessory thyroid tissue where islets of cells separate from the main organ. This ectopic tissue may be functional and localize to the trachea, thoracic inlet, mediastinum and descending aorta.

The parathyroid glands are also closely associated with the thyroid gland. Their chief function is the regulation of calcium homeostasis. Each thyroid lobe is linked to a pair of parathyroid glands located near the cranial and caudal poles. The cranial

parathyroids may be surrounding the thyroid, indented into its surface, or embedded within the parenchyma. The caudal parathyroids are often embedded[1].

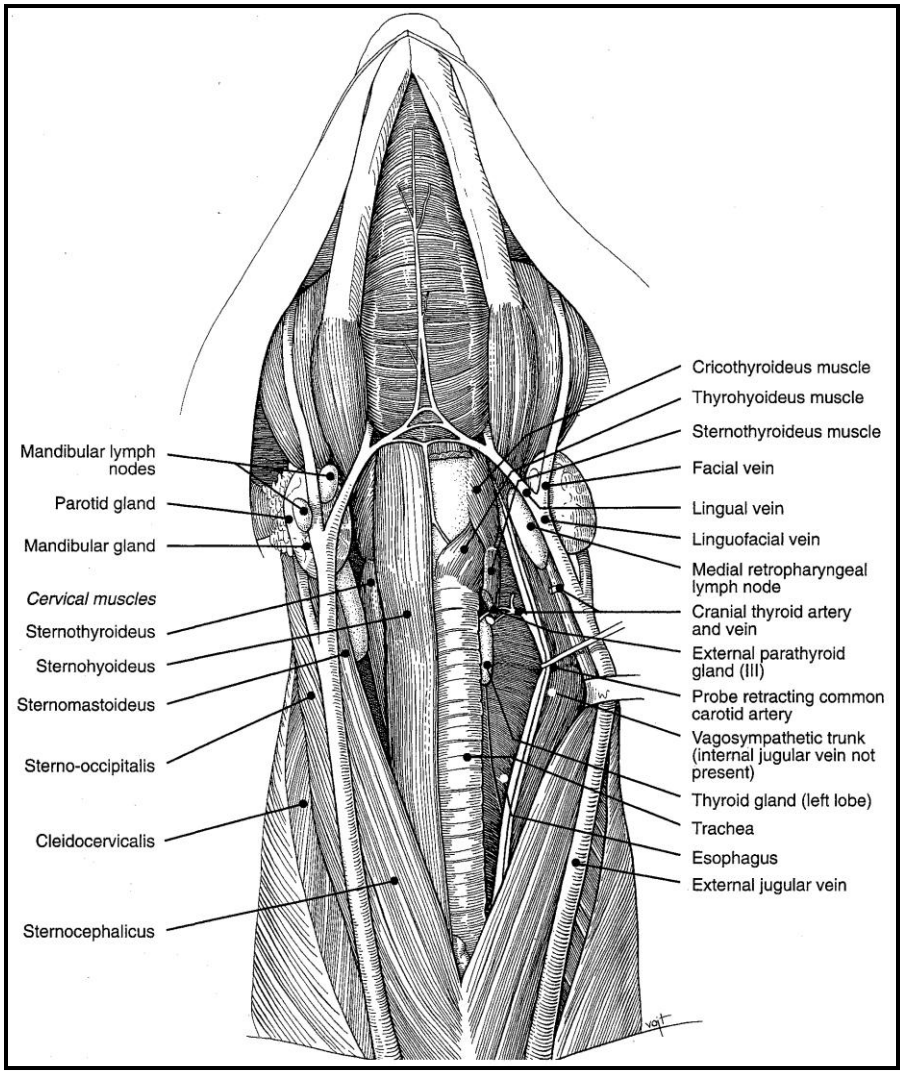

Figure 1-1 Thyroid and Parathyroid Glands
Reproduced with permission from: Anderson WD, Anderson BG. *Atlas of canine anatomy*.Pennsylvania: Lea & Febiger; 1994. p.375

The thyroid gland has rich blood and nerve supplies. The most prominent vessels are the cranial and caudal thyroid arteries which arise from the common carotid and

brachiocephalic arteries respectively, and anastomose along the lateral trachea[1]. Small branches arising from this union anastomose to form a network known as the *rete arteriosum* which divides into capillaries to surround the individual follicles and connective tissue. Venous output is regulated by the cranial and caudal thyroid veins which join the internal jugular vein. Lymphatic capillaries form larger vessels that accompany the blood vessels and drain to the cranial and caudal deep cervical lymph nodes. The thyroid nerve, formed by fibers from the cranial cervical ganglion and cranial laryngeal nerve, provides innervation to the thyroid gland and is closely associated with the cranial thyroid artery. Nerve bundles supply both the thyroid vasculature (vascular nerve plexuses) and parenchyma (interfollicular nerves)[2].

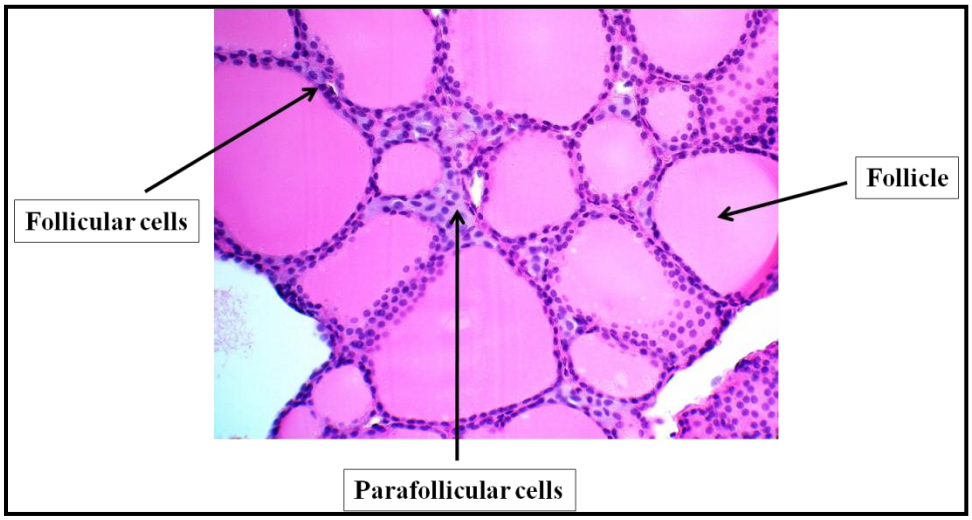

Figure 1-2 Histological section of a normal thyroid gland

The thyroid capsule (*capsula thyroideae*) separates the gland from other tissues and is a delicate structure adjoining the fasciae. Connective tissue form septae which roughly divide the gland into lobules. The most significant functional units within the thyroid gland are follicles (*folliculae thyroideae*), which are sphere-like structures of varying sizes[3] filled with a glycoprotein colloid and lined by a single layer of epithelium

(Figure 1-2). Parenchymal cells are predominantly follicular epithelial cells[4] and larger clear (C) cells. Follicular cells synthesize the protein thyroglobulin and release it into the colloid where it functions as a substrate for synthesis of the thyroid hormones tetraiodothyronine (T_4; thyroxine) and triiodothyronine (T_3). Three types of C cells responsible for synthesis of calcitonin have been described: intrafollicular (located between the follicular cells and follicular basement membrane), interfollicular (between follicular cells and possessing their own basement membrane), and parafollicular (adjacent to the follicular lining)[5]. Some authors use the terms parafollicular cell and C-cell interchangeably.

Follicular cells are capable of trapping iodide which is essential to the function of thyroid hormones[3]. Thyroid hormone synthesis is regulated by the release of thyroid stimulating hormone (TSH; thyrotropin) from the pituitary gland, which in turn is regulated by the release of thyrotropin releasing hormone (TRH) from the hypothalamus. Thyroxine (T_4) and a small amount of the active hormone (T_3) are synthesized from tyrosine and iodine when the follicular cells are stimulated by TSH. Both forms are released into the blood where T_4 is converted to T_3 by iodothyronine deiodinase (D_2) enzymes. Thyroxine provides negative feedback to the pituitary, ultimately inhibiting the release of TSH. Additionally, it regulates TRH production by manipulating expression of the TRH prohormone gene. T_3 is capable of stimulating osteoblasts directly or indirectly by inducing insulin-like growth factor-1 (IGF-1), cytokines, or fibroblast growth factor (FGF). TSH is also known to inhibit osteoclast activity, therefore decreased expression of TSH receptor leads to bone loss.

The roles of thyroid hormones in the body are diverse as they regulate the function of various organs and tissues[6]. They are essential for normal growth and development as they are required for the synthesis and function of growth hormone, the action of prolactin in the developing mammary gland, and synthesis of nerve growth factor during brain development[3]. The active hormone (T_3) contributes to the maintenance of homeothermy by increasing consumption of oxygen in the mitochondria, and activity of the sodium/potassium/ATPase (Na^+/K^+/ATPase) pump. It is also involved

in bone growth, intestinal glucose absorption, and synthesis of several enzymes. There are therefore many crucial physiological abnormalities associated with thyroid disease. Calcitonin, synthesized by the C cells, mainly functions to regulate postprandial hypercalcemia and inhibit osteoclastic bone resorption. While the secretion of calcitonin increases with hypercalcemia, it does not have significant effects on normal calcium regulation. At higher levels, it can induce increased calcium excretion by the kidneys[7].

EPIDEMIOLOGY OF THYROID TUMORS

Incidence

Literature have reported an incidence of 1.2 to 3.8% for canine thyroid tumors[8], representing approximately 15% of all head and neck tumors. They are largely adenomas and carcinomas of follicular origin (Figure 1-3).

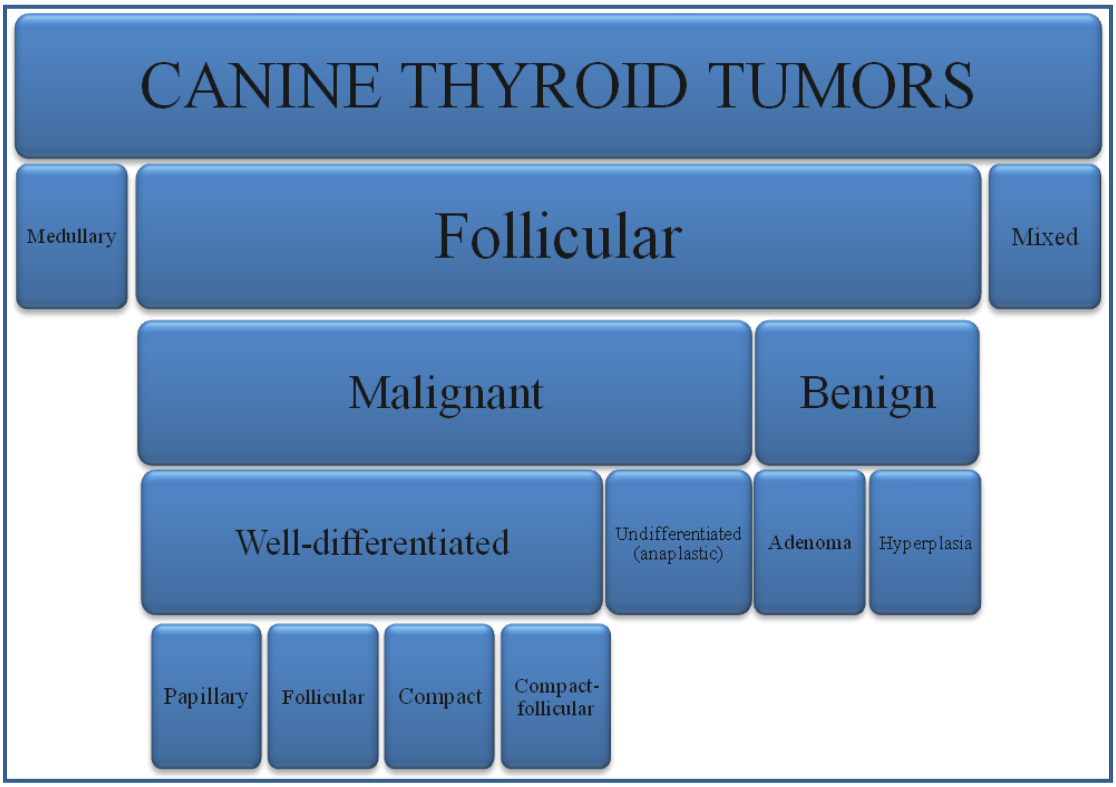

Figure 1-3 Classification of thyroid tumors in dogs

Of 26 dogs diagnosed with thyroid tumors at the University of Illinois Veterinary Teaching Hospital between 1977 and 1984, 23 were carcinomas and three were adenomas diagnosed at necropsy[9]. A larger study with data from 12 university hospitals reported 144 microscopically confirmed cases of primary thyroid neoplasia between 1964 and 1974. Twenty-five were adenomas and 119 were carcinomas[10]. More recently, 13 institutions reported 638 cases of thyroid cancer to the Veterinary Medical Data Base (VMDB) between 1995 and 2005. Of the 545 tumors that could be classified, 51 were adenomas, 490 were carcinomas, and four were tumors metastatic to the thyroid gland[11]. Generally, 51 to 100% of thyroid tumors are identified as carcinomas. The reported statistics are dictated by whether necropsy data are included, as adenomas are often incidental findings. Studies including necropsy data have described a 30 to 50% occurrence of adenomas[12,13]. Thyroid tumors in cats are generally benign and occur concurrently with hyperthyroidism. In dogs, although tumors are less common they are more likely to be malignant and non-functional[14].

Some cases do exist of canine adenomas and carcinomas that result in clinical signs associated with both the tumor lesion and functional tissue. An 11-year old Golden Retriever diagnosed with hyperthyroidism secondary to a follicular adenoma had histopathological evidence of a well circumscribed thyroglobulin-positive follicular tumor. Its presenting signs were progressive weight loss, polyuria, polydipsia, frequent vomiting and a movable cervical mass. Elevated T_3 and T_4 were discovered on further testing[15]. Another case report described a 10-year old Labrador retriever with hyperthyroidism secondary to thyroid carcinoma. In this case, the dog presented with weight loss, tachycardia, hyperactivity, anxiety, and excessive panting. Thyroxine and blood pressure were significantly elevated, and there was gross and microscopic evidence of muscular and vascular invasion by the tumor[16]. Only a few cases have been reported, and the estimated proportion of dogs with thyroid tumors showing signs of concurrent hypothyroidism or hyperthyroidism is only 30% and 10% respectively[17]. These data must be interpreted with caution; in addition to limitations due to the small number of

cases, some dogs with thyroid tumors may harbor unrelated illnesses resulting in the euthyroid sick syndrome.

In humans, thyroid nodules are encountered in 4 to 8% of adults by palpation and 13 to 67% by ultrasound[18]. Approximately 20% of these nodules have clinical significance and less than 5% are malignant. However, thyroid cancer is the most common primary endocrine malignancy in humans, with an estimated 44,670 diagnosed cases and 1,690 deaths in 2010[19]. It is the 8th most common neoplasm diagnosed in women, now more common than ovarian cancer[20]. It may appear that the incidence has been increasing over time. The reported age-adjusted incidence rate progressed from 7.5 per 100,000 in the year 2000 to 10.6 per 100,000 in 2006[19]. It is important to investigate whether these statistics reflect a true increase in incidence or an improvement in the ability to detect tumors, particularly those with diameters less than 2 cm. Additionally, mortality rates have remained relatively constant. The majority of adenomas in humans are non-functional but a small number of patients do exhibit signs of hyperthyroidism. These tumors are referred to as toxic adenomas, and thyroid hormones are produced without the influence of TSH. Differentiated thyroid carcinomas are rarely functional[21].

Risk factors

BREED AND ETHNICITY A number of epidemiological studies on canine thyroid tumors have reported over-representation of Golden Retrievers, Boxers, and Beagles[9,10,12]. In one such study, 40% of dogs with thyroid tumors were Boxers despite the fact that this breed accounted for only 7.3% of presenting dogs[12]. In another study evaluating the response to sodium iodide treatment in dogs with non-resectable thyroid tumors, of the 39 dogs included, 10 were Golden Retrievers[22]. A separate evaluation of radioiodide therapy in treatment of canine thyroid carcinoma reported that 23% of the cases were Boxers and Beagles[23]. Toy poodles are described as having relatively low risk[10]. In the VMDB study, Golden Retrievers, Beagles, and Siberian Huskies were over-represented[11]. The question remains whether these results are influenced by the relative popularity of breeds in different geographical locations, availability of resources, and

likelihood of owners of these breeds to seek veterinary care. In Scotland, an over-representation of Shetland collies, Old English Sheepdogs, and Cairn terriers was reported, while other combined studies reflected a large proportion of retrievers and mixed breeds[17].

In humans, race and ethnicity are associated with thyroid cancer incidence[24]. Age-adjusted rates suggest that both male and female Caucasians are more likely to develop thyroid tumors than Asians, and twice as likely as African Americans[25,26]. Relatively higher levels of TSH found in Caucasians support this trend[27]. However, another study reported that localized tumors were highest among African Americans. Interpretation of the findings in these studies should take into account the disparity that exists with respect to healthcare access and socioeconomic status in the United States[24]. Although, there is some recent evidence of under-diagnosis and less aggressive disease among African Americans, these data could not account for possible confounding by risk of radiation exposure, other environmental factors, or undiscovered predisposing genetic factors[28].

AGE As with many canine neoplasms, the risk of developing a thyroid tumor increases with age; it is more common in middle-aged and older dogs. Among the older studies, the reported median age of dogs presenting with thyroid neoplasia is nine to 10 years[9,10,12,13,29,30]. In a study of spontaneously occurring thyroid neoplasms in a colony of Beagle dogs, the incidence increased from 1.1% in dogs eight to 12 years old, to 4% in dogs 12 to 15 years old and 67% in dogs greater than 17 years[31]. In younger dogs however, there was a greater number of malignant tumors than benign ones. In the VMDB study, 32% of dogs with thyroid tumors were between seven and 10 years old, and 57% were between 10 and 15 years old. Dogs 10 – 15 years old were 6.9 times more likely to be diagnosed with a thyroid tumor than dogs of other ages[11].

A human Surveillance, Epidemiology and End Results (SEER) study including data from 1973 to 1991 reported that the median age of onset of thyroid cancer was 42 years, with a range of three to 98 years[32]. Age also influenced survival time for various

histologic subtypes. For minimally invasive carcinomas the mean age at presentation generally ranges from 36 to 65 years[33]. In patients over 80 years old, thyroid carcinoma accounts for one-third of all thyroid diseases. Compared to younger individuals, this age group also experiences more aggressive tumors, increased recurrence rates, higher mortality rates, and an increased incidence of anaplastic carcinomas[34]. Thyroid cancer is relatively uncommon in children[35].

GENDER All studies reviewed have agreed that there is no evidence of a gender predilection for canine thyroid tumors[9,10,11,12,30,31,36,37]. The only significant observation was that with advancing age, females showed a steeper increase in risk than males[10]. In contrast, women are three times more at risk than men[34], directly correlating with higher TSH levels[27]. This gap narrows with increasing age, as men over 70 years old have a relatively sharper increase in incidence of differentiated carcinomas[34]. Among pediatric patients[35], however, the ratio between girls and boys was found to be greater than 4 to 1.

RADIATION The thyroid gland is known to be sensitive to radiation, but a number of the early studies on the effect of ionizing radiation in animals involved rodent models. Later, the Collaborative Radiological Health Laboratory at Colorado State University investigated the effect of inducing Cobalt-60 (^{60}Co) gamma radiation exposure in perinatal beagles. Six groups of dogs were exposed to radiation at different time points; three during gestation and three post-natally. In this study, thyroid neoplasms were commonly encountered. Among the controls (dogs receiving a sham exposure), 28% developed at least one thyroid tumor, and 9.5% had multiple tumors. Euthyroid dogs receiving radiation at 70 days post partum and those receiving high-dose radiation at two days post partum had increased risk of developing both adenomas and carcinomas. Incidental carcinomas and adenomas detected at necropsy were increased in dogs irradiated at two and 70 days respectively[38]. These findings are similar to those from human studies of radiation and thyroid cancer risk.

The incidence of thyroid tumors in humans increases with exposure to neck radiation. Children treated with ionizing radiation for conditions such as enlarged thymus gland, tinea capitis, and cancer have been susceptible to thyroid tumors with exposure as low as 0.1 Gray (Gy)[39]. Similarly, ten years following the Chernobyl nuclear accident, there was a 100-fold increase in thyroid cancer among young individuals[40]. Survivors of the atomic bombing of Hiroshima by the United States experienced higher rates of thyroid cancer than those who were not exposed. The disparity between exposed and unexposed groups was greater for individuals exposed during childhood[41]. Further examination of seven human thyroid cancer studies demonstrated a relationship between dose and risk where it appeared that spreading the dose over time decreased the risk of developing cancer, possibly due to the induction of cellular repair mechanisms[42].

CONCURRENT THYROID DISEASES An interesting finding was reported in the Colorado State radiation study[38]. There was a higher incidence of thyroid neoplasia among dogs diagnosed with hypothyroidism than in euthyroid dogs. Approximately 55% of hypothyroid dogs in the non-irradiated control group developed at least one thyroid tumor, compared to 23% of euthyroid dogs. The irradiated group demonstrated a similar trend. Additionally, hypothyroid dogs had a higher incidence of carcinomas than adenomas, while the reverse was true for euthyroid dogs. In most cases, diagnosis of hypothyroidism was made using a combination of clinical signs, histopathologic evidence of follicular atrophy, serum hypercholesterolemia, and non-regenerative anemia. Therefore these results are limited by the fact that there may have been dogs with decreased T_4 in the absence of clinical signs and abnormal blood tests. The major cause of clinically detectable hypothyroidism was lymphocytic thyroiditis, however there were no tests performed to screen for antibodies indicative of autoimmune disease. Increased thyroid neoplasia in hypothyroid dogs may be linked to excessive TSH production which is thought to promote tumor growth and stimulate angiogenesis by inducing vascular endothelial growth factor (VEGF)[43]. In another survey of 144 dogs with thyroid

neoplasia, only four had clinical evidence of hypothyroidism, and one had lymphocytic thyroiditis[10].

In humans, the issue of an association between benign thyroid disease and thyroid neoplasia is still a controversial one[44]. In one study of individuals receiving partial or total thyroidectomy for benign thyroid disease, incidental papillary carcinoma (IPC) was detected in 12% (81/678) of patients. This included 68 females and 13 males. Patients with Hashimoto's thyroiditis (HT) had the highest tumor incidence, with 28% of them having evidence of IPC compared to 10% with follicular adenoma, 10% with multinodular goiter, and 8% with Graves' disease[45]. It has been suggested that HT is a precursor lesion for thyroid cancer. A high incidence of HT has been found in patients diagnosed with papillary carcinoma[46,47]. However, another survey found no significant association between the frequency of HT and papillary carcinoma lesions on examination of fine needle aspiration cytology of the thyroid glands of patients[48].

THYROID TUMOR CLASSIFICATION

Follicular tumors

These tumors originate from epithelial cells lining the follicles of the thyroid gland and are the most common thyroid tumors in dogs. There are benign and malignant types. Adenomas may be follicular or papillary although the former is much more common. Follicular adenomas are common in cats with hyperthyroidism but must be distinguished from multinodular hyperplasia which is not as well encapsulated, and more prevalent in older cats. Based on growth characteristics, adenomas may also be categorized as microfollicular, macrofollicular, or cystic. They do not frequently become clinically apparent. Well-differentiated follicular carcinomas are further classified into follicular, papillary, compact cellular (solid), and mixed (follicular and compact) based on their pattern of growth and histological characteristics[49] (Figure 1-3).

A follicular thyroid carcinoma (FTC) contains follicles of different sizes and shapes which produce colloid in varying quantities. The epithelial cells may be cuboidal to columnar and show little mitotic activity. Compact tumors contain layers or

aggregates of follicular epithelial cells surrounded by dense stroma[37,49]. There is generally no evidence of follicular organization or colloid production. Follicular-compact tumors have both solid and follicular characteristics although follicles tend to be smaller and produce smaller quantities of colloid than tumors which are entirely follicular (Figure 1-4).

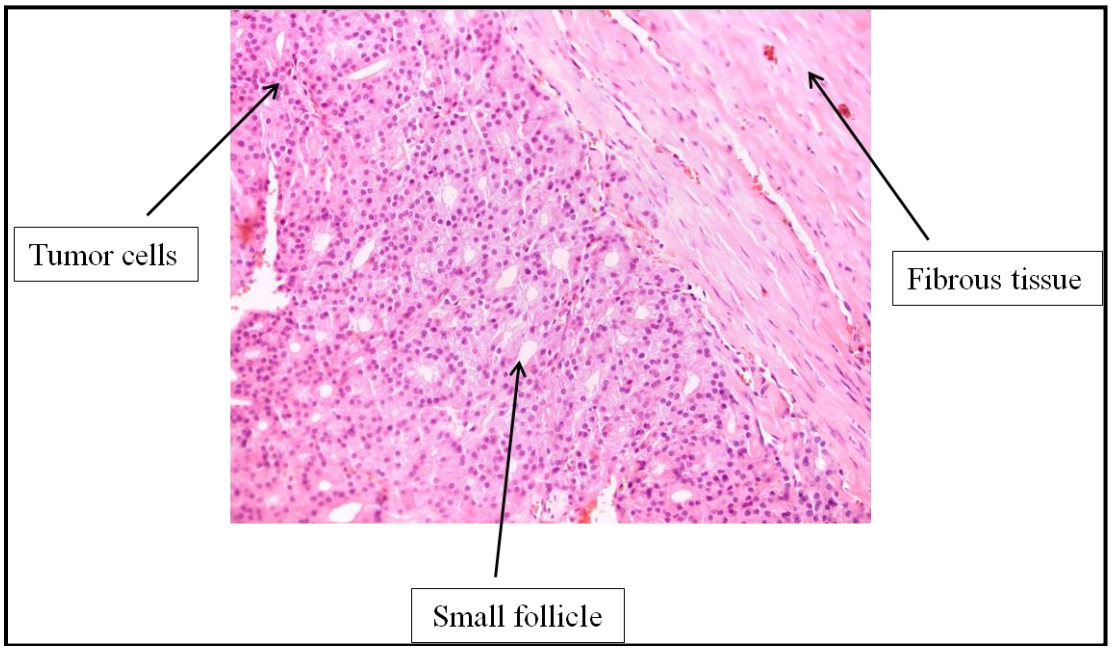

Figure 1-4 Histological section of a follicular-compact thyroid carcinoma

Papillary thyroid carcinomas (PTCs) which occur only occasionally in dogs, have characteristics of follicular carcinomas but are differentiated by overlapping nuclei with invaginations and a ground-glass appearance[23,50]. These tumors may also contain areas of small follicles and/or cells similar to those found in compact tumors[49]. Undifferentiated (anaplastic) carcinomas are also rare in dogs and are comprised of spindle cells that lack architecture but stain positively for thyroglobulin. Unlike follicular tumors, the mitotic activity is usually high.

In humans, FTC represents only 10% of thyroid malignancies and is more common in areas with iodine deficiency or where goiter is endemic[51]. The most common thyroid tumor in humans is PTC, accounting for approximately 80% of cases; however the incidence of both FTC and PTC appears to be increasing[52]. Many variants of PTC have been described, such as follicular, tall cell, columnar cell, diffuse sclerosing, encapsulated, and oncocytic. The follicular variant (FVPTC) is most common; it has the nuclear characteristics of PTC but a follicular growth pattern[53]. Hurthle or oncocytic cell tumors are composed of oncocytic cells and are considered follicular tumors. The incidence of adenomas in humans may be as high as 60% but this cannot always be accurately determined as they closely resemble hyperplastic lesions[54].

Medullary tumors

These tumors originate from C-cells and are less common than follicular carcinomas in dogs. Early reports suggested a prevalence of approximately 5%, however in another study 36% of their cases (12/33) were confirmed to be of medullary origin, suggesting that this tumor subtype may be under-diagnosed[30]. Medullary thyroid carcinomas (MTCs) may be differentiated from follicular carcinomas using cytochemistry and immunohistochemistry. In one study, 100% of C-cell tumors stained positively for calcitonin and a variable number stained positively for S-100 protein, neuron specific enolase, synaptophysin, somatostatin, gastrin, and serotonin[55]. Calcitonin is generally detected in 70 – 100% of canine medullary carcinomas[56]. They tend to be well encapsulated but may be difficult to differentiate from compact tumors by light microscopy alone[30,55]. A possible familial form similar to that seen in humans has been reported[57]. Four Alaskan malamute crosses belonging to the same family were diagnosed with calcitonin-positive thyroid tumors. Two of these cases also showed positive staining for thyroglobulin. In the human literature there are reports of medullary carcinomas concurrently expressing calcitonin and thyroglobulin[58,59].

In humans, MTCs account for 5 – 10% of all thyroid carcinomas. Up to 75% of them occur sporadically, and the hereditary form accounts for the other 25%[60].

Hereditary MTC may be a part of one of the multiple endocrine neoplasia (MEN) syndromes, or of familial medullary thyroid carcinoma (FMTC). It often occurs concurrently with C-cell hyperplasia and some authors have suggested that the latter is a precursor lesion. Mixed follicular/medullary tumors have also been reported.

FOLLICULAR THYROID CARCINOMA

Biological behavior

IMMUNOREACTIVITY In general, 90 – 100% of canine follicular thyroid tumors stain positively for thyroglobulin[30,56]. In one study, 90.5% of follicular tumors were positive for thyroglobulin. A similar percentage stained positively for thyroid transcription factor-1 (TTF-1), and the two markers together identified 95.2% of tumors. Both markers showed diffuse staining, with thyroglobulin being localized exclusively to the cytoplasm and TTF-1 to the nucleus. Additionally, TTF-1 stained solid areas of the tumor while thyroglobulin preferentially stained areas with differentiated follicles. However, TTF-1 was not exclusively found in thyroid tissue; it was also present in pulmonary carcinoma and normal bronchioloar and alveolar epithelial cells. Mixed staining of calcitonin and thyroglobulin has been reported in dogs whose tumor appears to be primarily medullary. This may be evidence of a tumor that is truly mixed, or thyroglobulin false positivity due to the tendency of this stain to become easily diffused[57].

INVASION Thyroid carcinomas in dogs generally grow rapidly and readily invade surrounding structures, while adenomas are slow-growing and tend to be well encapsulated[61]. Tumors that are purely follicular grow more rapidly than solid ones[49]. Sites of invasion include the esophagus, trachea, larynx, jugular veins, and carotid sheath. Generally the distinction between adenoma and carcinoma is made when there is invasion into the thyroid capsule. Vascular invasion is identified on histopathology when tumor cells are detected in the lumen of blood vessels or are attached as thrombi[33] but, categorization of FTC into levels of invasiveness has not been defined in dogs. Presence

of tumor thrombi in the cranial and caudal thyroid veins leads to pulmonary metastasis and could ultimately result in cranial vena cava syndrome[62].

In humans FTCs are classified according to their degree of invasion. Minimally invasive FTCs are described as those with capsular invasion only; moderately invasive FTCs have angioinvasion with or without capsular invasion; and widely invasive FTCs encompass invasion of the capsule and extrathyroidal tissue. These categories have implications both for clinical outcome (disease recurrence) and survival. In one study the minimally invasive group had a 10-year survival rate of 97.8% compared to 80% and 37.5% in the moderately and widely invasive groups respectively[63]. Papillary carcinomas have a lower tendency to become malignant and generally have a good prognosis if treated surgically, while FTC is considered to be more aggressive.

METASTASIS Follicular carcinomas metastasize most commonly to the lungs, and this is often related to tumor size. One study reported a positive correlation between tumor volume and rate of distant metastasis detected at autopsy in dogs[13]. In another study, the frequency of pulmonary metastasis detected by radiography was found to be 62.5% in dogs with thyroid carcinoma compared to 26% with transitional cell carcinoma, 9.4% with other epithelial neoplasms, and 10.8% with mesenchymal tumors[64]. Earlier studies detected metastasis in eight out of 21, and 12 out of 23 dogs respectively with thyroid carcinoma using thoracic radiography[9,12]. Most pulmonary lesions affect the connective tissue more severely than alveolar and bronchial structures and therefore may be at an advanced stage before being clinically detected.

Other sites of metastasis include the heart, kidney, adrenal gland, liver, bone, and brain[9,12,13]. Lymph node involvement is dictated by the cranial direction of lymphatic drainage with significance placed on the retropharyngeal and mandibular nodes, however the superficial cervical nodes may also be involved[61]. Carcinomas occur with similar frequency in the left and right lobes of the thyroid gland, and in 40% of canine patients they occur bilaterally. This has implications for the pattern of malignancy[65]. Dogs that had bilateral tumors were 16 times more likely to develop metastasis than those with a

single mass, while dogs with no indication of tumor progression had a significantly lower risk of metastasis and a non-significant decrease in time to metastasis. In a more recent study, successful clinical outcomes were observed with dogs undergoing bilateral thyroidectomies with or without complete parathyroidectomies; 7/14 cases were alive between 43 and 2180 days post-surgery[66].

ECTOPIC TUMORS During thyroid gland development accessory thyroid tissue may be formed. This occurs when rapidly proliferating cells separate from primordial tissue and colonize the brachium and thorax[62]. As a result, thyroid carcinoma may originate from structures such as the tongue, trachea, pericardium, heart base, and descending aorta[8]. In one report a 13-year old Labrador retriever presenting with exercise intolerance and a systolic murmur was diagnosed with intracardiac ectopic thyroid carcinosarcoma. The mass was discovered during necropsy and showed histological evidence of follicular epithelial cells as well as thyroid follicles containing colloid. A histologically normal thyroid gland ruled out the possibility that the lesion was a thyroid tumor metastatic to the heart[67]. Intracardiac tumors may also cause obstruction of the ventricular outflow tract[68]. Other cases of ectopic FTC have been reported in the cranial mediastinum[69] and tongue[70].

FUNCTIONALITY Most canine thyroid tumors are thought to be non-functional[71]. Sixty percent of patients are euthyroid, and approximately 30% have low T_4 and free T_4 (fT_4) suggesting concurrent hypothyroidism. Ten percent of dogs have functional tumors that result in signs associated with hyperthyroidism including restlessness, weight loss, excessive panting and tachycardia[17,72]. A patient's pre-treatment total T_4 has been found to predict survival outcome; for every increase of 10 nmol/L the risk of death at two years post-diagnosis increases by 1.86[73]. In humans, most patients are euthyroid but large or metastatic tumors may cause symptoms of hypothyroidism or hyperthyroidism[18].

Diagnosis

CLINICAL SIGNS For most dogs, the normal thyroid gland is not easily visible or palpable. Therefore, dogs with thyroid neoplasia most commonly present with a palpable mass in the ventral or ventrolateral neck and/or clinical signs due to compression of adjacent structures[72]. Signs may include coughing, gagging, retching, regurgitation, dysphonia, dysphagia and facial edema[9,30,74]. Differential diagnoses considered with these signs include abscesses, granulomas, salivary mucoceles, soft tissue sarcomas, and lymphoma. Invasion of cavernous sinuses may result in paralysis of the ocular muscles, leading to ptosis and prolapse of the nictitating membrane[75]. Fixed thyroid carcinomas that invade adjacent structures have potential to induce Horner's syndrome or vena caval syndrome. Mandibular or superficial cervical lymph nodes are sometimes enlarged when there is invasion or lymphatic obstruction. Signs that may indicate metastatic disease include exercise intolerance, weight loss, seizures, and incoordination[76].

CLINICAL STAGING Initial clinical staging of canine thyroid carcinomas involves complete blood count, serum biochemistry, urinalysis, three-view thoracic radiographs, and regional lymph node evaluation by cytology and/or histology. A mild normocytic normochromic nonregenerative anemia, hypercholesterolemia, and lipemia may be present in dogs that have concurrent hypothyroidism[72]. Considering the functional nature of some tumors it is advisable to evaluate serum concentrations of thyroxine and TSH. These are important considerations with respect to choice of therapy as hypothyroidism can increase anesthetic risk and complicate post-operative recovery[62]. Physical examination of the canine patient is important in determining the size of the mass, the extent to which it is fixed to underlying structures, and the presence of lymphadenopathy. Malignant carcinomas may be freely movable, but up to 67% are fixed and invasive[30]. Determination of the degree of fixation can be challenging in patients that are awake, therefore it is often recommended to conduct the physical examination under anesthesia. This will also facilitate additional imaging procedures.

Description of tumor stage is usually done according to the guidelines of the World Health Organization (WHO) tumor-node-metastasis (TNM) system[77] (Table 1-1).

Table 1-1 TNM classification of canine thyroid tumors

Clinical classification of canine thyroid tumors
T: Primary tumor
T0: No evidence of tumor T1: Maximum tumor diameter less than 2 cm T2: Maximum tumor diameter 2 to 5 cm T3: Maximum tumor diameter greater than 5 cm Substage a: Not fixed Substage b: Fixed
N: Regional lymph nodes (RLN)
N0: No evidence of RLN involvement (cervical) N1: Ipsilateral RLN involvement N2: Bilateral RLN involvement Substage a: Not fixed Substage b: Fixed
M: Distant metastasis
M0: No evidence of distant metastasis M1: Distant metastasis detected

Reproduced with permission from Owen LN (ed). TNM classification of tumours in domestic animals. Geneva,Switzerland. World Health Organization; 1980. p.52.

IMAGING Radiographs of the neck are useful in detecting soft tissue masses in the cervical region and may also identify compression and deviation of the trachea or larynx[61]. However, they do not adequately evaluate vascularity or invasion. Ultrasound may provide more information on these parameters, assess for bilateral disease, and guide fine needle aspirates[78]. Because it is non-invasive and simple to perform, it may serve as a screening test to evaluate patients as well as an adjunct to other diagnostics. The degree of local invasion may be more accurately determined by computed tomography (CT) or

magnetic resonance imaging (MRI); MRI generally offers superior soft tissue resolution. Thoracic and abdominal radiographs or CT scans are most commonly used for detecting metastatic lesions, an important step in determining the course of therapy. The degree of invasion determines whether patients are candidates for surgical resection or other options such as radiation therapy[8]. Although these tests offer many advantages, they may not provide information on functionality or presence of ectopic thyroid tissue[79].

Thyroid radionuclide scans display functional thyroid tissue – patients are injected with a tracer that is concentrated by the thyroid tissue. It is useful for diagnosis of thyroid abnormalities, staging ectopic tissue, evaluating distant metastasis, and determining the functionality of neoplastic and non-neoplastic tissue. Pertechnetate is commonly used as the tracer and is localized due to iodine trapping in thyroid cells. Other radioisotopes such as iodine-123 (^{123}I) and iodine-131 (^{131}I) may also be used. A common scintigraphic result noted in dogs is increased uptake compared to the parotid salivary gland[61]. One study reported abnormal scintigraphic results for all 29 dogs evaluated with thyroid tumors[80]. There was no association between uptake and histologic diagnosis; there was, however, an association between uptake and the degree of capsular invasion. Tumors with capsular invasion demonstrated heterogeneous uptake while those without invasion had homogeneous, well-circumscribed uptake. The authors noted that this method did not provide additional information when compared to thoracic radiography for detecting metastatic pulmonary lesions. A potential challenge associated with this procedure is the inability of some metastatic cells or anaplastic primary tumor cells to trap tracer substances due to their lack of differentiation.

CYTOLOGY AND HISTOPATHOLOGY Fine needle aspiration (FNA) and cytology are useful in differentiating among thyroid tumors, abscesses, cysts, salivary mucoceles, and enlarged lymph nodes but may not distinguish between benign and malignant thyroid neoplasms in dogs[81]. Because most thyroid carcinomas are highly vascular, this procedure may also result in severe hemorrhage. Peripheral blood contamination limits the diagnostic value of FNA cytology, but an ultrasound guided

procedure improves accuracy. Definitive diagnosis of thyroid carcinoma however, requires surgical biopsy. One study suggested that there was good correlation between cytological findings and histopathology in the diagnostic interpretation of canine thyroid carcinoma[82]. Five out of 12 cases showed identical cellular descriptions, however 33% of initial specimens contained only blood and there was frequently the need to obtain additional samples. They suggested that improved technique and applying gentle pressure to the biopsy site may improve the quality of the aspirate. It is important to note that false-negative results from FNA may delay treatment of patients, possibly with deleterious consequences. In a study of 100 human thyroid cancer patients, preoperative FNA failed to detect cancer in 14 cases. Three of these patients eventually developed metastatic disease[83]. A false-negative result delayed surgery by approximately 28 months and these patients were more likely to have vascular and capsular invasion, as well as persistent disease.

Excisional biopsies may be used for both diagnostic and therapeutic purposes in canine FTCs that are freely movable, while invasive tumors require incisional or core biopsies. These procedures have the disadvantage of significant hemorrhage. Malignant tumors are distinguished from adenomas by the presence of capsular invasion, and vascular invasion is also a common feature. It is often necessary to conduct immunohistochemical staining to separate tumors arising from follicular and C cells. For well-differentiated tumors in dogs, there has not been any documented evidence of a relationship between histologic subtype and prognosis[61,73]. The same is true for human thyroid cancer. There was no significant difference in survival time between patients diagnosed with PTC and FTC[84]. The estimation of prognosis therefore requires consideration of other parameters.

Treatment and prognosis

SURGERY When undertaking surgery for thyroid neoplasia it is important to consider the surrounding anatomical structures including large blood vessels and

embedded parathyroid glands. Injury to these structures could result in severe physiological consequences and significant hemorrhage[14]. Surgical decisions also depend on the size of the tumor, degree of invasion, presence of metastasis, and evidence of concurrent thyrotoxicosis[71]. Surgery is appropriate for tumors that are freely movable, while dogs with large invasive tumors are poor surgical candidates. Complete excision of adenomas is considered curative, and this may also be the case with carcinomas that are well circumscribed. The procedure involves a standard ventral approach to the neck (Figure 1-5), avoiding trauma to structures such as the esophagus, carotid sheath and recurrent laryngeal nerves[14].

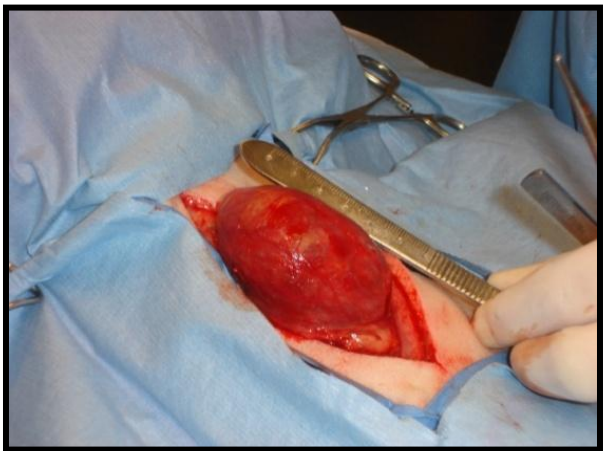

Figure 1-5 Standard ventral approach for surgical resection of a non-invasive thyroid carcinoma

Prior to excision, both the thyroid and parathyroid glands should be thoroughly evaluated and if possible, preservation of at least one parathyroid gland should be attempted to maintain adequate calcium homeostasis. Most unilateral, moveable tumors are resectable, and bilateral thyroid carcinomas or those that extend beyond the midline require bilateral thyroidectomy. In order to prevent excessive hemorrhage it may be necessary to ligate the common carotid artery and internal jugular vein.

The most common postoperative complication following bilateral thyroidectomy is hypocalcemia due to parathyroid gland injury or removal. Other less common concerns include recurrent laryngeal nerve damage, changes in phonation, hypothyroidism, and postoperative hemorrhage[14]. In some cases, it is possible to obtain a favorable prognosis using surgery alone[74]. Among five dogs with solid thyroid carcinoma, five with follicular carcinoma, and six with solid-follicular carcinoma that underwent surgery, the median survival time was 44, 24 and 17 months respectively. There was no significant association between histopathologic classification and survival time which may have been due to an insufficient number of cases in each category. Margins greater than 2 cm could not be achieved for any of the cases, and in 11 of the 16 dogs there was histological evidence of tumor cell infiltration into veins or lymphatic vessels. In another study, medullary tumors were more likely to be resectable than adenocarcinomas suggesting that they may be less invasive and more encapsulated[30]. Ten out of 12 dogs with medullary thyroid carcinoma had resectable tumors compared to 11 out of 21 dogs with thyroid adenocarcinoma. Of nine dogs with resectable medullary carcinomas that had follow-up data, 55% of them had a survival of at least six months and 33% had at least one year. Of nine dogs with resectable thyroid adenocarcinoma that had follow-up data, 78% had at least a six-month survival and 55% had at least one year.

In humans, total or near-total thyroidectomy is recommended for differentiated thyroid carcinoma. For papillary tumors, simultaneous central cervical lymph node dissection is done, and depending on the degree of spread, lateral neck lymph nodes may also be removed[85]. Following surgery, ablation of residual thyroid tissue and metastatic lesions is achieved by radioiodine treatment (^{131}I), and patients are managed with thyroxine to counteract TSH suppression[86]. The two major surgical treatment procedures, conventional thyroidectomy and minimally invasive video-assisted thyroidectomy (MIVAT), have similar outcomes when used to manage PTC[87].

RADIATION THERAPY Dogs with fixed invasive thyroid carcinomas are generally directed to radiation therapy. External beam radiation is also helpful in

controlling tumors that have not been completely resected. It can be used alone or as an adjunct to surgery or chemotherapy. Treatment protocols include the hypofractionated (nine Gy once weekly for four weeks), and fractionated (four Gy three times weekly for four weeks; or 18 to 20 fractions of 2.7 to three Gy each) protocols. The outcome of radiation therapy on dogs with invasive thyroid carcinoma has been reported[88]. One dog in this study had only radiation therapy and the other seven had tumors that were incompletely excised. All dogs responded completely within six months such that the tumors were not clinically detectable and there was no evidence of local recurrence. The median survival time was 24.5 months. Although the treatment plan was not delayed or discontinued, dogs experienced acute radiation reactions including esophageal, tracheal, and laryngeal mucositis (resulting in dysphagia), alopecia, and erythema.

Another study reported on the efficacy and toxicity of megavoltage irradiation in 25 dogs with localized non-resectable thyroid carcinomas. The mean progression-free survival time was 45 months while maximum tumor reduction was achieved in eight to 22 months. This slow response to therapy was previously described by other authors as resistance to radiation. There was local tumor progression in three dogs, concurrent progression and metastasis in three dogs, and metastasis in four dogs. One out of five dogs with pulmonary metastasis also had bone involvement, and abdominal metastases were detected in two dogs[65]. Acute radiation reactions were similar to the previous study; however it was necessary to delay therapy for four to seven days in three dogs due to severe dysphagia and weight loss. Chronic reactions included skin fibrosis, permanent alopecia, chronic tracheitis, and dry cough. This study was unable to identify significant prognostic factors in dogs with inoperable thyroid tumors. In contrast, treatment of papillary thyroid carcinoma with external beam radiation in humans has a better prognosis than that for follicular thyroid carcinoma[89].

RADIOIODIDE THERAPY This provides an alternative when external beam radiation is not available or practical. The radioisotope currently used, ^{131}I, emits beta particles and gamma radiation; the former is responsible for 80% of tissue damage

caused. It was initially believed that radioiodine therapy would benefit canine patients with functional thyroid tumors only. However studies have demonstrated that its benefit may be independent of thyroid hormone status. In dogs with non-resectable thyroid tumors, ^{131}I therapy prolonged survival time when used alone or in combination with surgery[22]. The median survival time for dogs with local tumors was significantly longer than that for dogs with metastasis, and the serum T_4 concentration before therapy did not influence survival time. However, three dogs experienced bone marrow suppression and died from complications due to anemia, neutropenia-induced sepsis, and thrombocytopenia-induced hemorrhage. The incidence of toxicosis was not associated with T_4 concentration unlike in humans where high thyroid hormone concentrations increase the risk of toxicosis.

In some cases, tumor cells may undergo de-differentiation resulting in inhibition of iodide uptake and resistance to therapy. Tumors of this type become more aggressive and have a greater tendency to metastasize[90]. In an earlier study, outcome data were compared for four treatment groups – no treatment, ^{131}I plus surgery, ^{131}I alone, and surgery alone. For the first three groups, the median survival time was three, 34, and 30 months respectively by the Kaplan-Meier method. The surgery alone group was not included in this analysis as eight of 15 dogs died or were euthanized for conditions not related to thyroid cancer[23]. However, log-rank statistical analysis showed that this group had better outcomes than all cases together.

In humans, radioiodide therapy is commonly performed after surgery to achieve ablation of tumor remnants. Adverse effects associated with low doses are not common but may include gastritis, thyroiditis and sialadenitis[91]. The effect of age on ^{131}I uptake has also been discussed. Decreased uptake has been associated with increasing age[92]; but one must consider that elderly patients are more likely to develop anaplastic carcinomas[34].

CHEMOTHERAPY Mainstream management involving chemotherapy for canine thyroid tumors has not been fully described. It is believed to be most effective

when there is only microscopic evidence of neoplasia[93]; however most cases are diagnosed well beyond this point, when there is already gross disease. Chemotherapy is often used when radiation therapy is not successful, when there is evidence of distant metastasis, or when the large size of some tumors suggests a high probability of metastatic lesions[72]. Doxorubicin is the drug of choice and is administered intravenously at a dose rate of 30 mg/m^2 every three to six weeks. Response to this drug has been variable and it has been suggested that combination with 5-fluorouracil, cyclophosphamide, or vincristine may improve the response. In dogs that fail to respond to doxorubicin or have recurrent disease, cisplatin or carboplatin is attempted.

The responses of 13 dogs with thyroid carcinoma were evaluated after treatment with cisplatin[93]. Of the 11 cases with information on tumor mobility, all of them were described as fixed to the underlying tissue. Six cases were previously treated with doxorubicin and one with surgery. After cisplatin therapy, only one case experienced complete remission; this patient had only microscopic evidence of disease prior to treatment. Six cases had partial remissions, three had stable disease and three had progressive disease. Some adverse effects included vomiting, mild azotemia, thrombocytopenia, and neutropenia. Seven patients were eventually euthanized as a result of progressive disease but no deaths were documented as a direct result of the cisplatin therapy. In humans with thyroid carcinoma, chemotherapy is reserved for patients who do not show appropriate responses to surgery, ^{131}I and other therapies. Due to its low toxicity, doxorubicin is commonly used as the first line drug. Patients can tolerate doses of 60 mg/m^2 every three weeks and respond better to this regimen than to 15mg/m^2 weekly[94]. Combination of doxorubicin with other drugs has not demonstrated an advantage[95].

NSAIDS AND THYROID HORMONE The use of non-steroidal anti-inflammatory drugs (NSAIDs) that target cyclooxygenase-2 (COX-2) is increasing for management of thyroid carcinomas. It was recently demonstrated by immunohistochemistry that COX-2 is expressed in canine thyroid tumors. All tumor types studied (adenomas, non-invasive carcinomas, and invasive carcinomas) had

significantly higher intensity and distribution of staining than normal thyroid tissue[96]. In humans, 20% of follicular adenomas, 40.9% of follicular carcinomas, and 81.3% of papillary carcinomas expressed COX-2[97]. There is evidence to suggest that it plays a role in the transition to malignancy. A study utilizing a murine model of human medullary thyroid carcinoma reported that indomethacin decreased tumor volume by up to 77% and also reduced plasma calcitonin[98]. Supplementation with thyroid hormone may also be useful supportive therapy due to its inhibition of TSH release and ultimately its negative effect on tumor growth[61].

GENETIC ALTERATIONS IN THYROID CANCER

Dogs

The genetic basis of canine thyroid cancer has not been extensively studied. One study sought to determine whether the tumor suppressor gene protein-53 (*p53*) plays an important role in its progression. In one of 23 follicular tumors evaluated, there was a missense mutation resulting in the substitution of arginine by leucine. The mutation was a 'G' to 'T' transversion located in a region considered to be a hotspot in human cancer. It also disrupted a *Haemophilus aegyptius* restriction enzyme (*HaeII*) recognition site, and tumor cells lost the wild-type allele and retained the mutant[99]. However, there is no clear evidence that p53 is important in the development of thyroid tumors in dogs. Thyroid transcription factor is expressed in neoplastic thyroid tissue but is also present in pulmonary carcinoma and cannot be used to differentiate between neoplastic lung tissue and thyroid tumors metastatic to the lung[56].

With respect to the concentration of TSH binding sites and binding affinity, there is no difference between normal thyroid tissue and primary thyroid carcinoma[100]. However, nine out of 10 metastatic tissues had reduced binding affinity, and lung metastases had both reduced affinity and concentration. Lower concentration of binding sites correlated with decreased uptake of pertechnetate, but no association was found between TSHR concentration and DNA-ploidy, TNM stage, histological grade, or T_4 and

TSH concentration. Binding could not be detected in lymph node metastases and tissues extracted from areas of local recurrence.

Humans

Thyroid cancer cells progressively develop genetic modifications over time[101]. In humans, follicular adenomas and carcinomas are characterized by aneuploidy and loss of heterozygosity (LOH) while papillary carcinomas are more likely to be diploid and less likely to show LOH[102]. Signaling via mitogen-activated protein kinases (MAPKs) may also contribute to tumor progression. Well-differentiated thyroid carcinomas involve deregulation of genes encoding components of this pathway. The proto-oncogene re-arranged during transfection (*RET*) is a receptor tyrosine kinase that activates several pathways, including MAPK, phosphatidylinositol 3-kinase (PI3K), and jun proto-oncogene (c-JUN)[103]. The RET gain-of-function mutations have been implicated in familial medullary thyroid carcinoma while the chimeric oncogene RET/PTC plays a role in the development of papillary carcinoma[104,105]. The expression of RET/PTC in normal thyroid cells is thought to induce inflammation that ultimately leads to cancer.

In cases where the oncoprotein is present, it lacks a transmembrane domain or signal peptide and is aberrantly expressed in follicular cells under a different promoter. Mutations in *BRAF* (v-raf murine sarcoma viral oncogene homolog B1) have been demonstrated in 29 – 69% of human papillary thyroid carcinoma, 13% of poorly differentiated thyroid carcinoma, and 35% of undifferentiated thyroid carcinoma. These mutations have been shown to correlate with severity of the disease and the presence of distant metastasis[106]. The reported incidence of rat sarcoma viral oncogene (Ras) mutations in human thyroid cancer is variable and may be due to differences in the detection techniques used. Additionally, the effect of estrogen has been described as a potential explanation of why women are at higher risk than men.

Other factors in humans that promote progression of thyroid cancer include alteration of adhesion and cell cycle regulation. Expression of fibroblast growth factor 2 (FGF2) and fibroblast growth factor receptor 1 (FGFR1), FGFR3, and FGFR4 have been

noted in thyroid carcinoma[107,108,109]. Members of the epidermal growth factor receptor (EGFR) and VEGF families are overexpressed in thyroid carcinoma while the receptor tyrosine kinase met proto-oncogene (MET) is overexpressed in 77 – 93% of papillary carcinomas[110,111,112]. The tumor suppressor gene *p53* is known to be mutated in a large number of human cancers, and its mutation in thyroid cancer is directly related to the aggressiveness of the tumor. In well-differentiated thyroid carcinoma the incidence is 0 – 9%, while in poorly differentiated and undifferentiated lesions, it may range from 17 – 38% and 67 – 88% respectively[113,114]. Thyroid stimulating hormone modulates the synthesis of thyroid hormone and growth of follicular cells by binding to the TSH receptor (TSHR) and activating the adenyl cyclase-cyclic adenosine monophosphate (cAMP) pathway. Gain-of-function mutations of TSHR are common in functional thyroid adenomas but are rare in malignant tumors[115].

GENE EXPRESSION PROFILING

Malignancies have largely been classified using clinical data, histopathology and immunophenotyping. However, there may be major differences in biological and clinical behavior of tumors even within the same subtype. Cellular phenotype depends on the level of functional proteins which is ultimately determined by mRNA expression[116]. Quantitative PCR is a very sensitive method of determining gene expression but can only accommodate a few genes at a time. Gene expression profiling allows for evaluation of the expression of thousands of genes simultaneously. DNA microarray analysis is often used to identify candidate genes of interest which are later validated by quantitative PCR. Since mRNA expression does not always correlate with protein expression, further validation may be necessary, most often by western blot or immunohistochemistry. Gene expression profiling has emerged as a high-throughput screening method of differentiating tumor subtypes and correlating these signatures with clinical outcome in patients. The information available from studies using this approach is mainly reflected in the human literature.

The gene expression in follicular carcinoma and adenoma from primary tumors in human surgical candidates has been compared[117]. One hundred and five genes were differentially expressed between the two groups, with 59 genes being up-regulated in carcinomas and 49 in adenomas. Among the genes expressed in carcinomas was *met* which was previously described as upregulated in PTC and FTC[118]. Results of semi-quantitative PCR correlated with microarray analysis, and the protein extracellular matrix metalloproteinase inducer (EMMPRIN) was confirmed by western blot to be upregulated in follicular carcinomas. In another study, 186 genes were differentially expressed in normal tissue extracted from thyroid glands with and without tumors[119]. These genes were identified within several ontology groups including cytoskeletal organization, cell adhesion, cellular matrix, signal transduction, and the immune response. They were comparable to genes expressed in adenomas, suggesting that normal tissue in close proximity to tumor tissue may exhibit genomic instability. Adenomas and carcinomas could be differentiated using a 43-gene cluster. In a similar manner, papillary carcinomas could be distinguished from adenomas and follicular carcinomas using 23 and 52 genes respectively. These gene sets were associated with protein metabolism, cellular trafficking, transport proteins, and transcription. Successful differentiation between follicular carcinomas and adenomas has recently been achieved using the 3 genes cyclin D2 (CCND2), proprotein convertase subtilisin/kexin type 2 (PCSK2), and placental bone morphogenetic protein (PLAB)[120]. Other genes with potential roles in thyroid malignancy have been reported and are related to signal transduction, transcription, post-transcriptional regulation, and metabolism of protein, fat, carbohydrate, and nucleic acid[121].

THE DOG AS A MODEL OF HUMAN CANCER

The dog has been used as a model for human muscular dystrophy and has promise for new therapeutic discoveries[122]. There is also increasing evidence that canine and human cancers share many features in common including histological description, genetic alterations, biological behavior, and molecular targets[123]. There is a need for

adequate models to study the pathogenesis of human tumors that have traditionally been studied in rodents. There are many challenges associated with mouse models. For example, they may involve the use of transgenics and xenograft models in cases where spontaneous tumors do not develop in mice. There may also be other confounding factors such as lifespan, body size, and presence of concurrent conditions unrelated to the tumor being evaluated. Therefore interpretation of results may be difficult. In the case of breast cancer, mouse models inadequately reflect the heterogeneous nature of tumors as well as the necessary microenvironment and association with steroid hormones. Using an incremental approach to gene expression analysis, it was demonstrated that dogs and humans share a number of deregulated pathways in common with respect to mammary cancer. These included phosphatidylinositol-3 kinase/v-akt murine thymoma viral oncogene homolog (PI3K/Akt), KRas, phosphatase and tensin homolog (Pten), wingless type MMTV integration site (Wnt-beta catenin), and MAPK[123]. The authors noted the potential for using the dog as a model for targeting these pathways.

Thyroid cancer occurs spontaneously in dogs and although the incidence of FTC differs between humans and dogs, these tumors show similar biological characteristics in both species. Mouse models of thyroid cancer are sometimes induced by decreasing thyroxine levels, leading to an increase in circulating TSH and proliferation of follicular cells[124]. Due to the shorter half life of thyroid hormone in mice, and issues with the incidence and distribution of tumors, this model is not appropriate to study all aspects of thyroid cancer[125]. Furthermore, the use of xenografts in severe combined immunodeficient (SCID) mice presents challenges associated with development of inappropriate microenvironments, lack of metastasis, abnormal immune function, and multiple unrelated tumors. Since thyroid cancer involves many different subtypes and converging molecular pathways, it is also difficult to obtain a genetically engineered mouse that accurately represents the true nature of the disease. A transgenic model of FTC created by the introduction of a dominant-negative mutation (PV) provided some reasonable representation of human FTC but there was often elevation of T_3 and T_4 while human tumors are mainly non-functional[126].

There are many features of cancer in dogs that provide useful information about the pathogenesis in humans[127]. A major advantage is that in contrast to laboratory animals, dogs are outbred, and therefore represent the genetic diversity characteristic of the human population. Also, with increasing knowledge of the canine genome, it is apparent that humans and dogs share a close genetic relationship. An examination of the neutral rate of evolution revealed that there are many similarities between humans and dogs with respect to genes implicated in malignant conditions[128]. These similarities are more significant than those between humans and mice and encompass risk factors such as age, gender, nutrition; histological grading; molecular alterations, and heterogeneity of biological behavior. Additionally most of the surgical and medical management techniques used in veterinary medicine are similar to those used in human patients. The dog as a model for human therapy offers the advantage of superior definition of malignant traits, representation of the time involved in tumor development and response to treatment, and presence of an appropriate microenvironment.

CHAPTER 2

GENE EXPRESSION OF OSTEOPONTIN AND VEGFA IN FOLLICULAR THYROID CARCINOMA COMPARED TO NORMAL THYROID TISSUE IN DOGS

Follicular thyroid carcinoma (FTC) is a highly aggressive tumor in dogs with little known about its molecular pathogenesis. The overall goal of this study was to determine whether the biological behavior of canine FTC correlates with its gene expression. Microarray analysis was performed on a pilot group of five FTC-affected dogs and four healthy dogs, and then validated with quantitative PCR of thyroid tissue from non-invasive FTC, invasive FTC, and healthy dogs. On microarray analysis, 489 transcripts were differentially expressed between FTC and normal thyroid: 242 transcripts were down-regulated and 247 were up-regulated. A number of differentially expressed genes had pathways relevant to cancer, however, osteopontin expression was markedly increased in tumor tissue, with low expression in normal thyroid tissue. One of its upstream regulators, *VEGFA*, was also differentially expressed. Interest in studying these genes further stem from the fact that there is evidence from human studies of these two genes working together to promote progression of aggressive tumors. In the present study, quantitative PCR confirmed the differential gene expression of osteopontin in both tumor types (invasive and non-invasive) compared to normal thyroid tissue. There is therefore justification for further investigation of osteopontin as a potential molecular marker and adjunctive diagnostic tool for canine FTC.

INTRODUCTION

Follicular thyroid carcinoma (FTC) is a highly aggressive tumor, accounting for the majority (up to 90%) of malignant thyroid tumors in dogs[9,12,37]. Although it is the most common canine head and neck tumor, little is known about its etiology and pathogenesis. These tumors are typically poorly encapsulated, they grow rapidly, are

highly vascular and have a propensity for invasion and metastasis[8]. Dogs generally present with a palpable mass in the ventral to ventrolateral neck and/or signs such as dysphagia, dyspnea, coughing and dysphonia, which are related to compression of surrounding anatomical structures[14]. Definitive detection by histopathology, along with the physical exam, and imaging modalities such as computed tomography (CT) and magnetic resonance imaging (MRI) ultimately determine the management approach. However, as in humans, histological grade and evidence of capsular and/or vascular invasion are not direct determinants of prognosis[84,129]. Therefore the question of what molecular events cause early invasiveness of canine FTC remains unanswered. Historically, studies of FTC have focused on epidemiological and pathological features, and have been unable to explain its invasiveness. It is possible that changes leading to invasion occur at the genetic level; these changes may occur early in tumor formation, even before the tumor is detected visually or by palpation.

Much of the gene expression work to date addressing this tumor type has been performed in affected human patients. Investigators have successfully used gene signatures to differentiate among follicular carcinomas, papillary carcinomas, adenomas and normal thyroid tissue[117,119,120]. Additionally, this information has been applied to evaluating novel therapies and improving diagnostic accuracy[90,130]. In the present study, 489 transcripts were differentially expressed between FTC and normal thyroid tissue by microarray analysis. Osteopontin and VEGFA were chosen for further investigation because of their relationship to promoting angiogenesis and tumor progression. Osteopontin was expressed at consistently high levels in FTC and very low levels in normal thyroid tissue, the fold change was high (134), pathway analysis identified it as significant within the data set, and it is up-regulated in human papillary thyroid carcinoma.

Osteopontin (OPN), also referred to as secreted phosphoprotein 1 (SPP1), is a secreted protein that can be detected in body fluids and is a promising marker for cancer detection, monitoring, and therapy. It is produced by different cell types and encompasses diverse biological functions, a number of which revolve around CD44/αvβ3

integrin receptor signaling[131]. It is involved in bone remodeling[132], anchoring of osteoclasts to bone matrix[133], adhesion and migration of leukocytes, wound healing, induction of cytokine production[131], and apoptosis evasion[134]. The interaction of osteopontin with membrane receptors implicates it in the progression of cancer. It is up-regulated in human papillary thyroid cancer (PTC) and one group demonstrated that treatment of human PTC cells with exogenous osteopontin induced invasion *in vitro* and resulted in activation of the ERK pathway, a pathway known for promotion of cancer cell proliferation[135]. Many studies have shown that VEGFA is important in tumor progression by promoting angiogenesis and stimulating motility of endothelial cells[136-138].

In a breast cancer study, an RNA aptamer designed to inhibit osteopontin successfully decreased expression of cell proliferation pathways, and inhibited migration and invasion *in vitro*[139]. Baseline and serial measurements of plasma osteopontin also have significant applications with respect to determining severity of breast cancer and duration of survival[140]. Further evidence for the use of osteopontin as a marker of aggressive cancers was presented in a comprehensive review and meta-analysis of 228 studies. This involved data correlation between tissue and plasma osteopontin, severity of tumors, and survival of human patients[141]. There was a negative correlation between osteopontin levels and survival time, and osteopontin was considered a good predictor of survival time in patients. High plasma osteopontin consistently identified groups of individuals with short survival times and was generally associated with a poorer prognosis. Osteopontin was found to be strongly associated with factors driving tumor progression, and its elevation may indicate the need for more aggressive therapy in many cases.

In the present study, the question of the molecular pathogenesis of canine FTC was approached. We sought to discover which genes were differentially expressed between dogs with non-invasive and invasive FTC and clinically healthy (normal) dogs. This is the first step in discovering molecules that could reliably and consistently identify dogs with this disease.

METHODS

Microarray analysis

RNA samples from thyroid tissue of nine dogs (five FTC and four histologically normal thyroid glands) were obtained from Iowa State University Veterinary Teaching Hospital. RNA quality was assessed using the Agilent® 2100 bioanalyzer. All samples used for microarray analysis were free from degradation as evidenced by the presence of distinct 28S and 18S ribosomal bands on gel electrophoresis and distinct peaks on the electropherogram. Array hybridization and scanning were performed at the University of Minnesota Biomedical Genomics Center (BMGC) Microarray Facility using the Affymetrix Canine 2.0 array platform. The array contained 43,042 canine probe sets and ten canine control probe sets. It interrogated over 20,000 canine genes. Controls used on the chip were added as a cocktail, and included four spike controls for labeling (*lys, phe, thr*, and *dap* genes from *Bacilus subtilis*), four exogenous spike controls for hybridization (*bioB, bioC, bioD* from *E. coli* and *cre* from P1 bacteriophage), and the housekeeping genes *GAPDH* and *β-actin* for quality assessment.

Microarray intensity raw data were pre-processed by using the Expressionist® Refiner module (Genedata, Basel, Switzerland). The data quality was assessed by evaluation of scatter plots as well as the $3'/5'$ ratios of housekeeping genes. The probe set expression indices were summarized by MAS5 algorithm and normalized by linear scaling to a median of 100. Expression values for FTC and normal were compared using a two sample t-test, $\alpha = 0.001$. The error discovery rates were evaluated by EDR[142] and BH[143] methods. Transcripts were considered to be differentially expressed if the fold change between the two groups was two or greater. Gene information was obtained from Affymetrix Canine 2.0 annotation (2010) and the Ensembl® gene browser (http://useast.ensembl.org). A Fisher test was performed to determine differences based on gene ontology biological processes ($\alpha = 0.05$).

PCR case selection and experimental design

Validation of candidate genes using quantitative real-time PCR required a larger sample size therefore additional cases were recruited from the University of Minnesota Veterinary Teaching Hospital. Clients participating in this study did so with informed consent. All procedures were approved by the Institutional Animal Care and Use Committee (IACUC). Dogs with thyroid masses were included in the study if they had histopathological confirmation of FTC. Controls were selected from dogs euthanized for reasons unrelated to thyroid pathology and were included in the study if they had histologically normal thyroid glands. Histological analysis was performed by a pathologist and involved microscopic evaluation of tissue sections stained with hematoxylin and eosin. Tumors were categorized based on the pathologist's reports of their degree of invasion: those with tumor cells confined within the thyroid capsule only were considered non-invasive and those reported as having capsular and vascular invasion (including invasion of surrounding anatomic structures) were considered invasive. Tumor stages were also noted, including the size of the tumor, evidence of lymph node invasion, and metastasis. Based on sample size analysis conducted using 'R' statistical software (version 2.9.2), it was determined that nine samples in each category were necessary. Therefore nine samples each were sought from healthy dogs with normal thyroid glands, dogs with non-invasive FTC, and dogs with invasive FTC.

Sample collection and RNA processing

Tumor tissue samples were obtained from surgically excised thyroid masses presumed to be FTC. The surgical procedure followed a standard ventral approach to the thyroid gland where a unilateral or bilateral thyroidectomy was performed depending on the extent of the tumor. Normal thyroid tissues were obtained using the same surgical approach from clinically healthy dogs. In each case, a 1-2cm^3 section of tissue was placed in a 15-ml conical tube containing 10 ml of RNA later®. This was performed immediately after removal from the patient. The tissue was incised in several locations to ensure uniform exposure to the RNA later®. The tube was kept at 4°C for 24 hours to

allow the RNA later® to adequately infiltrate the tissue, and then it was stored at -20°C until extraction. A second tissue section was placed in formalin for confirmatory histopathology. RNA was extracted from tissues using the RNeasy total RNA midi kit (Qiagen®, Germany) according to the protocol outlined for RNA extraction from animal tissue. RNA concentration was measured using a Nanodrop® spectrophotometer. Samples were visualized by agarose gel electrophoresis to assess quality and only those with no evidence of degradation were used for further analysis.

Quantitative PCR

Two genes were selected for validation by quantitative PCR; osteopontin and vascular endothelial growth factor A (*VEGFA*). The housekeeping gene beta actin was chosen as the internal reference gene. Gene-specific primers were designed using Primer-3 Plus **(**http://www.bioinformatics.nl/cgi-bin/primer3plus/primer3plus.cgi**).** The BLAST algorithm (http://blast.ncbi.nlm.nih.gov/Blast.cgi) was utilized to ensure primer specificity to the target gene. The primers used for beta actin (*ACTB*), were previously published[144] (Table 2-1).

Table 2-1. Primer sequences used for amplification of osteopontin, VEGFA, and beta actin from follicular thyroid carcinoma and normal thyroid tissue cDNA samples

Gene	Forward primer (5′ to 3′)	Reverse primer (5′ to 3′)	Product size (bp)
OPN	TCAATGCCGTCCTACTTTCC	TTGGCTGACAAGTTCACTGC	224
VEGFA	CCAGGAGTACCCTGACGAGA	GCTGCAGGAAACTCATCTCC	188
ACTB	CCAGCAAGGATGAAGATCAAG	TCTGCTGGAAGGTGGACAG	100

Semi-quantitative PCR was performed on one control sample with a temperature gradient to determine the optimal temperature for amplification using all three primers. Based on agarose gel electrophoresis of PCR products, the optimal temperature was

chosen as the one with the most distinct band. PCR products were evaluated to ensure the correct sized band was obtained based on the expected product size from Primer-3 plus. Reverse transcription was performed using the Quantitect® Reverse Transcription kit (Qiagen®, Germany). The cDNA samples were analyzed in triplicate on 96-well non-skirted Stratagene® PCR plates.

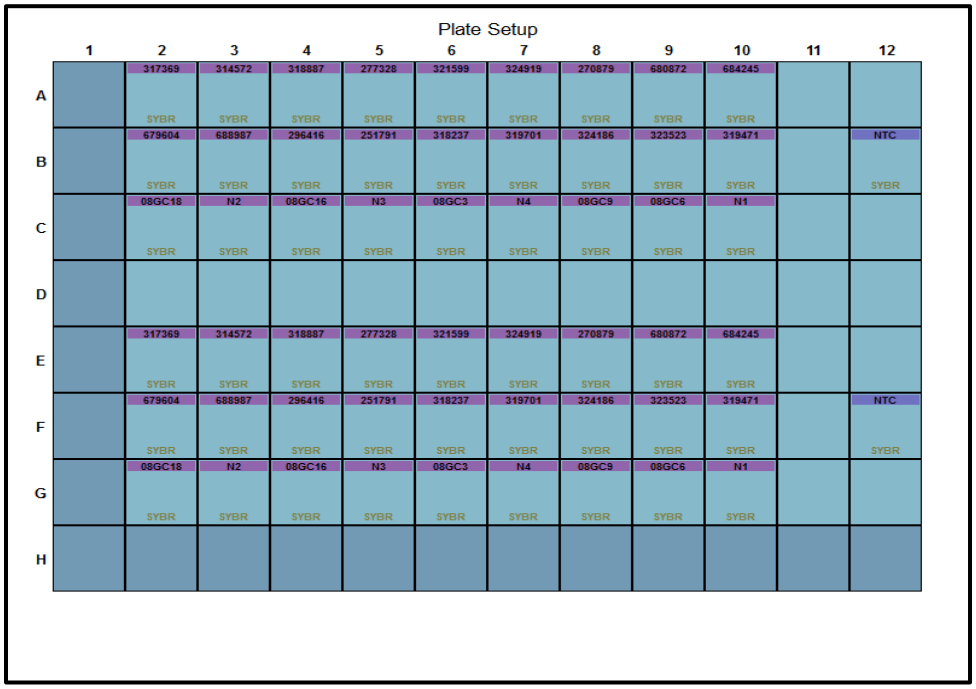

Figure 2-1 Plate set-up for quantitative PCR amplification of genes in non-invasive and invasive follicular thyroid carcinoma and normal thyroid tissue cDNA samples
Samples in upper three rows were amplified using primers for the target gene; samples in lower three rows were amplified using primers for the reference gene (beta actin); NTC = no-template control

Real-time PCR analysis was performed using the PerfeCTa™ FastMix kit (Quanta Biosciences) with SYBR green detection, and the Stratagene® Mx3005P™ qPCR system. Each PCR reaction included 10 µl of the 2X SYBR green master mix, 5 µl of cDNA template (total 50 ng), 0.5 µl each of 10 µM forward and reverse primers and 4 µl

nuclease free water. The thermal profile (Figure 2-2) was based on previous primer optimization.

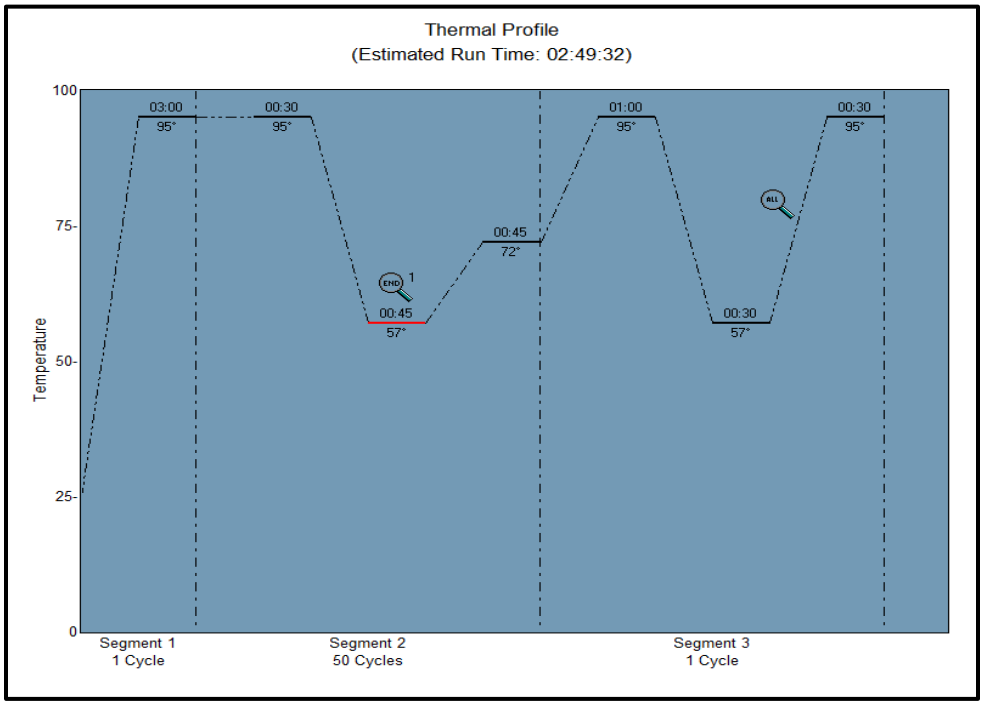

Figure 2-2 Thermal profile for quantitative PCR amplification of genes in non-invasive and invasive follicular thyroid carcinoma and normal thyroid tissue cDNA samples

Beta actin (*ACTB*) was included as the reference gene on each plate. No-template controls were included on each plate for each gene (Figure 2-1). Amplification plots (fluorescence values measured against the cycle threshold, Ct) for each sample were analyzed for appropriate shape (Figures 2-3; 2-5). Dissociation curves (fluorescence values measured against temperature) were evaluated to ensure correct product melting temperatures and to rule out primer-dimer interference (Figures 2-4; 2-6).

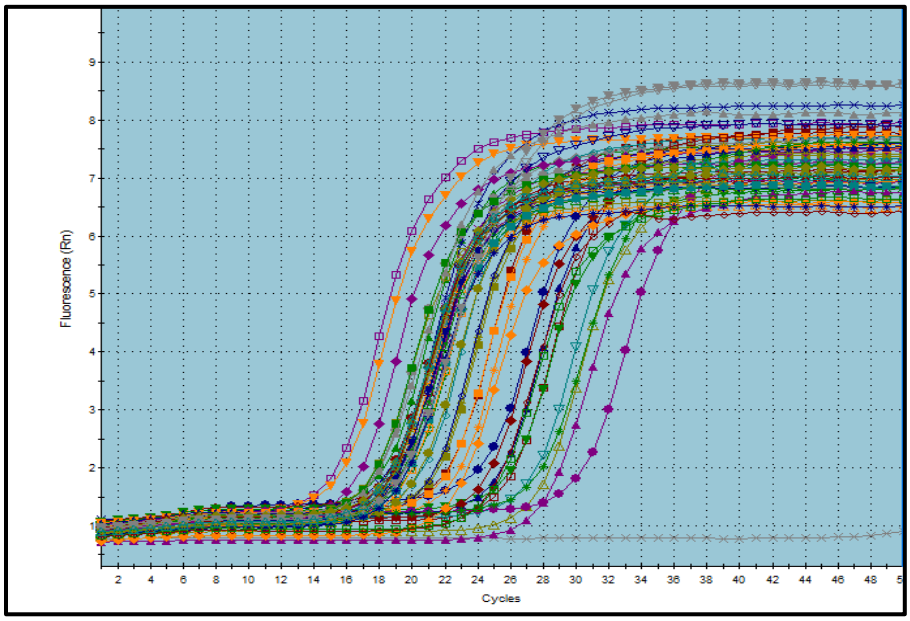

Figure 2-3 Amplification plots from quantitative PCR amplification of osteopontin and beta actin in non-invasive and invasive follicular thyroid carcinoma and normal thyroid tissue cDNA samples

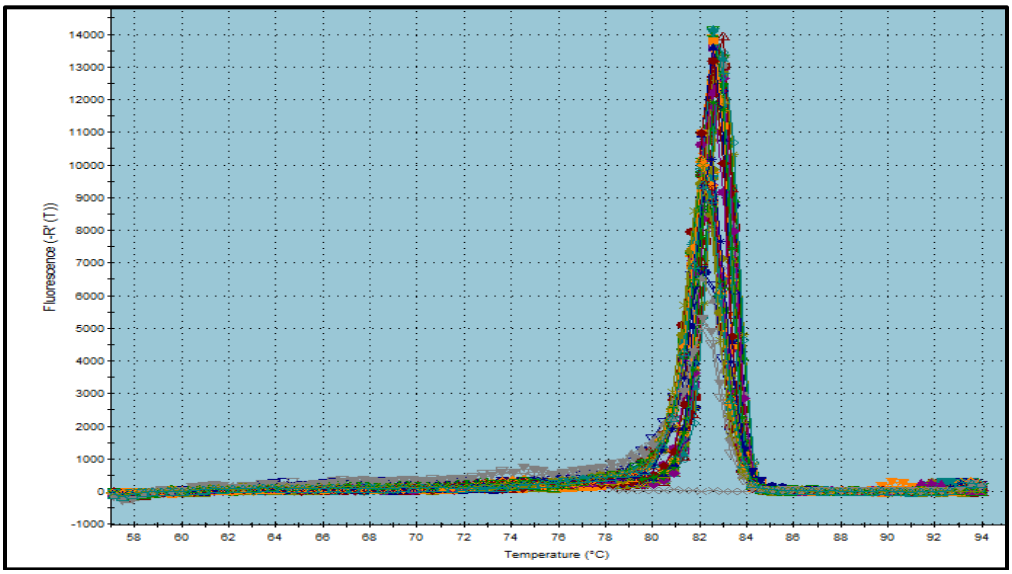

Figure 2-4 Dissociation curves from quantitative PCR amplification of osteopontin and beta actin in non-invasive and invasive follicular thyroid carcinoma and normal thyroid tissue cDNA samples. The melting temperature for both osteopontin and beta actin PCR products was 82° C

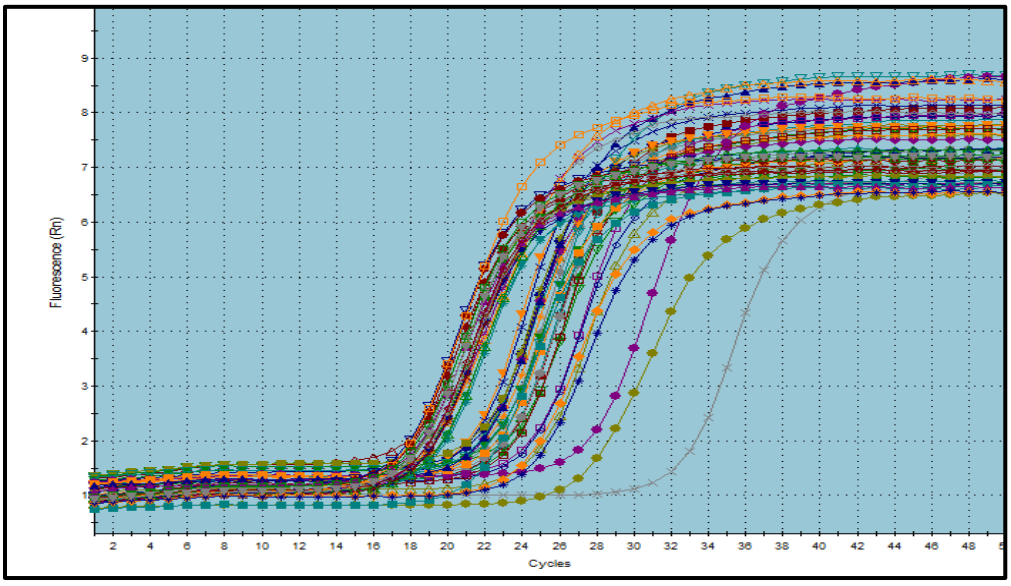

Figure 2-5 Amplification plots from quantitative PCR amplification of VEGFA and beta actin in non-invasive and invasive follicular thyroid carcinoma and normal thyroid tissue cDNA samples

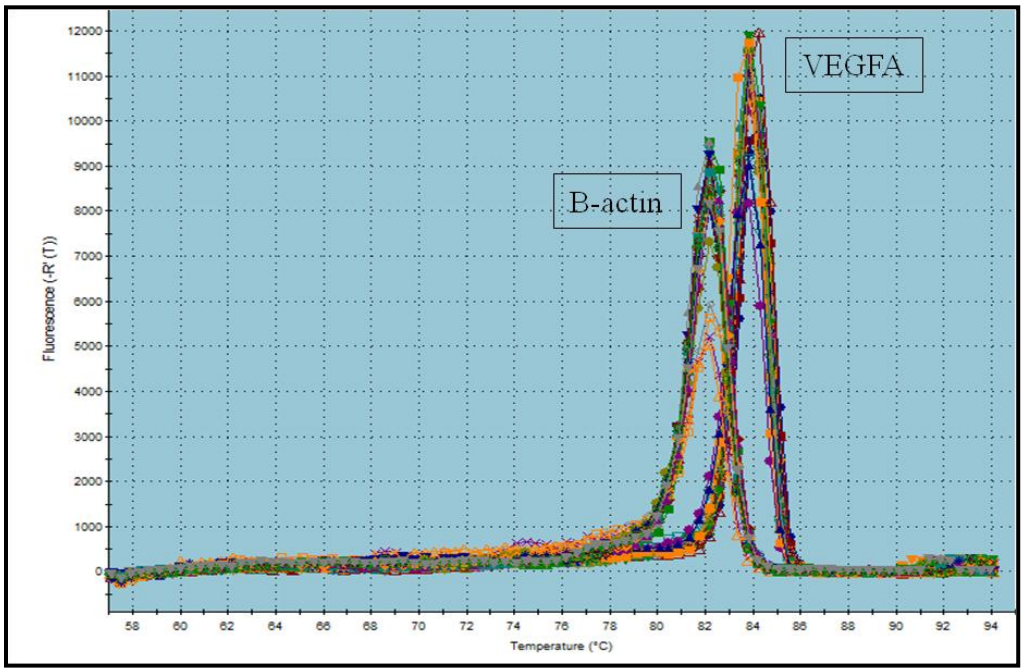

Figure 2-6 Dissociation curves from quantitative PCR amplification of VEGFA and beta actin in non-invasive and invasive follicular thyroid carcinoma and normal thyroid tissue cDNA samples The melting temperature for beta actin PCR products was 82°C and that for VEGFA was 83.6°C

No-reverse-transcription controls were analyzed for each sample to rule out genomic DNA contamination. Products were again evaluated on an agarose gel to ensure that a single product was amplified for each gene and each sample. For each gene, representative PCR products were sequenced and determined to be the correct gene using the Sequencher® and the BLAST algorithm.

PCR Data analysis

For each sample, an average Ct value was obtained by calculating the mean of the three replicates for a particular gene. Primer efficiency was estimated by the LinReg® PCR software and expression for each sample was calculated using the following formula, where E = primer efficiency[145]:

$$\text{Expression} = \frac{(E_{ref})^{Ct\,sample}}{(E_{target})^{Ct\,sample}}$$

Mean expression among the three groups was compared by analysis of variance (ANOVA) and Tukey's multiple comparison test on log-transformed data. Fold changes were calculated by dividing mean expression values between groups. To assess for correlation between *OPN* and *VEGFA* expression among the samples, the Spearman's rank correlation was calculated.

RESULTS

Microarray analysis

Comparison of gene expression in the FTC and normal groups demonstrated significant differences in 777 transcripts. These transcripts had a fold change of two or

greater and were considered differentially expressed. A large number of these transcripts were not characterized in major gene databases and did not have adequate information on location, name and function. Therefore 489 characterized transcripts were differentially expressed with 242 being down-regulated and 247 up-regulated (Table 2-2). Some gene ontology biological processes that were significantly different included regulation of cell shape, cell adhesion, regulation of MAP kinase activity, angiogenesis, and regulation of cell migration. Twenty-three up-regulated transcripts had a fold difference greater than ten (Table 2-3). Seventy-one down-regulated transcripts had a fold difference greater than ten (Table 2-4).

The mean expression of osteopontin was 134.7 times higher in FTC than normal thyroid tissue. All normal samples consistently recorded low expression values and all FTC samples recorded high expression values (Figure 2-7). The expression of one of its upstream regulators, *VEGFA* was 2.25 times higher in FTC tissue samples than normal thyroid gland tissue (Figure 2-8).

Table 2-2. Fold changes of transcripts differentially expressed between follicular thyroid carcinoma and normal thyroid tissue (microarray analysis)

Fold change	Up-regulated in FTC	Down-regulated in FTC	**Total**
> 100	2	15	**17**
10 - 100	21	56	**77**
5.0 - 9.9	36	60	**96**
3.0 - 4.9	50	40	**90**
2.0 - 2.9	138	71	**209**
Total	**247**	**242**	**489**

Table 2-3 Genes that were significantly up-regulated with fold changes greater than ten in follicular thyroid carcinoma compared to normal thyroid tissue

Gene Symbol	Gene Title	Fold
OPN	osteopontin	134.7
SBSN	suprabasin	103.5
CHI3L1	chitinase 3-like 1 (cartilage glycoprotein-39)	47.55
CHRDL2	chordin-like 2	39.5
SLIT1	slit homolog 1 (Drosophila)	30.11
PRSS53	protease, serine, 53	24.44
SLC2A9	solute carrier family 2, member 9	21.31
ACP5	acid phosphatase 5, tartrate resistant	20.5
RRM2	ribonucleotide reductase M2	20.09
CDCA3	cell division cycle associated 3	16.48
CRLF1	cytokine receptor-like factor 1	15.31
CRABP2	cellular retinoic acid binding protein 2	14.03
SLC7A11	solute carrier family 7, member 11	13.43
ADAMTSL2	ADAMTS-like 2	13.34
ACP5	acid phosphatase 5, tartrate resistant	13.14
MIOX	myo-inositol oxygenase	12.89
CENPH	centromere protein H	12.61
AQP5	aquaporin 5	12.4
COL16A1	collagen, type XVI, alpha 1	12.17
CD40	CD40 molecule, TNF receptor superfamily member 5	11.09
HSPH1	heat shock 105kDa/110kDa protein 1	10.83
ST6GALNAC6	ST6 (alpha-N-acetyl-neuraminyl-2,3-beta-galactosyl-1,3)	10.21
PGF	placental growth factor	10.03

Table 2-4 Genes that were significantly down-regulated with fold changes greater than ten in follicular thyroid carcinoma compared to normal thyroid tissue

Gene Symbol	Gene Title	Fold
CRSP-2	calcitonin receptor-stimulating peptide-2	469.20
CALCB	calcitonin-related polypeptide beta	410.40
SNAP25	synaptosomal-associated protein, 25kDa	337.30
GFRA4	GDNF family receptor alpha 4	297.20
CHGB	chromogranin B (secretogranin 1)	231.30
SCG5	secretogranin V (7B2 protein)	222.50
CALB1	calbindin 1, 28kDa	215.50
SLC18A1	solute carrier family 18, member 1	197.00
CHGB	chromogranin B (secretogranin 1)	177.80
CASR	calcium-sensing receptor	177.40
CASR	calcium-sensing receptor	176.90
SCG2	secretogranin II	135.50
SCGN	secretagogin, EF-hand calcium binding protein	132.10
SCGB1C1	secretoglobin, family 1C, member 1	114.30
CALCA	calcitonin/calcitonin-related polypeptide, alpha	112.20
SCG5	secretogranin V (7B2 protein)	68.71
CALB1	calbindin 1, 28kDa	58.25
PCSK2	proprotein convertase subtilisin/kexin type 2	55.55
GCG	glucagon	54.39
FXYD2	FXYD domain containing ion transport regulator 2	40.25
DPT	dermatopontin	34.55
PNMT	phenylethanolamine N-methyltransferase	32.88
TNMD	tenomodulin	31.19
LMO7	LIM domain 7	31.08
SLC30A3	solute carrier family 30, member 3	30.95
SCG3	secretogranin III	28.47
CFH	complement factor H	28.28
FMO2	flavin containing monooxygenase 2	28.27
CPE	carboxypeptidase E	27.39
RASSF10	Ras association domain family (N-terminal) member 10	27.22
VEPH1	ventricular zone expressed PH domain homolog 1 (zebrafish)	26.54
ELMOD1	ELMO/CED-12 domain containing 1	25.36
FXYD3	FXYD domain containing ion transport regulator 3	24.31
CACHD1	cache domain containing 1	24.27
NNAT	neuronatin	23.93
SST	somatostatin	23.54

Table 2-4 cont'd Genes that were significantly down-regulated with fold changes greater than ten in follicular thyroid carcinoma compared to normal thyroid tissue

Gene Symbol	Gene Title	Fold
MMRN1	multimerin 1	23.06
SCGB1C1	secretoglobin, family 1C, member 1	22.71
LMO7	LIM domain 7	21.91
PHACTR3	phosphatase and actin regulator 3	21.80
TBX1	T-box 1	20.49
PHEX	phosphate regulating endopeptidase homolog, X-linked	19.54
ASCL1	achaete-scute complex homolog 1 (Drosophila)	19.35
SCARA5	scavenger receptor class A, member 5 (putative)	18.93
CPE	carboxypeptidase E	18.59
RSPO3	R-spondin 3 homolog (Xenopus laevis)	17.72
DPP4	dipeptidyl-peptidase 4	17.39
KLK11	kallikrein-related peptidase 11	16.15
SLC18A1	solute carrier family 18, member 1	16.00
PCSK5	proprotein convertase subtilisin/kexin type 5	15.31
GPX3	glutathione peroxidase 3	14.96
ECE2	endothelin converting enzyme 2	14.72
RARRES2	retinoic acid receptor responder (tazarotene induced) 2	14.39
PAPPA2	pappalysin 2	14.22
PTPRN2	protein tyrosine phosphatase, receptor type, N polypeptide 2	14.00
CLGN	calmegin	13.85
LMO7	LIM domain 7	13.41
NEDD4	neural precursor cell expressed, developmentally down-regulated 4	12.97
DTNA	dystrobrevin, alpha	12.83
AKAP12	A kinase (PRKA) anchor protein 12	11.92
VWA2	von Willebrand factor A domain containing 2	11.80
PHACTR3	phosphatase and actin regulator 3	11.52
SLC39A8	solute carrier family 39, member 8	11.40
C1QL1	complement component 1, q subcomponent-like 1	11.33
VTN	vitronectin	10.99
IL17RB	interleukin 17 receptor B	10.55
DPT	dermatopontin	10.46
SNCA	synuclein, alpha (non A4 component of amyloid precursor)	10.38
CASR	calcium-sensing receptor	10.26
SEZ6L2	seizure related 6 homolog (mouse)-like 2	10.26
LYVE1	lymphatic vessel endothelial hyaluronan receptor 1	10.01

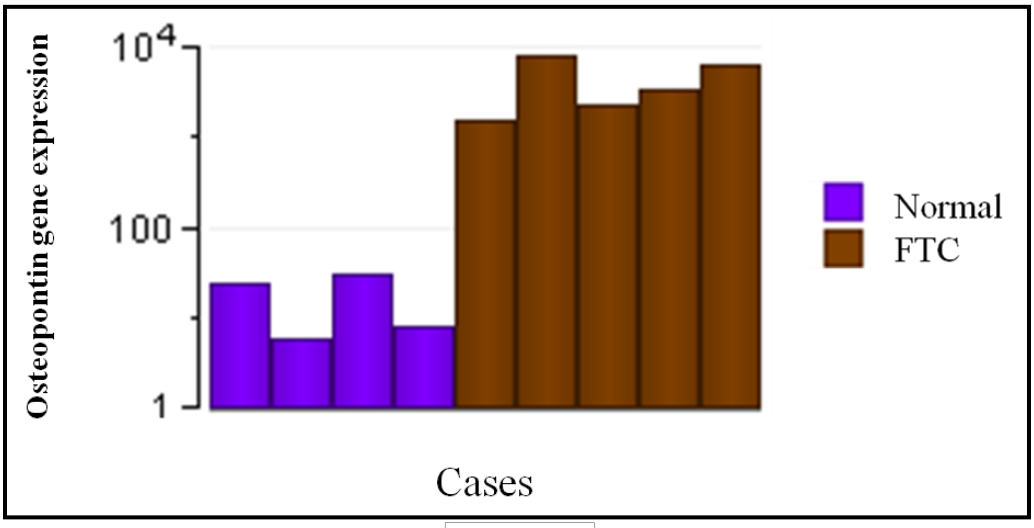

p < 0.0001

Figure 2-7 Osteopontin gene expression in normal thyroid tissue and follicular thyroid carcinoma (microarray analysis)

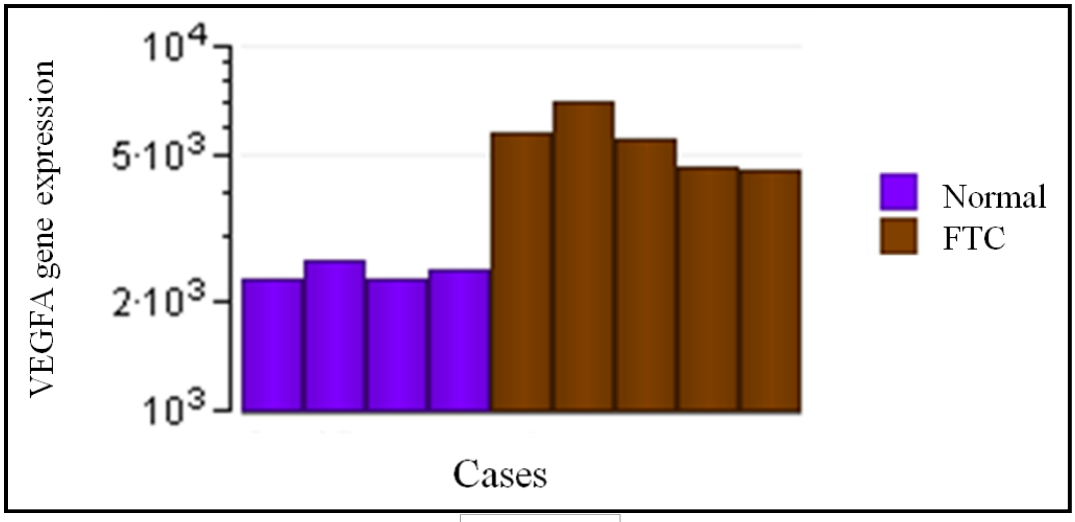

p = 0.0007

Figure 2-8 VEGFA gene expression in normal thyroid tissue and follicular thyroid carcinoma (microarray analysis)

Descriptive analysis of PCR cases

Eighteen FTC cases (nine non-invasive and nine invasive) were evaluated by quantitative PCR. The overall median age of presentation for dogs with FTC was 10.1 years, consistent with previous reports[12]. The median age of dogs presenting with non-invasive FTC was 11.2 years (range 5.92 – 12.92 years); and that for invasive FTC was 8.8 years (range 5.25 – 12.17 years). There was no statistical difference in presentation age between the two groups (Figure B-1). The number of male and female FTC cases was evenly distributed, with nine males (four non-invasive and five invasive) and nine females (five non-invasive and four invasive). There were several breeds represented among the cases, however 22% (4/18) were Golden Retrievers (Figure B-2). The majority of dogs (12/18) presented with a visible or palpable cervical mass; some dogs presented with signs suggestive of thyroid disease (neck stiffness or signs of hyperthyroidism); while other dogs presented with non-specific clinical signs or for a routine procedure (Figure B-3). Among the normal controls, the breeds represented were five hound crosses, three beagles, and one Border collie: their median age was 1.75 years.

Of the 18 FTC cases, serum T_4 was evaluated in only 5/9 non-invasive and 3/9 invasive cases. Among the five non-invasive cases, one had an elevated T_4 while the other four were within the normal range. However, one of the cases with normal T_4 was due to treatment with thyroxine for concurrent hypothyroidism. Among the three invasive cases, one had an elevated T_4 and the other two were within the normal range.

Quantitative PCR

The mean expression of osteopontin was higher in non-invasive and invasive FTC compared to healthy controls (Table 2-5; Figure 2-9). Osteopontin expression was 22.93 times higher in non-invasive FTC than healthy controls and 14.3 times higher in invasive FTC than healthy controls (Table 2-6). Among the cases, the expression was highly variable; therefore, the non-invasive and invasive groups were not different from each other. The mean expression of *VEGFA* did not differ among any of the three groups

(Table 2-5; Figure 2-10). There was no correlation between osteopontin and *VEGFA* expression (Spearman's rank correlation; p = 0.52).

Table 2-5 Mean gene expression values for osteopontin (OPN) and VEGFA in non-invasive and invasive follicular thyroid carcinoma and normal thyroid tissue (quantitative PCR)

	Mean expression ± SEM			**p-value**
	Non-invasive FTC (n = 9)	**Invasive FTC (n = 9)**	**Normal thyroid tissue (n = 9)**	
OPN	1.2412 ± 0.7399 (a)[1]	0.7741 ± 0.3414 (a)	0.0541 ± 0.0407 (b)	0.0003
VEGFA	0.1026 ± 0.0228 (a)	0.1951 ± 0.0964 (a)	0.0858 ± 0.0236 (a)	0.4962

[1]Values within a row that are represented by the same letter in parenthesis are not statistically different.
SEM = standard error of the mean

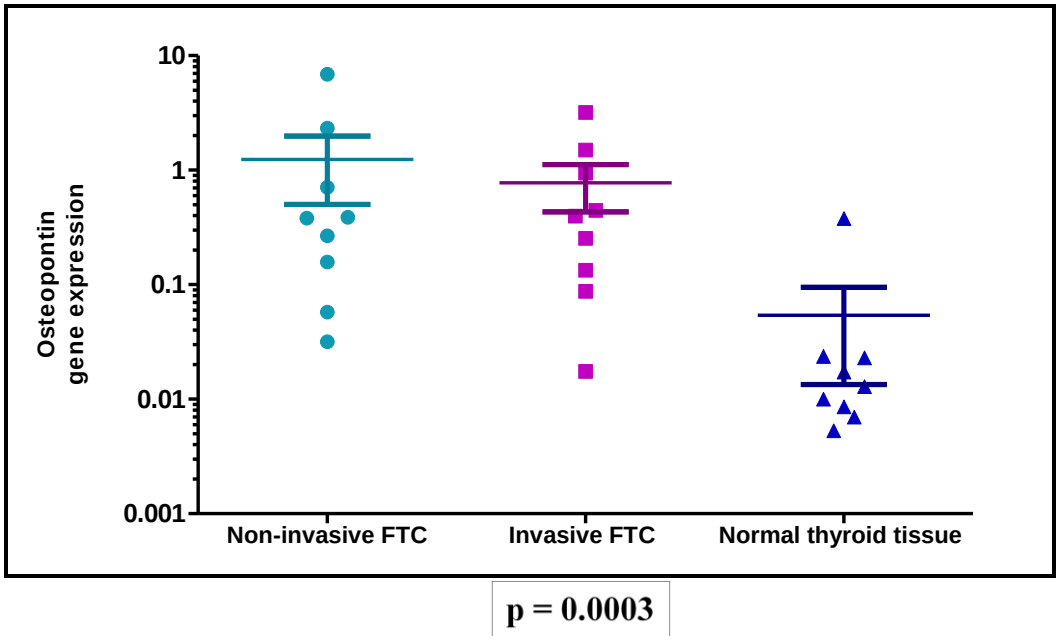

Figure 2-9 Osteopontin gene expression in non-invasive and invasive follicular thyroid carcinoma compared to normal thyroid tissue (quantitative PCR)

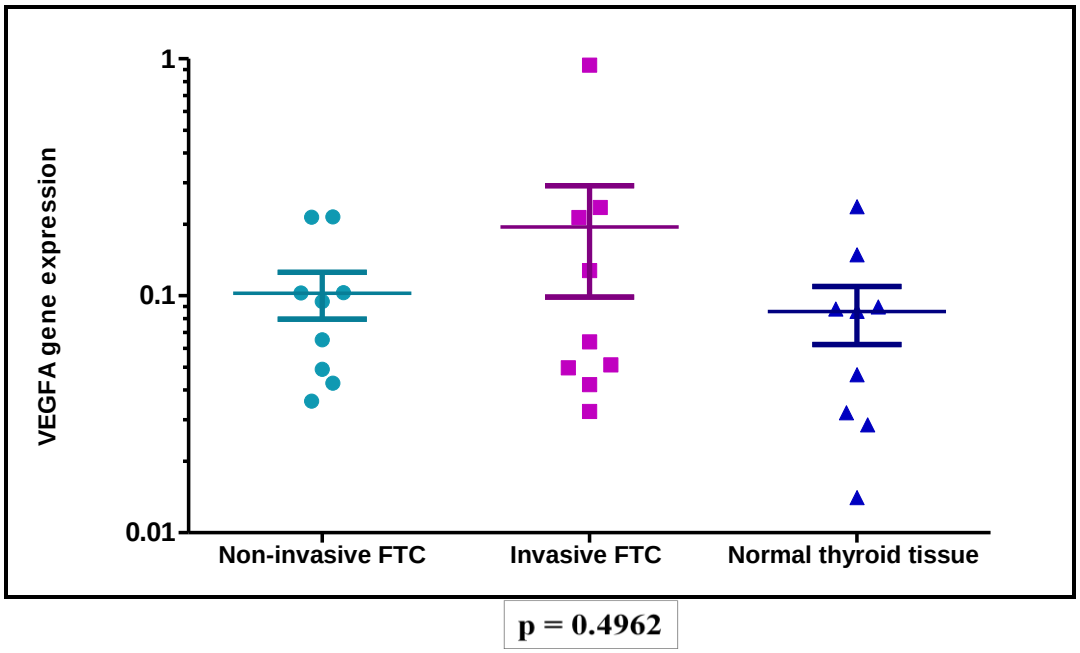

Figure 2-10 *VEGFA* gene expression in non-invasive and invasive follicular thyroid carcinoma compared to normal thyroid tissue (quantitative PCR)

Table 2-6 Osteopontin (OPN) and VEGFA fold differences between non-invasive and invasive follicular thyroid carcinoma and normal thyroid tissue (quantitative PCR)

Gene	Groups compared	Fold difference
OPN	Non-invasive *vs* healthy	22.93
	Invasive *vs* healthy	14.3
	Non-invasive *vs* invasive	1.6
VEGFA	Non-invasive *vs* healthy	1.19
	Invasive *vs* healthy	2.27
	Non-invasive *vs* invasive	0.53

DISCUSSION

Canine FTC is an aggressive tumor characterized by high vascularity and early invasiveness[61]. The molecular characteristics of this condition have not been extensively researched in the dog. To date and to the authors' knowledge, there have been no genome-wide studies. Gene expression profiling has proven to be a valuable tool in characterizing human cancer subtypes, understanding the biological behavior of tumors, and predicting response to therapy and prognosis[90,117,120]. In the present study, differential expression of 489 characterized transcripts was identified by microarray analysis between tissues from FTC and histologically normal thyroid tissue. This was based on the Affymetrix® Canine 2.0 microarray chip which interrogates over 20,000 genes. Differentially expressed genes belonged to several gene ontology categories including regulation of cell shape, cell adhesion, regulation of MAP kinase activity, angiogenesis, and regulation of cell migration. Molecular functions included cell differentiation, development, signaling, apoptosis, protein metabolism, transport, transcription/translation regulation, and cell cycle regulation. FTC cells therefore differ from normal thyroid cells in their level of transcriptional and post-transcriptional activity as well as their ability to exploit pathways that enhance growth and motility of transformed cells.

Osteopontin expression was significantly up-regulated in FTC compared to normal thyroid tissue, and the potential significance to tumor progression justified further analysis of this gene. Quantitative PCR confirmed that osteopontin was in fact expressed in normal thyroid tissue at lower levels than thyroid tissue from dogs with FTC. Due to the high vascularity and rapid growth rate of canine FTC, VEGFA, one of the upstream regulators of osteopontin was also chosen for analysis. Studies have shown that osteopontin enhances tumor progression and angiogenesis driven by VEGFA[146], and experimental inhibition of tumor growth negatively affects the expression of these two genes[147]. The main function of VEGFA in tumors is the promotion of angiogenesis and migration of endothelial cells. Osteopontin, which is secreted by transformed epithelial cells, has been implicated in the progression of aggressive human tumors[148,149,150] as well

as in human papillary thyroid cancer[135]. Its cellular functions include the inhibition of apoptosis and induction of migration, invasion and angiogenesis. In the present study, the up-regulation of osteopontin in dogs with both non-invasive and invasive FTC compared to normal dogs suggests that this gene may have a role in the progression of the tumor. There was a disparity between fold differences observed by microarray analysis and quantitative PCR. Such changes have been reported in the literature. Additionally, a conservative approach was used for quantitative PCR analysis by incorporating the primer efficiency in calculation of gene expression. The variability in osteopontin expression observed among FTC cases likely reflects differences in tumor size and distribution as well as the time period between tumor initiation and patient presentation. Additionally, it is unclear at what point in tumor development osteopontin is induced.

While significant differences were not found between non-invasive and invasive tumors, it is important to consider that the criteria for determining degree of invasiveness were based on histopathological detection of capsular and vascular invasion. Tumors may also have been at different stages of development, resulting in variable expression. The fold difference between non-invasive FTC and healthy was greater than that between invasive FTC and healthy. This finding, although not statistically significant, was unexpected since osteopontin expression often correlates with invasion. A possible explanation is that invasive tumors may express osteopontin at high levels in tumor cells located at the invasive front, which may not have been fully represented in the samples from which RNA was extracted. Alternatively, depending on their stage of development, non-invasive tumors could have cells with a greater potential to become malignant, which therefore may express a higher level of osteopontin. There was no significant difference noted for *VEGFA* expression between groups. However, some studies have reported subtle changes in *VEGFA* expression, which resulted in larger osteopontin differences and influenced tumor invasion[146]. *VEGFA* may also have been expressed earlier in the development of the tumor or alternatively, the osteopontin response may be induced by an alternative pathway. It must be noted that control dogs used in this study represented different breeds and genders, but were not age-matched. This was partly due to the

availability of younger institutional dogs. It was also less likely that the thyroid glands of younger dogs contained pathological changes.

The results of this study are similar to those of human carcinomas that demonstrate aggressive biological and clinical behavior. We therefore need to consider the clinical significance of osteopontin up-regulation in FTC cases. There is justification for further investigation of osteopontin for its potential as a molecular marker of canine FTC.

CONCLUSIONS

We have demonstrated by microarray analysis that there is differential gene expression between tissue from FTC and normal thyroid tissue. The differential expression of osteopontin was also validated by quantitative PCR. However, the expression of *VEGFA* was not different among groups. Osteopontin is a promising candidate for enhanced diagnostic accuracy and monitoring of canine FTC.

CHAPTER 3

EXPRESSION OF OSTEOPONTIN AND VEGFA PROTEIN IN CANINE FOLLICULAR THYROID CARCINOMA COMPARED TO NORMAL THYROID TISSUE

Follicular thyroid carcinoma (FTC) is an aggressive tumor affecting dogs. Previous gene expression analysis demonstrated that osteopontin is over-expressed in non-invasive and invasive FTC compared to normal thyroid tissue. VEGFA, implicated along with osteopontin in tumor progression, showed non-significant expression differences among the patient groups. The goal of the present study was to examine the protein expression of osteopontin and VEGFA in the same tissues and to determine whether there is a correlation between gene and protein expression. Nine formalin-fixed paraffin-embedded tissues from each group were tested using immunohistochemistry and evaluated based on the intensity and distribution of the immunoreactivity as well as the total IHC score. Osteopontin expression was higher in non-invasive and invasive FTC compared to normal thyroid tissues but there was no difference between the two tumor groups. VEGFA differed only in its distribution score between invasive FTC and normal thyroid tissue. Osteopontin was consistently expressed in tumor tissues and absent in the majority of normal tissues and is a promising marker for identification of canine FTC.

INTRODUCTION

Thyroid tumors occur in approximately 1 to 4% of the canine population and up to 90% are carcinomas, largely of follicular origin[9-12,29,37]. Tumors tend to grow, invade, and metastasize rapidly, leading to patient morbidity and decreased quality of life[14]. Many studies have addressed the question of what causes such rapid tumor progression. In human thyroid tumors, osteopontin and VEGFA may work synergistically to promote tumor progression and angiogenesis[146]. In some cases, small changes in VEGFA

expression results in larger osteopontin responses, affecting tumor invasion. Additionally experimental inhibition of tumor growth negatively affects the expression of these two genes[147].

Osteopontin is an extracellular matrix protein that has been extensively studied in human medicine. It has a wide range of cellular functions, and is secreted into body fluids such as blood and urine[151]. Cells such as osteocytes, dendritic cells, macrophages, myoblasts, endothelial cells and chondrocytes produce osteopontin in the normal cell. Integrin receptors facilitate signaling, and major functions include bone remodeling[132], adhesion and migration of leukocytes, wound healing, and induction of cytokine production[131]. However, the interaction of osteopontin with membrane receptors also aids its ability to induce neoplastic growth. The CD44 receptors to which osteopontin bind induce pathways of proliferation and migration in both normal and tumor cells[151]. In one study, OPN was up-regulated in human papillary thyroid carcinoma[135], and another demonstrated that most papillary, all medullary, and all anaplastic carcionomas were positive for osteopontin[152]. Its ability to secrete into body fluids has also made it possible to investigate it as a potential biomarker. Compared to healthy controls, it has been found in higher concentrations in the blood of human patients with ovarian[153], breast[140,154], pancreatic[155], prostatic[156] and papillary thyroid[135] carcinomas, as well as non-small cell lung cancer[157], and multiple myeloma[158].

In the previous study, gene expression was examined by microarray analysis in a small group of FTC and normal thyroid tissue as well as by quantitative PCR among non-invasive FTC (tumors with capsular invasion only), invasive FTC (tumors with capsular and vascular invasion) and normal thyroid tissue[159]. Both methods demonstrated the up-regulation of osteopontin in FTC compared to normal thyroid tissue. In order to further understand the biological relevance of osteopontin, it was necessary to investigate whether the gene expression translated to protein expression in the tissues of these same patients. Because VEGFA is often implicated along with osteopontin in cancer progression, its protein expression was also examined. We hypothesized that FTCs

would have a higher protein expression of osteopontin and VEGFA than healthy thyroid tissue and that invasive FTC would have a higher expression than the non-invasive form.

METHODS

Case selection and experimental design

Tumor tissue samples were obtained from surgically excised thyroid masses presumed to be FTC. The surgical procedure followed a standard ventral approach to the thyroid gland where a unilateral or bilateral thyroidectomy was performed depending on the extent of the tumor. Normal thyroid tissues were obtained using the same surgical approach from clinically healthy dogs. A section of tissue was placed in formalin for fixation and a portion of this was later stored as paraffin-embedded blocks. Tissues were reviewed by an independent pathologist for confirmation of FTC diagnosis in cases and normal thyroid structure in healthy controls. The cases chosen for immunostaining were the same as those chosen for quantitative PCR in the previous study. Nine cases were evaluated from each patient group; non-invasive FTC (tumors with capsular invasion only), invasive FTC (tumors with capsular and vascular invasion), and normal thyroid tissue. These numbers were obtained by sample size analysis using 'R' statistical software (version 2.9.2). Antibodies were commercially available, and purchased from Santa Cruz Biotechnology, Inc. Immunohistochemistry staining was conducted at IHC Services (Smithville, Texas).

Immunohistochemistry

Staining protocol for osteopontin

Five-micron sized sections were cut, placed on positively charged microscope slides and allowed to dry at room temperature. Sections were de-paraffinized using two series of the clearing agent ProPar (Anatech, Michigan) for five minutes each. Hydration was achieved by passing the slides through a series of alcohols, and then they were pre-treated with Proteinase K for two minutes at room temperature. Sections were rinsed

briefly in Tris buffer and then covered in protein blocking solution for 30 minutes. This was followed by a second Tris rinse and protein block using Power Block™ for five minutes. Another Tris rinse was followed by application of the specific antibody (OPN) to the tissue sections. The osteopontin polyclonal antibody was used at a dilution of 1:100. Negative control slides were prepared using an irrelevant antibody (*Helicobacter pylori* polyclonal antibody reactive only in bacilli). Slides were rinsed in Tris buffer followed by addition of biotinylated goat anti-mouse IgG and incubation for 30 minutes. They were again rinsed in Tris buffer and after the linking reagent, streptavidin-alkaline phosphatase, was added, they were incubated for 30 minutes. Slides were then rinsed in Tris buffer and New Fuchsin substrate was applied. Development of color was monitored by light microscopy. The slides were then washed using distilled water and counterstained by applying Mayers' hematoxylin for one minute. Slides were briefly rinsed in ammonia water and distilled water, followed by dehydration with a series of alcohols. ProPar clearing agent was applied and the slides were mounted.

Staining protocol for VEGFA

Five-micron sized sections were cut, placed on positively charged microscope slides and allowed to dry at room temperature. Sections were de-paraffinized using two series of the clearing agent ProPar (Anatech, Michigan) for five minutes each. Hydration was achieved by passing the slides through a series of alcohols. Slides were heated in 10mM citrate buffer (pH 6.0), maintained between 95-100°C for 6 minutes, and then allowed to cool at room temperature for 20 minutes. After a brief rinse in water, sections were covered with a protein blocking solution for 30 minutes. All slides were rinsed in 50mM Tris buffer (pH 7.60) and an Avidin/Biotin blocking reagent applied for 30 minutes. This was followed by a rinse in Tris, a protein block ("Power Block", Pierce Chemical Co., Rockford, IL) for 5 minutes, and another Tris rinse. The specific VEGFA polyclonal antibody was then applied to the sections and the irrelevant antibody applied to the negative control slides. The incubation time was one hour. Each slide was rinsed in Tris buffer and a biotinylated goat anti-rabbit IgG applied and incubated for 30

minutes. A Tris buffer rinse was again applied followed by a streptavidin-alkaline phosphatase linking reagent incubated for 30 minutes, another Tris rinse, and a New Fuchsin substrate. Color development was monitored microscopically. Slides were then washed in distilled water and counterstained in Mayers' hematoxylin for one minute. After a brief rinse in ammonia water, the slides were washed in distilled water, dehydrated up a series of alcohols and mounted using Propar.

Scoring and data analysis

Scoring of slides was based on evaluation of intensity and distribution of staining supervised by a blinded pathologist. Semi-quantitative scoring was based on a four point scale for staining intensity and a five-point scale for stain distribution. For distribution, scores were assigned as 0 = no evidence of stain, 1 = 1–25% of cells stained, 2 = 26–50%, 3 = 51–75%, and 4 = greater than 75% cells stained. For intensity, scores were assigned as 0 = no stain, 1 = weak staining, 2 = moderate staining, and 3 = strong staining in most cells[160]. Scores for distribution and intensity were averaged over ten microscopic fields. Staining intensity was assessed in comparison to the positive controls; canine kidney in the case of osteopontin and canine small intestine in the case of VEGFA. All samples were compared to a matched negative control; a section of tissue from the same sample stained with the irrelevant antibody in order to detect non-specific staining. Scores for distribution and intensity were summed to obtain total IHC scores. Therefore, any particular sample could have a maximum score of seven. Samples with total scores equal to or less than two were considered to have stained negatively, and those with total scores greater than two were considered positive[152]. Scores were compared between the three patient groups (non-invasive FTC, invasive FTC and normal thyroid tissue) using a Mann-Whitney U test at a significance level of 0.05.

A Spearman rank correlation was used to examine the correlation between osteopontin and VEGFA protein expression; the correlation between gene and protein expression for both osteopontin and VEGFA; and the correlation between osteopontin

and VEGFA IHC score and age, gender and tumor size for all cases. All analyses were performed using Prism® software.

RESULTS

For osteopontin, canine kidney was used as the positive control. Staining was strongly positive (4+), multifocal and cytoplasmic in renal tubular epithelial cells (Figure 3-1). No staining was detected in glomeruli. In thyroid tumor tissues, osteopontin staining in epithelial cells was diffusely cytoplasmic. In some cases, staining was observed throughout most of the tissue section and in other cases it was patchy and limited to smaller areas. In cases where a regional pattern was detected, staining was more prominent but not limited to the epithelial cells lining follicles.

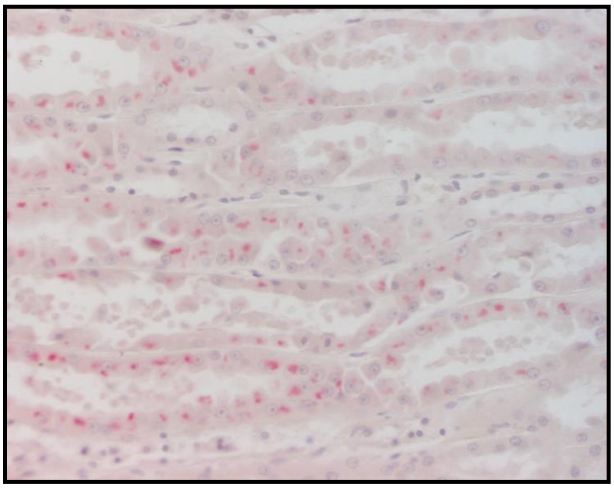

Figure 3-1 Section of canine kidney showing positive staining for osteopontin in renal tubular epithelial cells

All nine non-invasive and nine invasive FTC cases were osteopontin positive, having total IHC scores greater than two (Table 3-1). Among the non-invasive tissues, four showed weak staining and five showed moderate staining (Figure 3-4). Cases also varied in the distribution of staining. In two cases, stain was detected in 26-50% of cells; in four cases there was staining in 51-75% of cells; and in three cases, stain was detected

in 76-100% of cells. Among the invasive cases, three showed weak staining and six showed moderate staining (Figures 3-2; 3-3).

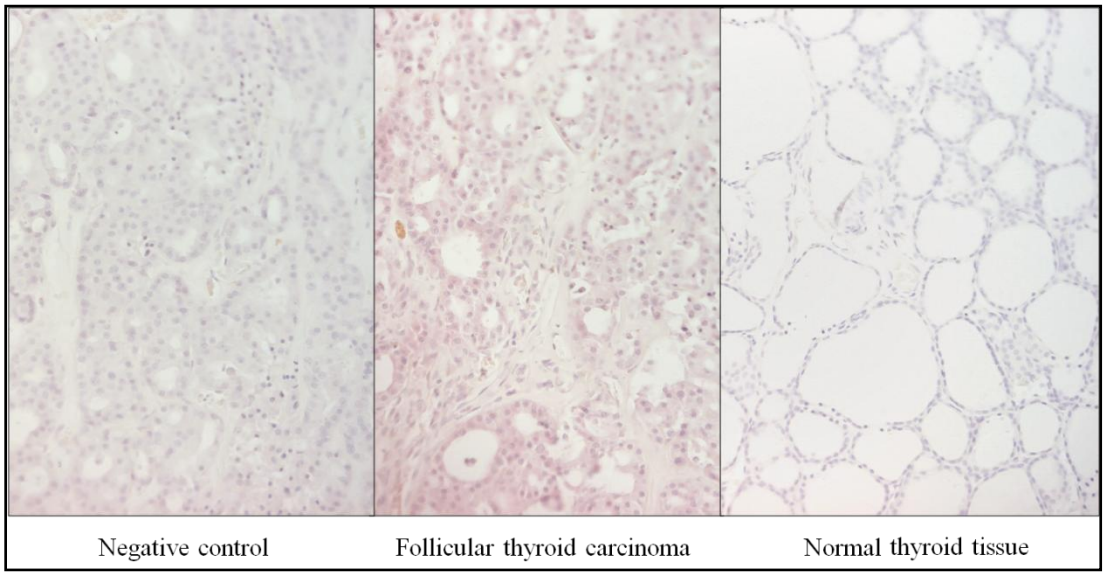

Figure 3-2 An example of follicular thyroid carcinoma tissue with moderate diffuse osteopontin staining (middle) compared to its negative control (left) and a negative normal thyroid tissue sample (right); (magnification 20X)

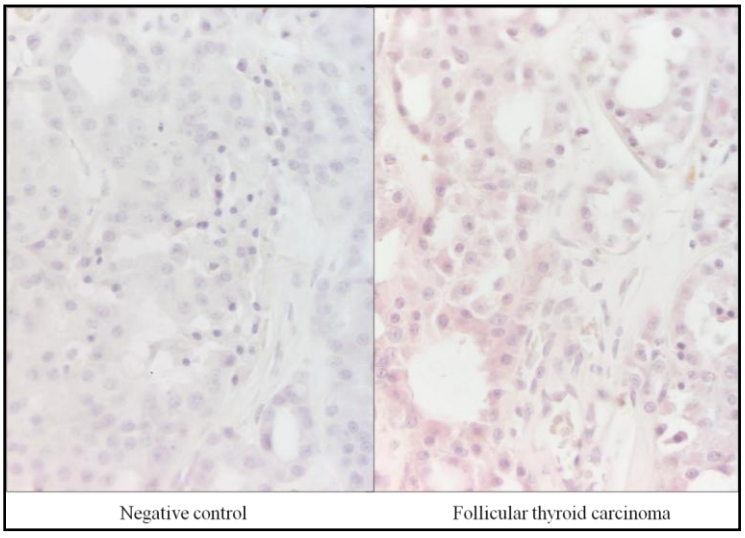

Figure 3-3 An example of follicular thyroid carcinoma tissue with moderate diffuse osteopontin staining (right) compared to its negative control (left); (magnification 40X)

Table 3-1 Individual osteopontin intensity, distribution and total IHC scores for non-invasive and invasive follicular thyroid carcinoma and normal thyroid tissue

	Sample	Intensity score	Distribution score	Total IHC score	Comment
Non-invasive FTC	1	2	4	6	Positive
	2	2	4	6	Positive
	3	1	2	3	Positive
	4	1	3	4	Positive
	5	2	3	5	Positive
	6	1	2	3	Positive
	7	2	3	5	Positive
	8	1	3	4	Positive
	9	2	4	6	Positive
Invasive FTC	1	2	4	6	Positive
	2	1	4	5	Positive
	3	1	3	4	Positive
	4	2	4	6	Positive
	5	2	4	6	Positive
	6	2	4	6	Positive
	7	2	4	6	Positive
	8	2	4	6	Positive
	9	1	2	3	Positive
Normal thyroid tissue	1	0	0	0	Negative
	2	0	0	0	Negative
	3	0	0	0	Negative
	4	0	0	0	Negative
	5	1	1	2	Positive
	6	1	1	2	Positive
	7	0	0	0	Negative
	8	0	0	0	Negative
	9	0	0	0	Negative

With respect to distribution, one tissue had staining in 26-50% of its cells; one tissue had staining in 51-75% of its cells; and in seven tissues staining was detected in 76-100% of its cells. No tumor tissues showed strong positive staining for osteopontin. Two normal thyroid tissues stained positively for osteopontin. In both cases there was weak staining with 1-25% of cells showing reactivity. The other seven normal thyroid tissues had no evidence of stain.

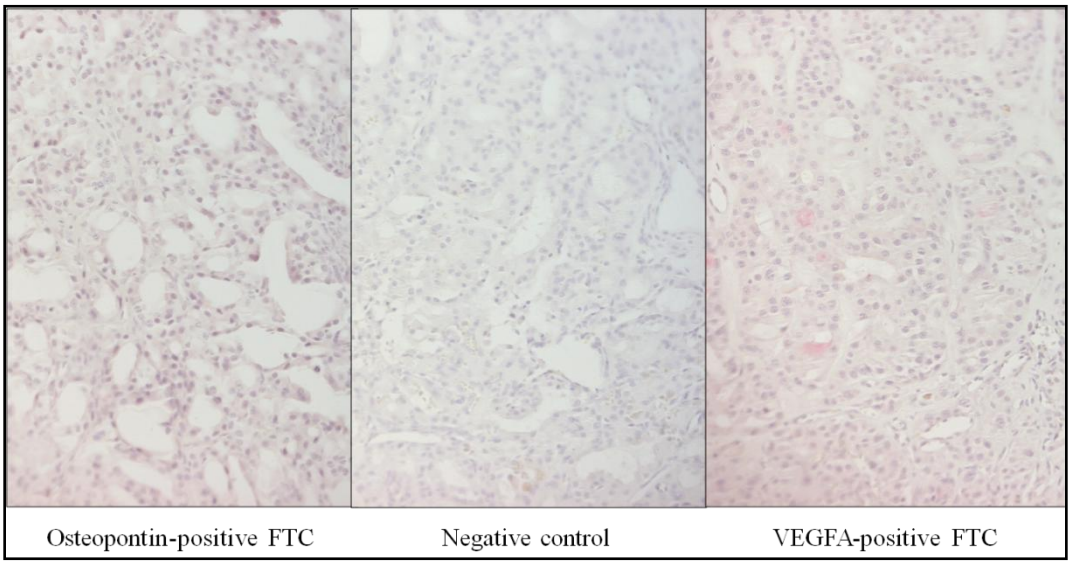

Figure 3-4 An example of follicular thyroid carcinoma tissue with moderate diffuse staining for both osteopontin (left) and VEGFA (right) compared to the negative control (middle); magnification 20X

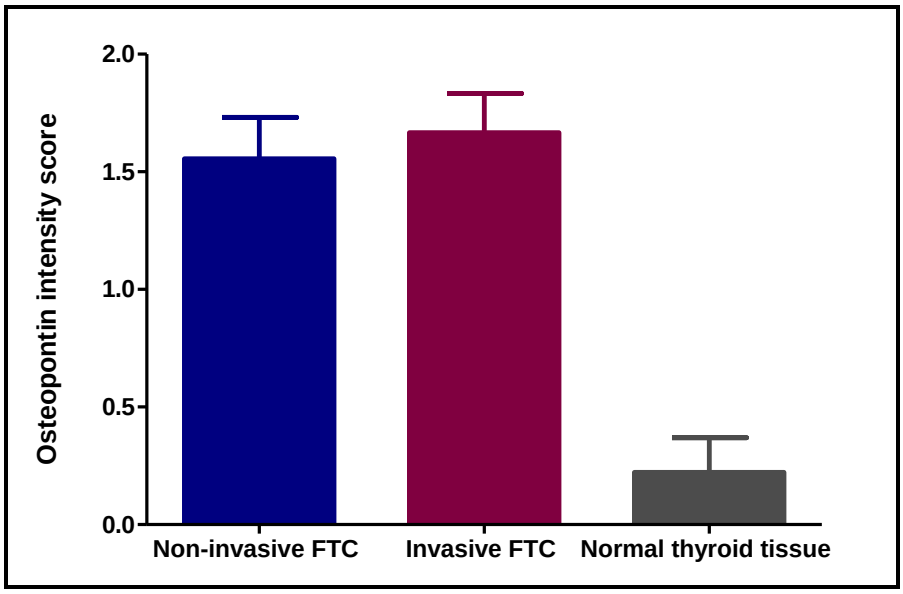

Figure 3-5 Staining intensity scores for osteopontin in non-invasive and invasive follicular thyroid carcinoma (FTC) and normal thyroid tissue

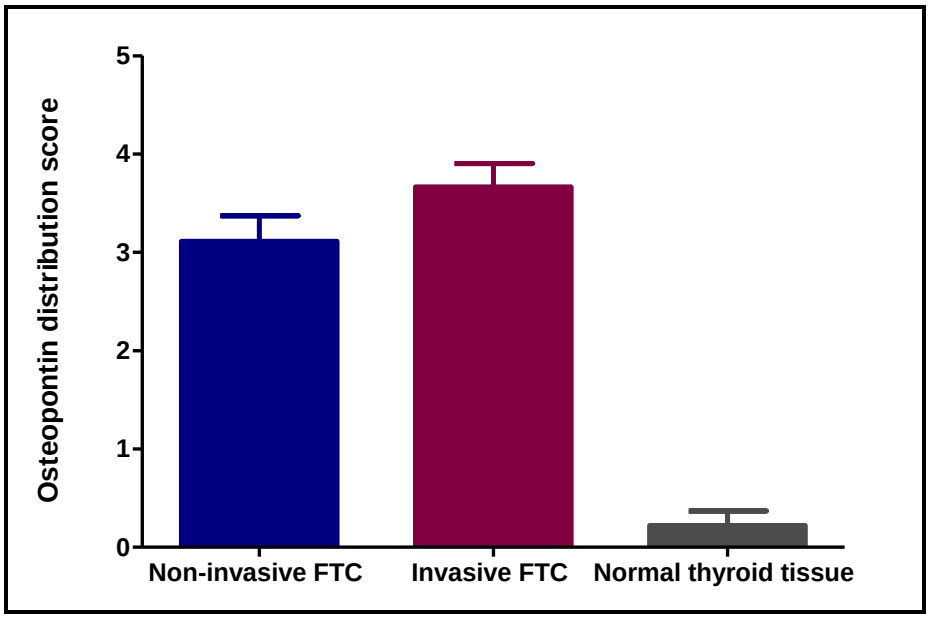

Figure 3-6 Staining distribution scores for osteopontin in non-invasive and invasive follicular thyroid carcinoma (FTC) and normal thyroid tissue

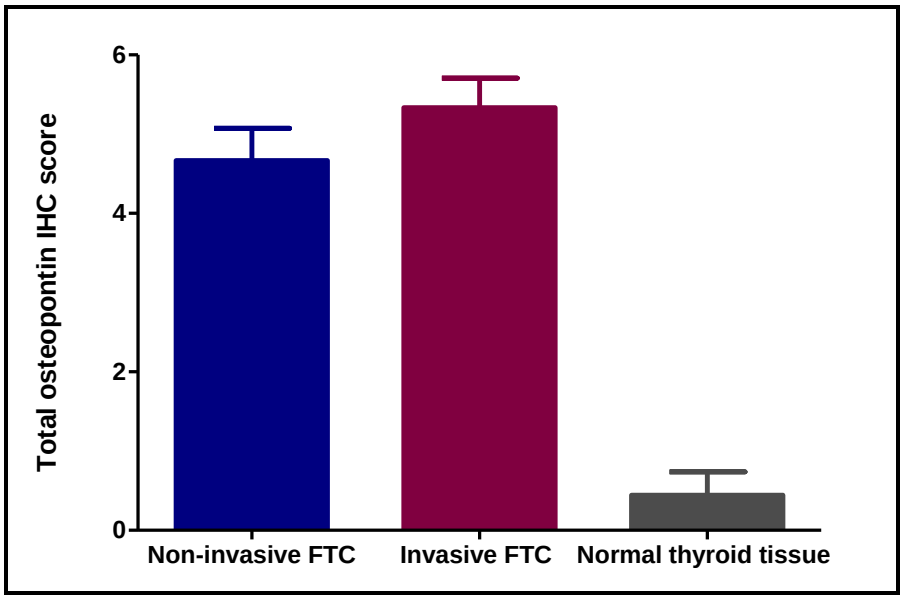

Figure 3-7 Total IHC scores for osteopontin in non-invasive and invasive follicular thyroid carcinoma (FTC) and normal thyroid tissue

Pair-wise comparison of the three patient groups was performed with a Mann-Whitney U test. Both non-invasive and invasive FTC tissues had significantly higher stain intensity, stain distribution and total IHC scores than normal thyroid tissues (Table 3-2). The non-invasive group had lower intensity, distribution, and total scores than the invasive group but this trend was not significant (Figures 3-5; 3-6; 3-7).

Table 3-2 Comparison of osteopontin staining between non-invasive and invasive follicular thyroid carcinoma and normal thyroid tissue

Category	Groups compared	p-value
Osteopontin staining intensity	Non-invasive *vs* healthy Invasive *vs* healthy Non-invasive *vs* invasive	0.0007 0.0005 0.6762
Osteopontin staining distribution	Non-invasive *vs* healthy Invasive *vs* healthy Non-invasive *vs* invasive	0.0002 0.0002 0.1044
Osteopontin total IHC score	Non-invasive *vs* healthy Invasive *vs* healthy Non-invasive *vs* invasive	0.0003 0.0002 0.2168

For VEGFA, canine small intestine was used as the positive control (Figure 3-8). Stain was detected in villous epithelial cells and was diffusely cytoplasmic.

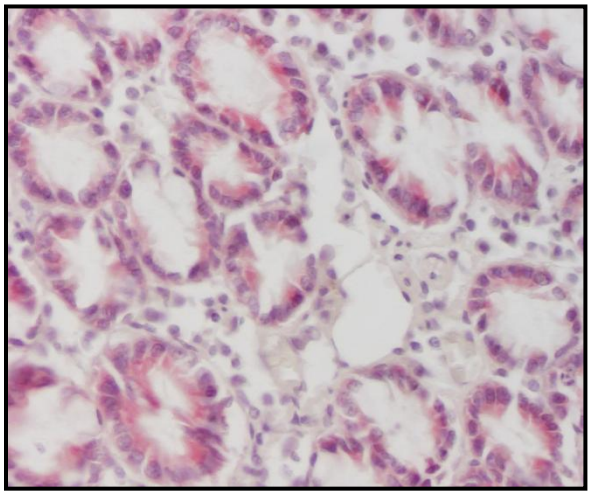

Figure 3-8 Section of canine small intestine showing positive staining for VEGFA in villous epithelial cells

Eight of nine non-invasive FTC tissues were VEGFA positive (Table 3-3). Of those, five tissues stained with weak intensity and three with moderate intensity. In five tissues, stain was detected in 26-50% of cells and the other three tissues had stain in 76-100% of cells. Eight of nine invasive tissues were also VEGFA positive. Three of those tissues stained with weak intensity and five with moderate intensity. With respect to distribution, one tissue had staining in 26-50% of cells, four had staining in 51-75% of cells, and the other three tissues stained positively in 76-100% of cells. Six of nine normal thyroid tissues were VEGFA positive while the other three had no evidence of stain. Two of the positive normal tissues had weak staining and four had strong staining (Figure 3-9). With respect to distribution, two tissues had 1-25% of cells stained; two had 26-50% stained and two had 51-75% of cells stained.

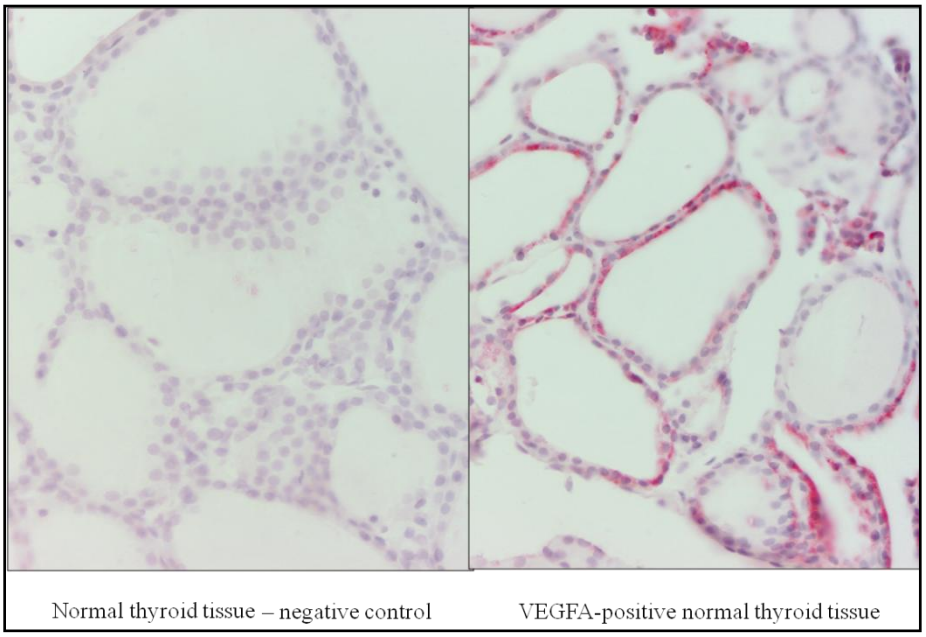

Figure 3-9 An example of normal thyroid tissue with strong VEGFA staining (right) compared to the negative control (left); magnification 40X

Table 3-3 Individual VEGFA intensity, distribution and total IHC scores for non-invasive and invasive follicular thyroid carcinoma and normal thyroid tissue

	Sample	Intensity score	Distribution score	Total IHC score	Comment
Non-invasive FTC	1	2	4	6	Positive
	2	2	4	6	Positive
	3	0	0	0	Negative
	4	1	2	3	Positive
	5	1	2	3	Positive
	6	1	2	3	Positive
	7	1	2	3	Positive
	8	1	2	3	Positive
	9	2	4	6	Positive
Invasive FTC	1	1	2	3	Positive
	2	2	4	6	Positive
	3	2	3	5	Positive
	4	0	0	0	Negative
	5	2	4	6	Positive
	6	2	3	5	Positive
	7	1	3	4	Positive
	8	2	4	6	Positive
	9	1	3	4	Positive
Normal thyroid tissue	1	3	3	6	Positive
	2	3	3	6	Positive
	3	3	1	4	Positive
	4	3	2	5	Positive
	5	1	2	3	Positive
	6	0	0	0	Negative
	7	0	0	0	Negative
	8	1	1	2	Positive
	9	0	0	0	Negative

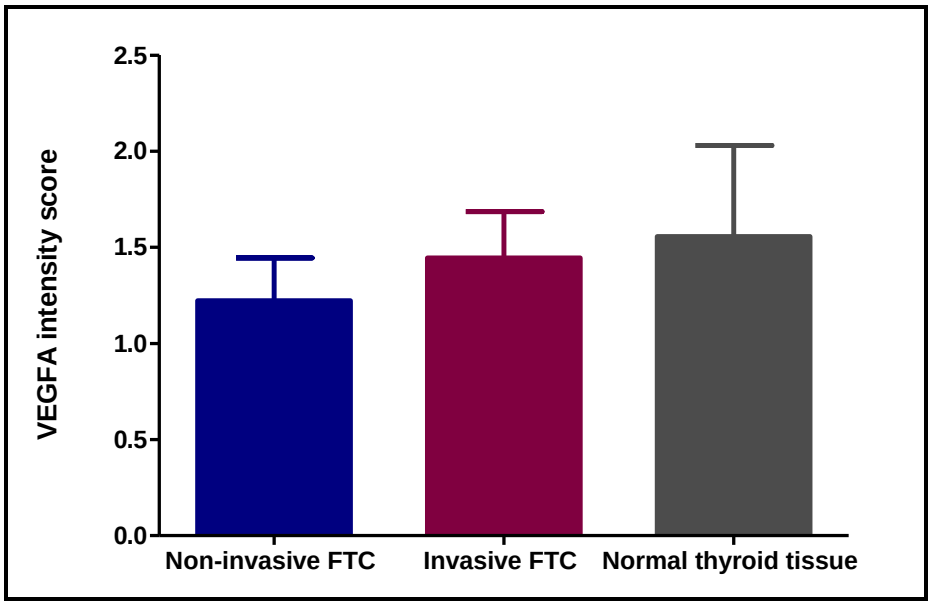

Figure 3-10 Staining intensity scores for VEGFA in non-invasive and invasive follicular thyroid carcinoma (FTC) and normal thyroid tissue

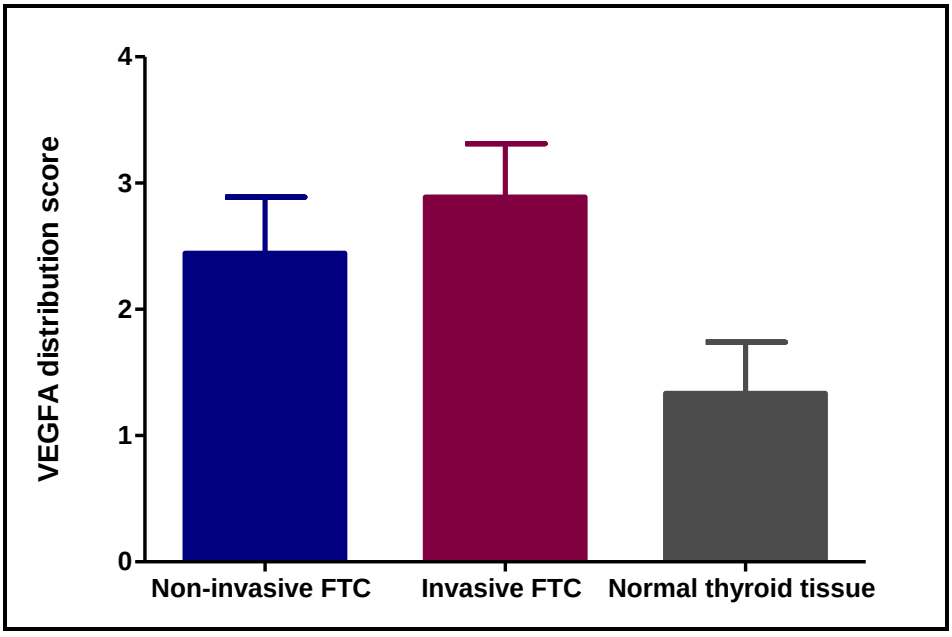

Figure 3-11 Staining distribution scores for VEGFA in non-invasive and invasive follicular thyroid carcinoma (FTC) and normal thyroid tissue

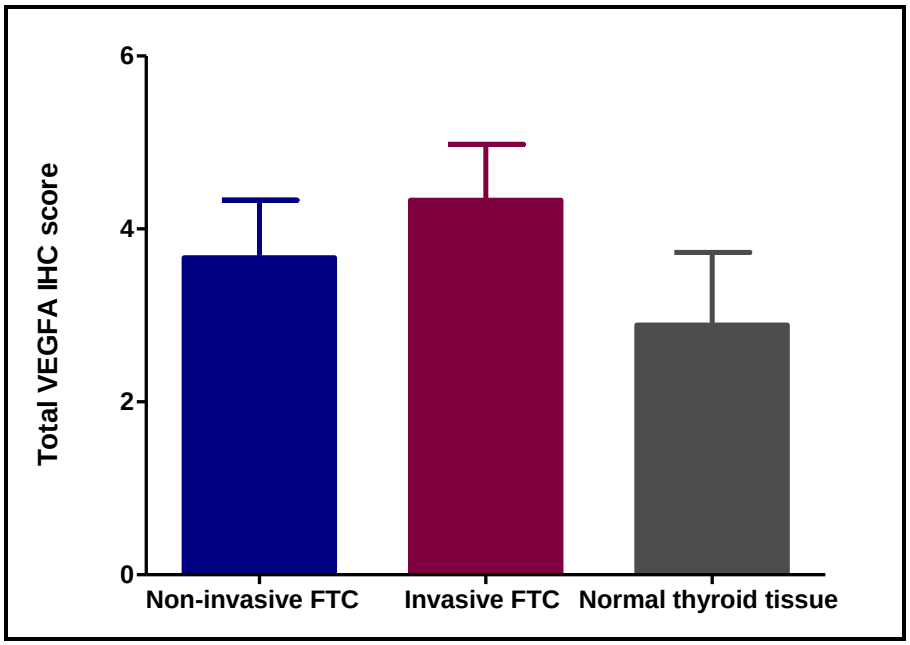

Figure 3-12 Total IHC scores for VEGFA in non-invasive and invasive follicular thyroid carcinoma (FTC) and normal thyroid tissue

There was no significant difference among groups for intensity of staining and total IHC score, however there was an increasing trend from normal thyroid tissue to non-invasive FTC and then to invasive FTC (Figures 3-10; 3-12). Invasive FTC had significantly higher distribution of staining than healthy thyroid tissue but neither group was different from non-invasive FTC (Table 3-4; Figure 3-11). While most positive tissues showed a diffuse pattern of staining, the normal tissues that were VEGFA positive showed regional patchy staining with several areas of the tissue having no evidence of reactivity.

Table 3-4 Comparison of VEGFA staining between non-invasive and invasive follicular thyroid carcinoma and normal thyroid tissue

Category	Groups compared	p-value
VEGFA staining intensity	Non-invasive *vs* healthy Invasive vs healthy Non-invasive vs invasive	0.7470 0.8912 0.4661
VEGFA staining distribution	Non-invasive *vs* healthy Invasive vs healthy Non-invasive vs invasive	0.1083 0.0205 0.3809
VEGFA total IHC score	Non-invasive *vs* healthy Invasive vs healthy Non-invasive vs invasive	0.5222 0.2413 0.3830

There was no correlation between the protein expression of osteopontin and that of VEGFA. The protein expression of osteopontin showed a strong correlation with patient age (Table 3-5) but no correlation with gender or tumor size. There was also a strong correlation between osteopontin protein expression and gene expression. There was no correlation between VEGFA protein expression and patient age, gender, tumor size or tissue gene expression.

Table 3-5 Correlation between osteopontin and VEGFA protein expression and patient parameters

Variable 1	Variable 2	r sq value	p-value
Osteopontin protein expression	Osteopontin gene expression	0.746	0.000008
	Age	0.664	0.0002
	Gender	-0.311	0.115
	Tumor size	0.368	0.132
VEGFA protein expression	VEGFA gene expression	-0.184	0.358
	Age	0.300	0.128
	Gender	-0.034	0.865
	Tumor size	0.043	0.866
	Osteopontin protein expression	0.340	0.083

DISCUSSION

Osteopontin plays an important role in the functioning of normal epithelial cells as well as the survival and progression of neoplastic cells. Osteopontin and VEGFA are known to work synergistically in the progression of aggressive human tumors[146] but their role has not been studied in canine FTC, a tumor that is known to be aggressive and highly vascular. In order to understand the significance of our gene expression data, we examined how the proteins were expressed in tissues from the same patient groups. Over-expression of osteopontin protein has been demonstrated in tissues from human thyroid cancer[152]. In that study, the intensity of osteopontin immunoreactivity showed an increasing trend from normal thyroid tissue to benign and malignant thyroid tissue. Osteopontin was weakly expressed in a few normal thyroid tissues, and there was strong expression in papillary thyroid carcinomas. The authors noted that expression of osteopontin and carcinoembryonic antigen-related cell adhesion molecule 1 (CEACAM1) may be useful in diagnosis and management of human thyroid cancer.

The expression of osteopontin protein in the present study was weak in two normal thyroid tissues and weak to moderate in tumor tissues. In most cases the staining was diffuse but more intense in epithelial cells directly lining the follicles. Tumor tissues therefore expressed osteopontin protein at higher levels and in a larger percentage of cells than normal thyroid tissues. Compared to the positive control, no tissues had strong staining and this may reflect osteopontin's secretive properties. There was no significant difference in osteopontin protein expression between non-invasive and invasive FTC. This finding concurred with the previously determined gene expression data[159]. Osteopontin mRNA was significantly up-regulated in both non-invasive and invasive FTC compared to normal thyroid tissue, with fold changes of 22.9 and 14.3 respectively. No difference was observed between the tumor groups.

One of osteopontin's up-stream regulators, VEGFA, showed no significant difference in intensity and total IHC scores among the three study groups. This was in agreement with previous gene expression data, however in both studies there was an increasing trend from normal thyroid tissue to non-invasive FTC and invasive FTC. The lack of significance is partly explained by the fact that there was strong VEGFA expression in four of the normal thyroid tissues. These four dogs were all two years old and increased VEGFA expression may be a response to areas of hypoxia within the thyroid gland, possibly related to development. There is not enough evidence to reasonably determine whether there was a true age effect. There was a significant difference in the distribution of the protein in invasive FTC tissues compared to normal thyroid tissue. This might suggest that the invasive tumors developed new vasculature over a wider area than non-invasive tumors increasing the ability of tumor cells to enter blood vessels.

Protein expression in the present study may have been influenced by different factors. Microscopic analysis of tumor tissues showed various stages of development and differences in the percentage of follicles that could be recognized even within a study group. It is possible that tumors with mixed follicular characteristics have different protein expression than those that are purely follicular. A larger sample size is necessary

to examine this further. Additionally, tumors were categorized as non-invasive and invasive based only on histopathological evidence of tumor cells in blood vessels. Other factors may need to be taken into account in determining these categories.

There was a strong correlation between osteopontin protein expression (total IHC score) and the gene expression determined in the previous study. Therefore tissues expressing the gene at high levels also expressed the protein at relatively high levels despite not having strong staining intensity. The correlation of osteopontin protein expression with age of the patient was an unexpected finding since invasive FTC showed an increasing trend of protein expression compared to non-invasive FTC, and patients with non-invasive FTC tended to be older than patients with invasive FTC. Finally, the fact that VEGFA had high expression in four normal tissues and there was only weak osteopontin staining in two normal tissues, might explain why there was no correlation between osteopontin and VEGFA protein expression.

CONCLUSIONS

Non-invasive and invasive canine FTC express higher levels of osteopontin protein than normal thyroid tissue. There is no difference in osteopontin protein expression between non-invasive and invasive FTC. Normal thyroid tissue may express high levels of VEGFA suggesting localized responses to hypoxia and/or development in younger dogs.

CHAPTER 4

PLASMA OSTEOPONTIN AND VEGFA CONCENTRATION IN DOGS WITH FOLLICULAR THYROID CARCINOMA COMPARED TO NORMAL DOGS

Osteopontin and VEGFA often work synergistically to enhance angiogenesis, invasion and metastasis in aggressive carcinomas. We have previously demonstrated that osteopontin gene and protein expression is higher in dogs with follicular thyroid carcinoma (FTC) than in normal dogs. The goals of the present study were (1) to determine plasma concentrations of VEGFA and osteopontin in dogs diagnosed with FTC and compare them to clinically healthy dogs; and (2) to compare the plasma levels of these proteins before and after surgical resection of the tumor. Blood samples were collected from prospective cases and matched controls. Proteins were measured using commercially available canine-specific ELISA kits. Both VEGFA and osteopontin had significantly higher plasma concentrations in dogs with FTC compared to healthy dogs. Some of these cases showed decreased levels after surgery. This study justifies further research to determine how these findings can be used in the diagnosis and management of canine FTC.

INTRODUCTION

Canine follicular thyroid carcinoma (FTC) is relatively uncommon and has not been extensively studied. The incidence of thyroid tumors in dogs is approximately 1-4%[10,11,12,13] and they are more likely to be malignant tumors of follicular origin[61]. The molecular basis of their rapid growth and aggressive nature warrant investigation, particularly since, as in humans, histopathological classification by itself is not a good predictor of biological behavior or prognosis[84,129]. In addition, there are many challenges associated with management of invasive cases including side effects of radiation therapy and surgical complications such as excessive hemorrhage.

We previously demonstrated that 247 up-regulated and 242 down-regulated genes distinguish FTCs from normal thyroid tissue. The gene osteopontin was consistently expressed at high levels in FTC and very low levels in normal tissue samples[159]. Compared to normal thyroid tissue, its expression in non-invasive (tumors with only capsular invasion) and invasive (tumors with capsular and vascular invasion) FTC was 22.9 and 14.3 times higher respectively. Immunohistochemical analysis of the same tissues revealed a strong correlation between gene and protein expression. Both osteopontin and VEGFA are secreted into the bloodstream and there is a previously described relationship between them that enhances angiogenesis-driven tumor progression[146,161]. They both act directly in the lumen of blood vessels to induce migration and proliferation of endothelial cells one of the primary roles of VEGFA[136-138].

Our previous data revealed that VEGFA gene and protein expression were similar in FTC and normal thyroid tissues. Some human studies have reported that plasma VEGF levels in cancer patients were significantly higher than in controls and in some cases predicted survival and response to therapy[162-168].

Osteopontin is secreted from tumor cells and can be detected in blood, urine and seminal fluid[151]. It is over-expressed in the tissues of human papillary thyroid carcinoma and induces invasion in *in vitro* models[135,152]. Human studies have also found higher levels of serum and plasma osteopontin concentrations in patients with different types of cancers and are investigating it as a means of detecting disease and monitoring progress[140,153-158,169].

In the present study, we sought to determine the difference in plasma osteopontin and VEGFA concentration between normal dogs and dogs diagnosed with FTC before and after surgical excision of the tumor. We hypothesized that plasma osteopontin and VEGFA was higher in dogs diagnosed with FTC compared to normal dogs and that among the FTC cases the post-surgical concentrations of these proteins will be lower than the pre-surgical concentrations.

METHODS

Case selection and experimental design

Cases were recruited from the University of Minnesota Veterinary Teaching Hospital, with client participation based on informed consent. Based on sample size analysis using SAS® statistical software (version 9.1), a minimum of 10 samples were required at a significance of 0.05 and power of 0.8. Blood samples were collected from prospective FTC cases at the time of a tentative diagnosis and included in the study based on histopathological confirmation of FTC. For cases that had surgical resection of the thyroid tumor, a second blood sample was obtained two weeks after surgery (at the time of suture removal). Dogs presenting for annual physical exams and/or vaccines were recruited as normal controls. They were matched to the FTC cases by age and gender. Dogs were excluded as normal controls if there was evidence of thyroid disease, tumors or other diseases on history or physical examination.

Sample processing

Three to five ml of blood were collected by jugular venipuncture and placed in a blood tube containing EDTA. Samples were centrifuged immediately after collection at 1000g for 15 minutes at room temperature. Plasma was extracted and stored in cryovials at -80°C. Samples with gross hemolysis were excluded from the assay.

Osteopontin ELISA protocol

Plasma osteopontin concentration was measured using a canine-specific ELISA (Uscn Life Science Inc, Wuhan). It is a sandwich enzyme immunoassay designed for use in research as a quantitative measurement of canine osteopontin in plasma and other biological fluids. A standard curve was evaluated by measuring absorbance of seven different dilutions of the standard diluent. Plasma samples were diluted 10-fold for the assay and run in duplicate. The microtiter plates contained wells that were pre-coated with a biotin-conjugated polyclonal antibody specific to osteopontin. Seven wells were

designated for use with the standards, one for a blank and the remaining for the test samples. These were all incubated for two hours at 37°C after which the liquid was removed from each well. Avidin conjugated to Horseradish Peroxidase was added to each well and incubated, followed by TMB substrate solution incubated for 25 minutes and protected from light. At this step, wells containing canine osteopontin, biotin-conjugated antibody and enzyme-conjugated Avidin exhibited a color change from colorless to blue. The enzyme-substrate reaction was terminated by adding a sulphuric acid Stop solution to each well, at which time a yellow color was noted. All samples were measured spectrophotometrically at a wavelength of 450nm. The value for any particular sample was the mean of the duplicated samples. Osteopontin concentration was determined by comparing the optical density of samples to the standard curve.

VEGFA ELISA protocol

Plasma VEGFA concentration was measured using the Procarta cytokine assay (Affymetrix® Inc, Santa Clara, California). The kit is based on Luminex technology with canine-specific standard buffers and assay buffers. A standard curve was prepared as instructed in the protocol using eight dilutions. Columns one and two were reserved for duplicate standards and the other columns for test samples. The filter plate was pre-wet by adding reading buffer, then incubated for five minutes and cleared. Antibody beads were added to each well, washed with wash buffer, and then removed by vacuum filtration. Standards and samples were added to their designated wells and the plate was shaken at 500 rpm for 60 minutes. Solution was removed by vacuum filtration and the wells were washed with wash buffer. The detection antibody was added to each well followed by the biotinylated secondary antibody and streptavidin-PE. After each of these three steps, the plate was shaken at 500 rpm for 30 minutes followed by vacuum filtration and rinsing with wash buffer. Reading buffer was then added to each well and the plate was shaken at 500 rpm for 15 minutes. The plate was immediately read on the Luminex machine.

Data analysis

Mean plasma osteopontin and VEGFA concentrations for clinically healthy dogs and dogs with FTC were compared using a two-sample t-test, $\alpha = 0.05$. Relative operating characteristic (ROC) curves were constructed to evaluate the sensitivity and specificity of osteopontin and VEGFA ELISA tests for detection of dogs with FTC.

RESULTS

Osteopontin

Validation of the osteopontin ELISA kit was performed by the manufacturer using a control canine population. In this population the plasma osteopontin ranged from 4.78 to 23.45 ng/ml. In the present study, the kit performed with a sensitivity of 0.64 ng/ml. Plasma samples from 10 cases and 10 age and gender matched normal controls were available for analysis. The plasma osteopontin concentration in healthy dogs ranged from 6.5 to 25.2 ng/ml. Nine of these samples were within the range of the control population used by the manufacturer for validation. The concentration in FTC samples was more variable and ranged from 9.6 to 66.5 ng/ml; six of these samples were greater than 20 ng/ml. The mean FTC plasma concentration was significantly higher than the mean concentration for normal patients (Table 4-1; Figure 4-1).

Table 4-1 Mean osteopontin and VEGFA plasma concentrations in normal dogs and dogs with follicular thyroid carcinoma before surgery

Patient group	**Mean plasma concentration ± SEM**	
	VEGFA (pg/ml); n =8	Osteopontin (ng/ml); n = 10
FTC Healthy	32.91 ± 5.578 16.18 ± 2.585	28.79 ± 5.928 13.68 ± 1.812
p-value	0.0165	0.0254

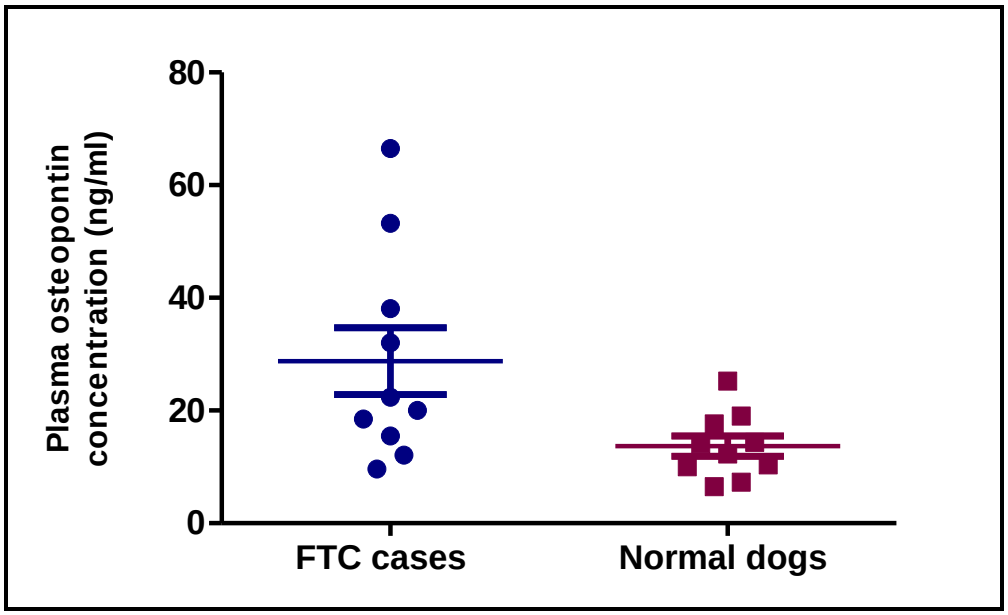

Figure 4-1 Plasma osteopontin concentration in dogs with follicular thyroid carcinoma and normal dogs

Pre- and post-surgical osteopontin data are available for five FTC cases. The post-surgical plasma concentration in three cases decreased by 23, 55 and 57% respectively. For two of these cases, the pre-surgical and post-surgical concentrations were within the range recorded by normal controls. The third case had a pre-surgical concentration that was significantly higher than the normal samples, but this decreased to within the normal range after surgery. Two cases had plasma osteopontin concentrations that increased by 9 and 21% respectively after surgery. In both cases the pre- and post-surgical concentrations were within the range recorded by normal controls.

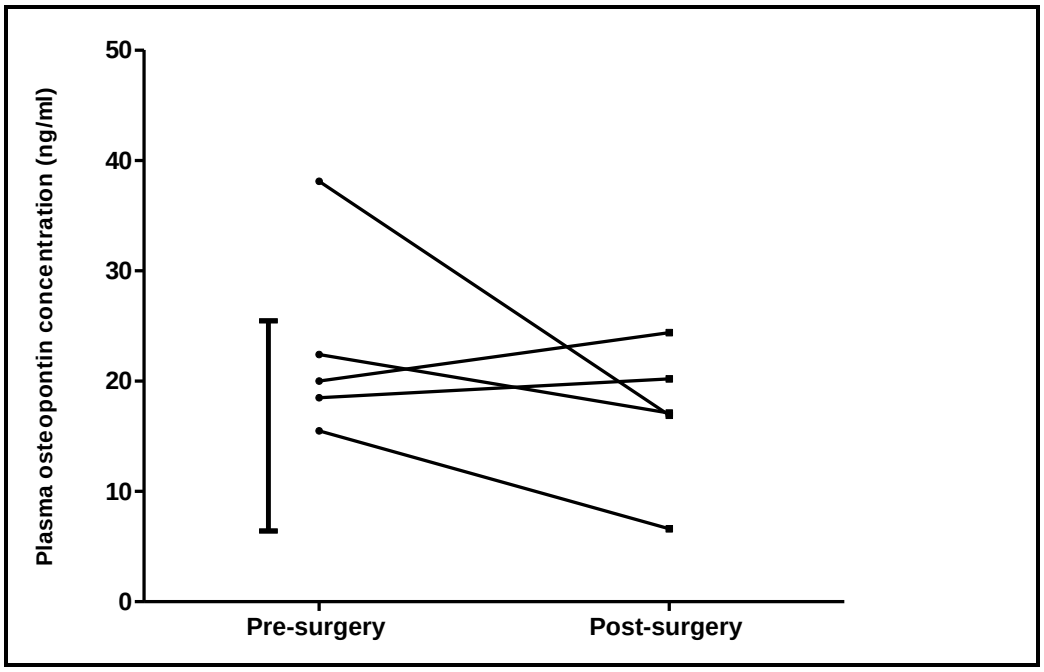

Figure 4-2 Plasma osteopontin concentration in follicular thyroid carcinoma cases at the time of diagnosis (pre-surgery) and two weeks after thyroidectomy (post-surgery). The vertical line represents the concentration range among normal controls

VEGFA

The VEGFA ELISA kit performed with a sensitivity of 4.0 pg/ml. Within the allocated time period, it was possible to recruit only eight FTC cases. Plasma samples from these cases were analyzed as well as 8 samples from age and gender matched healthy controls. Among the FTC samples, plasma VEGFA concentration ranged from 8.2 - 49.2 pg/ml and healthy samples ranged from 2.5 - 28.4 pg/ml. The mean FTC plasma concentration was significantly higher than the mean concentration for healthy patients (Table 4-1; Figure 4-3).

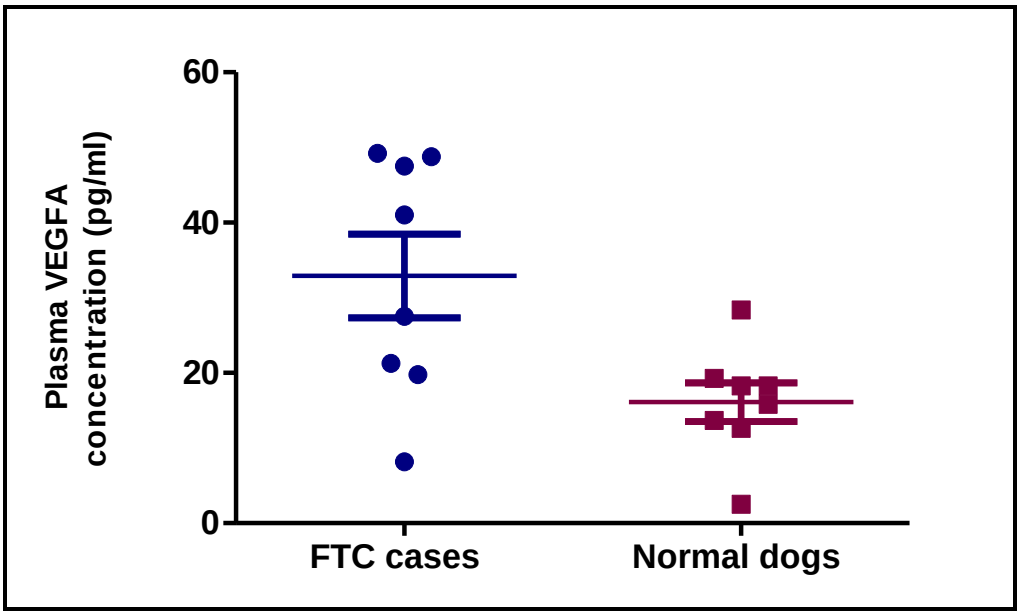

Figure 4-3 Plasma VEGFA concentration in dogs with follicular thyroid carcinoma and normal dogs

Pre- and post-surgical VEGFA data are available for four FTC cases. The post-surgical plasma concentration in three cases decreased by 4, 25, and 30% respectively (Figure 4-4). For two of these cases the pre- and post-surgical concentrations were higher than the range recorded by normal controls. The third case recorded pre- and post-surgical concentrations within the normal range. The plasma VEGFA concentration of the fourth case was the same both before and after surgery and these values were within the normal range.

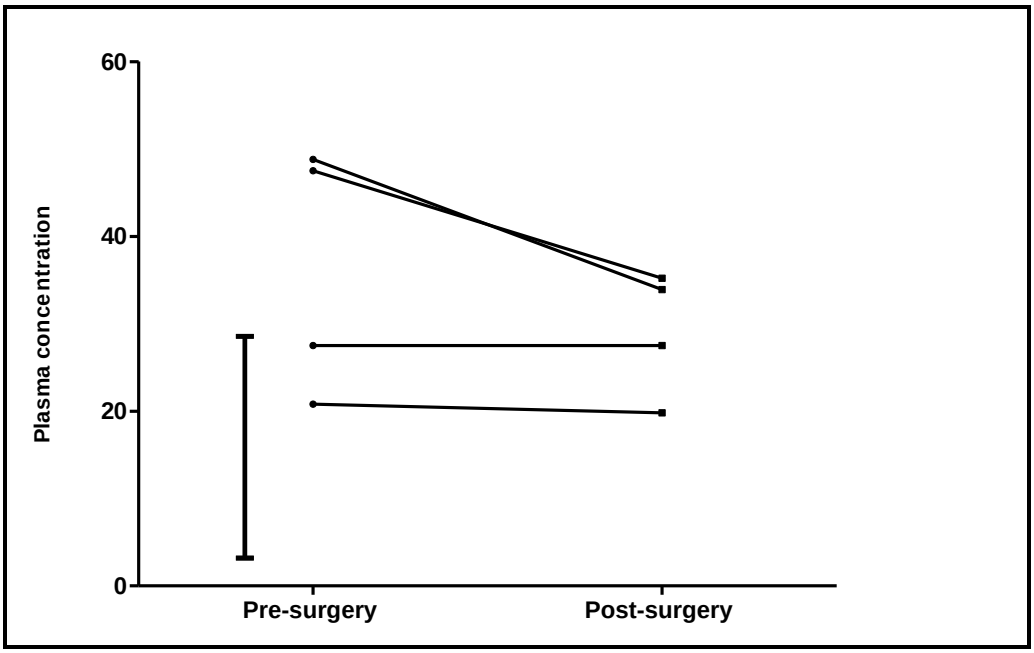

Figure 4-4 Plasma VEGFA concentration in follicular thyroid carcinoma cases at the time of diagnosis (pre-surgery) and two weeks after thyroidectomy (post-surgery) The vertical line represents the concentration range among normal controls

Sensitivity and specificity

There was some degree of overlap with respect to plasma osteopontin concentrations between the two study groups (normal dogs and dogs with FTC). The sensitivity and specificity of the assay varied according to the concentration cut-off point examined (Table 4-2; Figure 4-5). At higher sensitivities (greater than 90%), the specificity was very low and at higher specificities, the sensitivity was low. The test performed optimally at a cut-off point greater than 18.05 ng/ml. At this point, the sensitivity was 70% and the specificity was 80%.

Table 4-2 Sensitivity and specificity of the canine osteopontin ELISA for identification of dogs with follicular thyroid carcinoma at different concentration cut-off points

OPN concentration (ng/ml)	Sensitivity	95% CI	Specificity	95% CI
> 6.900	1.0	0.6915 to 1.000	0.1	0.0025 to 0.4450
> 8.450	1.0	0.6915 to 1.000	0.2	0.0252 to 0.5561
> 9.800	0.9	0.5550 to 0.9975	0.2	0.0252 to 0.5561
> 10.20	0.9	0.5550 to 0.9975	0.3	0.0667 to 0.6525
> 11.25	0.9	0.5550 to 0.9975	0.4	0.1216 to 0.7376
> 12.20	0.8	0.4439 to 0.9748	0.4	0.1216 to 0.7376
> 13.20	0.8	0.4439 to 0.9748	0.5	0.1871 to 0.8129
> 14.25	0.8	0.4439 to 0.9748	0.6	0.2624 to 0.8784
> 14.95	0.8	0.4439 to 0.9748	0.7	0.3475 to 0.9333
> 16.55	0.7	0.3475 to 0.9333	0.7	0.3475 to 0.9333
> 18.05	0.7	0.3475 to 0.9333	0.8	0.4439 to 0.9748
> 18.75	0.6	0.2624 to 0.8784	0.8	0.4439 to 0.9748
> 19.50	0.6	0.2624 to 0.8784	0.9	0.5550 to 0.9975
> 21.20	0.5	0.1871 to 0.8129	0.9	0.5550 to 0.9975
> 23.80	0.4	0.1216 to 0.7376	0.9	0.5550 to 0.9975
> 28.60	0.4	0.1216 to 0.7376	1.0	0.6915 to 1.000
> 35.05	0.3	0.0667 to 0.6525	1.0	0.6915 to 1.000
> 45.65	0.2	0.0252 to 0.5561	1.0	0.6915 to 1.000
> 59.85	0.1	0.0025 to 0.4450	1.0	0.6915 to 1.000

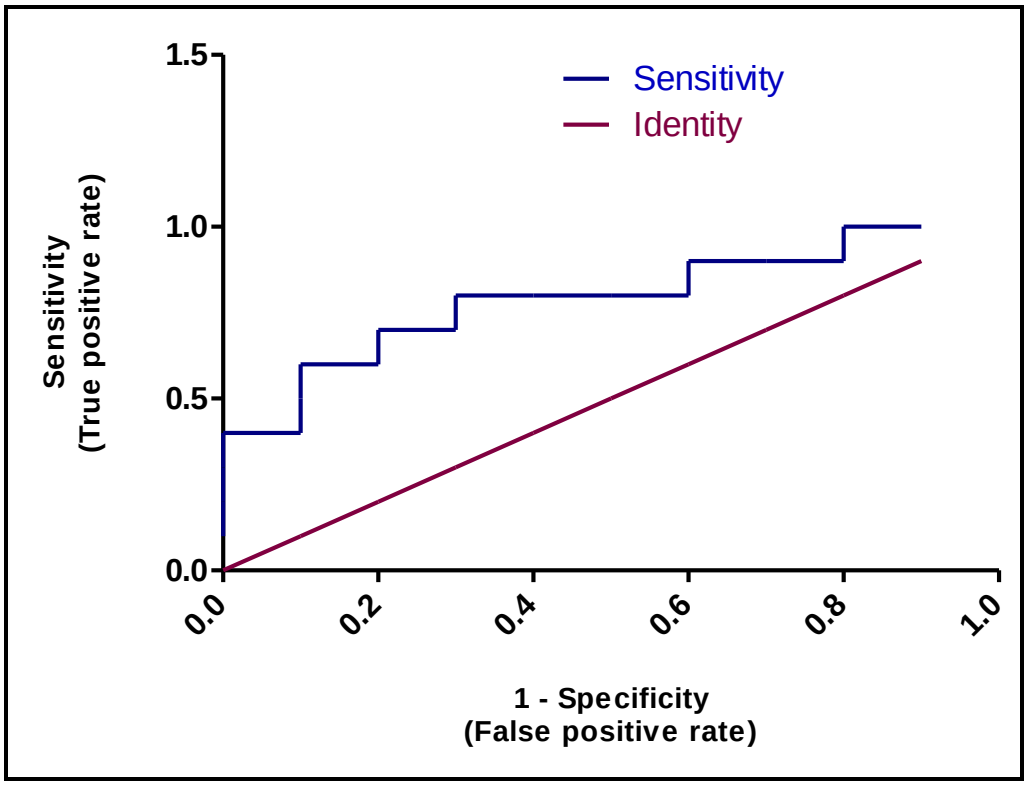

Figure 4-5 ROC curve showing the rate of true positives (follicular thyroid carcinoma cases with elevated plasma osteopontin) against false positives (normal cases with elevated osteopontin)

The identity line represents the point at which the test is unable to distinguish between the two study groups

The plasma VEGFA concentrations also overlapped between the two study groups. The sensitivity and specificity trends of the canine VEGFA assay were similar to that of the canine osteopontin assay (Table 4-3; Figure 4-6). The test performed optimally at a cut-off point greater than 19.55 pg/ml. At this point, the sensitivity and specificity were both 87.5%.

Table 4-3 Sensitivity and specificity of the canine VEGFA ELISA for identification of dogs with follicular thyroid carcinoma at different concentration cut-off points

VEGFA concentration (pg/ml)	Sensitivity	95% CI	Specificity	95% CI
> 5.350	1.000	0.6306 to 1.000	0.125	0.0032 to 0.5265
> 10.40	0.875	0.4735 to 0.9968	0.125	0.0032 to 0.5265
> 13.15	0.875	0.4735 to 0.9968	0.250	0.0318 to 0.6509
> 14.75	0.875	0.4735 to 0.9968	0.375	0.0852 to 0.7551
> 17.05	0.875	0.4735 to 0.9968	0.500	0.1570 to 0.8430
> 18.80	0.875	0.4735 to 0.9968	0.750	0.3491 to 0.9681
> 19.55	0.875	0.4735 to 0.9968	0.875	0.4735 to 0.9968
> 20.55	0.750	0.3491 to 0.9681	0.875	0.4735 to 0.9968
> 24.40	0.625	0.2449 to 0.9148	0.875	0.4735 to 0.9968
> 27.95	0.500	0.1570 to 0.8430	0.875	0.4735 to 0.9968
> 34.70	0.500	0.1570 to 0.8430	1.000	0.6306 to 1.000
> 44.25	0.375	0.0852 to 0.7551	1.000	0.6306 to 1.000
> 48.15	0.250	0.0318 to 0.6509	1.000	0.6306 to 1.000
> 49.00	0.125	0.0032 to 0.5265	1.000	0.6306 to 1.000

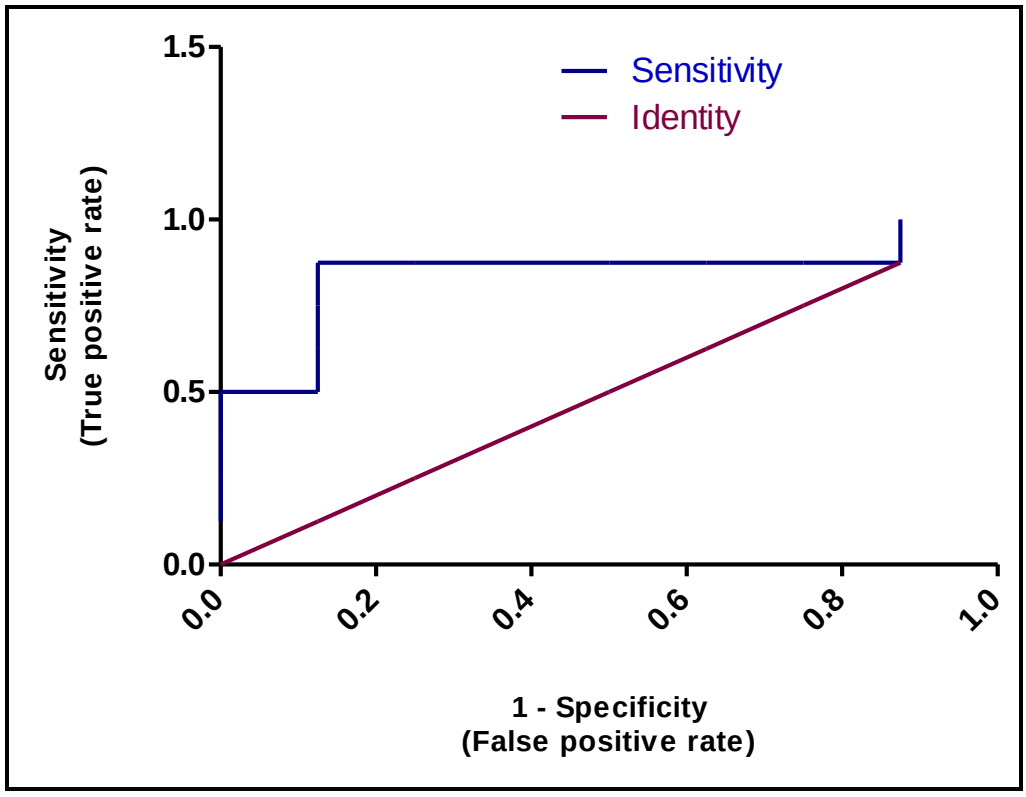

Figure 4-6 ROC curve showing the rate of true positives (follicular thyroid carcinoma cases with elevated plasma VEGFA) against false positives (normal cases with elevated VEGFA)

The identity line represents the point at which the test is unable to distinguish between the two study groups

DISCUSSION

Dogs with FTC often present with evidence of invasion to structures in the neck or other complications suggestive of metastasis[14,64]. Therefore many of these tumors are not detected at an early stage, and management options often involve surgical resection of the tumor, radiation therapy, chemotherapy or radioiodide therapy. All of these treatments can have risks and complications. It is therefore desirable to have a greater understanding of plasma protein indicators of disease that may aid in earlier detection and guide therapy. The goal of this study was to determine the plasma concentrations of VEGFA and osteopontin in dogs diagnosed with FTC and to compare them with that in clinically healthy (normal) dogs. Both proteins can be measured in serum and plasma but

studies have shown that plasma values are more reliable and of greater diagnostic value[163,170,171].

In the current study, we demonstrated that the plasma concentration of both VEGFA and osteopontin are significantly higher in dogs diagnosed with FTC than clinically healthy dogs. For osteopontin, this trend correlated with the gene expression previously determined by quantitative PCR and the protein expression determined by immunohistochemistry. With respect to VEGFA, the previous studies found no difference in gene and protein expression between tumor tissues and healthy thyroid. In those cases, normal thyroid tissues expressed VEGFA at levels comparable to the tumor tissues. It is unclear to what extent the age of the controls influenced that result as healthy controls were much younger than the FTC cases. In this study, however, controls were matched to cases by age and gender and there is confidence that the differences are in fact significant.

The plasma concentrations before and after surgery were compared. In the case of VEGFA, three cases decreased by 4, 25, and 30% respectively while a fourth case showed no change in concentration. For osteopontin, three cases decreased by and 23, 55, and 57% respectively; however two cases increased by 9 and 21% respectively. It is possible that cases which showed increased concentrations after surgical removal of the tumor may have had metastatic lesions that went undetected, since many of these cases did not have full imaging evaluations. At optimal performance, the canine osteopontin assay had a sensitivity of 70% and a specificity of 80%. The relatively low sensitivity is reflected in the fact that some dogs with FTC had a plasma osteopontin concentration that was comparable to normal dogs. Additionally, the variability in concentrations among FTC cases may be due to different tumor sizes and stages. The test was more accurate at identifying healthy dogs as most normal controls had low concentrations. For VEGFA, the assay had a relatively high sensitivity and specificity (87.5%) at optimal performance. However there was some overlap between the two study groups. It must be considered that the sample size was very small and may not have been sufficient to detect significant differences in a population of dogs that is so diverse and with tumors that are at different

stages. In the case of VEGFA, the minimum of 10 cases per group was not obtained due to time limitations. A larger sample size will likely yield results that are more clinically applicable.

Another important point is that the biological behavior of osteopontin in canine peripheral blood is unclear, therefore we are unsure whether the two-week post-surgical timepoint was appropriate. This timepoint was chosen since it was convenient to collect the second blood sample when clients returned with their dogs for suture removal and it was prior to initiation of adjunctive treatments (radiation or chemotherapy). It would be ideal to obtain serial blood samples to monitor the patterns until death of the dog. In the breast cancer study[140], blood samples were taken at the time of diagnosis and post-therapy samples at designated intervals until the patients died. These data revealed that pre-treatment osteopontin levels were strong indicators of clinical outcome and survival time. High levels consistently identified patients with poor prognosis and shorter survival times. Additionally, plasma levels decreased post-therapy, increased again when tumors recurred or metastases were detected, and were highest just prior to death.

Opportunities for further work in our research therefore include evaluation of serial plasma samples and monitoring progress over a longer period of time. A long term goal of this study is to correlate the findings with clinical outcome, recurrence and survival time in these dogs. Finally, in order to determine the specificity of osteopontin, it may be necessary to evaluate plasma levels in other canine carcinomas.

CONCLUSIONS

VEGFA and osteopontin can be accurately measured in the plasma of dogs. Plasma concentrations of VEGFA and osteopontin are higher in dogs diagnosed with FTC compared to age and gender matched healthy controls. In some cases, levels decreased after surgical resection of the tumor. This can be better evaluated using a larger sample size and serial blood samples.

CHAPTER 5

CONCLUSIONS AND FUTURE DIRECTIONS

Canine FTC is the most common head and neck tumor in dogs and it is highly aggressive. It is important to gain an understanding of the molecular characteristics of these tumors in order to investigate means of early detection and monitoring. The sequence of the tumor suppressor gene p53 was studied in tissues from dogs with follicular tumors[99]. However, a single base pair mutation was noted in only one case. In another study, the expression of thyroid transcription factor-1 was noted in neoplastic thyroid tissue but also in pulmonary carcinomas, therefore it was difficult to differentiate between neoplastic lung tissue and metastatic thyroid tissue[56]. In the present study a genome-wide approach identified 489 differentially expressed transcripts, 242 of which were down-regulated and 247 up-regulated in FTC compared to normal thyroid tissue. Although this is a considerable number of genes, when categorized by functional analysis, it was noted that processes important to cancer progression were significantly up-regulated, including cell differentiation, signaling, transcription/translation regulation, cell cycle regulation, angiogenesis, and regulation of apoptosis.

The gene osteopontin was selected for further analysis for four reasons. First, there was a large fold difference between FTC and normal by microarray analysis (fold change 134). Second, all tumor samples consistently recorded high expression values and all normal samples recorded very low expression values. Third, the functional importance of osteopontin was established by examining its relevance to the canine FTC data set by pathway analysis. Finally, osteopontin is significantly up-regulated in human thyroid carcinoma tissues, and an *in vitro* model demonstrated its role in promoting cellular invasion[135]. There were similarities noticed in the results of this study and our findings in dogs. In the present study, the gene expression of osteopontin was validated by quantitative PCR and the protein expression validated by immunohistochemistry. Non-invasive and invasive thyroid carcinomas expressed osteopontin at higher levels

than normal thyroid tissues. The gene and protein expression of its upstream regulator, VEGFA, was not different among groups mainly because some normal cases expressed high levels of VEGFA protein in their tissues. It is unclear the extent to which there was a true age effect in this analysis. Dogs diagnosed with FTC had an average age of 10.1 years while the average age of normal dogs was 1.75 years. These control dogs were readily available as they were utilized in student laboratory sessions and were therefore euthanized for reasons unrelated to the study. It is likely that very young dogs may experience periods of thyroid gland proliferation unrelated to any pathological changes. All affected and normal dogs were represented by different breeds and there was an equal distribution of males and females. Interestingly, 22% of cases were Golden Retrievers, consistent with previous reports of this breed being over-represented in epidemiological studies[9-12].

There was no difference in osteopontin gene and protein expression between non-invasive and invasive FTC. Since osteopontin and VEGFA are directly related to angiogenesis and invasion of tumor cells, it was expected that invasive tissues would have higher expression of these two molecules than the non-invasive tumors. The criterion for placing tumors into these two categories was whether there was documented evidence of vascular invasion based on histopathology reports. Histopathology sections were from small areas of the tumor and may not be representative of the entire tumor. Therefore some tumors that were listed as non-invasive may actually have invasive properties and vice versa. Not all cases were completely staged; therefore there was not enough information on whether there might have been evidence of invasion or metastasis to other tissues. Some lymph node aspirates were non-diagnostic due to the presence of large amounts of blood. Serum T_4 and TSH were only available for a few cases; with more data it would be interesting to note how these parameters affect the protein expression since TSH impacts follicular cell hypertrophy and also has a role in inducing VEGF[112].

Additionally if a tumor on physical examination is fixed to underlying tissue, it is generally assumed that it is locally invasive (in the absence of confirmation by imaging

modalities). For six cases histopathologicallly classified as non-invasive, veterinarians reported that three of them were fixed and three were freely movable. For six cases classified as invasive, it was reported that none of them were fixed. It must be considered however that fixed tumors may reflect fibrous adhesions in the absence of true neoplastic invasion. Also, there may be micrometastases or early invasion of tumor cells to surrounding structures without gross evidence of fixation. Of nine non-invasive tumors, surgeons reported complete excision in five cases and for the other four cases it was uncertain. Of nine invasive tumors, complete excision was reported in three cases; marginal excision was reported in two cases; two cases were uncertain; and for two cases the surgeon was certain that there was not complete excision. It is also possible that within any tumor there exists a localized area that expresses markers of invasiveness, for example at the invasive front and that other areas of the tumor are not yet primed for this activity. This also applies to tumors that are heterogeneous in nature. It is unclear at what point the increased expression of osteopontin is turned on in these neoplastic cells. With respect to histopathological characterization of canine FTCs, there is need for more specific categories based on degree of invasion that is similar to those in humans.

Both VEGFA and osteopontin are proteins that are secreted into the bloodstream. This in part reflects their site of action in promoting angiogenesis. VEGFA directly stimulates proliferation of endothelial cells and this function is supported by osteopontin in neoplastic conditions. The finding that both proteins were increased in the plasma of dogs with FTC compared to matched healthy controls was therefore expected. A larger sample size is required to appreciate true changes in protein levels after surgical removal of the tumor. Also, serial blood samples should be evaluated until the death of the dogs. In the breast cancer study, serial sampling was very useful in monitoring response to treatment and clinical outcome. This is an opportunity for further work with the ultimate goal of determining how plasma VEGFA and osteopontin correlate with survival time in dogs and recurrence of tumors. There is need however for complete staging and imaging particularly to determine whether there is evidence of metastasis. In some cases this might be difficult as micrometastases are not easily detected and clinical indications of

metastatic lesions in the brain and bones are often found when the disease has progressed considerably. Since histopathology by itself does not dictate clinical outcome[61,73], the expression of osteopontin can be eventually used as a criterion in determining prognosis. Before this can be implemented, however, we need to evaluate more dogs from the time of diagnosis until death and appreciate how osteopontin expression changes with the course of the disease. These trends can then be applied to prospective cases.

Finally, in dogs follicular thyroid carcinoma is the most commonly diagnosed thyroid tumor and papillary carcinomas (PTCs) are rarely identified. In contrast, papillary carcinomas are more likely in humans, and follicular carcinomas are less commonly encountered. In the human thyroid tumor studies over-expression of osteopontin, was reported mainly in papillary carcinomas. According to the literature, there is a subtle difference between FTCs and PTCs. Papillary carcinomas generally have a follicular growth pattern and differ from FTCs by the presence of overlapping nuclei with invaginations and a ground-glass cytoplasmic appearance[23,50]. Papillary tumors may also have cells similar to compact tumors[49]; in our study, some of the tumors were mixed follicular-compact. It may be possible that canine FTC has molecular similarity to human PTC. But it is also likely that PTCs in dogs are under-diagnosed. Also, the cases in the present study were identified as having cells of follicular origin. Further investigation of osteopontin expression and plasma concentration in different tumor types may yield information on whether these tests can be used adjunctively to differentiate FTC and PTC in dogs. We considered the possibility that other cell types in the tumor may contribute to its gene and protein expression. In some cases tumor cells of medullary carcinomas are difficult to differentiate from those of compact follicular tumors[30,55]. The ultimate solution to this is the use of laser microdissection of tissues to separate the true follicular tumor cells from surrounding cells. This was not possible in our study. As an alternative, the program used for microarray analysis (Expressionist® analyst) included a step for 'virtual dissection'. In this case, the genes that were not directly related to tumor initiation and progression, for example those that were

characteristic of secondary lymphocytic infiltration, were excluded. This can also be applied to rule out other types of thyroid tumors.

The findings of this study provide justification for further analysis of osteopontin expression in dogs with FTC and its impact on identification of disease, biological behavior of the tumor and clinical course. The usefulness of VEGFA may also be evaluated since our findings indicate that its concentration in plasma also differentiated some dogs with FTC from normal dogs. In the long term, since we have seen similarities in osteopontin expression with human papillary carcinomas, the dog might be useful as a model of human disease.

REFERENCES

1. Hullinger RL. The endocrine system. In: Evans HE; *Miller's Anatomy of the Dog* 3rd ed. Pennsylvania: WB Saunders & Co; 1993. p. 567-571.

2. Anderson WD, Anderson BG. *Atlas of canine anatomy*. Pennsylvania: Lea & Febiger; 1994. p. 382.

3. Hadley ME, Levine JE. *Endocrinology, 6th ed*. New Jersey: Pearson Prentice Hall;2007. p. 293-314.

4. Nunez EA, Belshaw BB, Gershon MD. A fine structural study of the highly active thyroid follicular cell of the African basenji dog. *Am J Anat*. 1972;133(4):463-481.

5. Roediger WE. A comparative study of the normal human neonatal and the canine thyroid C cell. *J Anat*. 1973;115(2):255-276.

6. Reece WO. *Functional anatomy and physiology of domestic animals* 4th ed. Iowa: Wiley-Blackwell; 2009. p. 165-167.

7. Schenck PA. Calcium homeostasis in thyroid disease in dogs and cats. *Vet Clin Small Anim.* 2007;37:693-708.

8. Page RL. Tumors of the endocrine system. In: Withrow SJ, MacEwen EG (eds): *Small animal clinical oncology* 3rd ed. Pennsylvania: Saunders; 2001. p. 423-427.

9. Harari J, Patterson JS, Rosenthal RC. Clinical and pathologic features of thyroid tumors in 26 dogs. *J Am Vet Med Assoc*. 1986;188(10):1160-1164.

10. Hayes HM Jr, Fraumeni JF Jr. Canine thyroid neoplasms: epidemiologic features. *J Natl Cancer Inst*. 1975;55(4):931-934.

11. Wucherer KL, Wilke VL. Thyroid cancer in dogs: an update based on 638 cases (1995 – 2005). *J Am Anim Hosp Assoc*. 2010;46(4):249-254.

12. Brodey RS, Kelly DF. Thyroid neoplasms in the dog: a clinicopathologic study of fifty-seven cases. *Cancer*. 1968;22(2):406-416.

13. Leav I, Schiller AI, Rijnberk A, *et al*. Adenomas and carcinomas of the canine and feline thyroid. *Am J Pathol*. 1976;83(1):61-122.

14. Radlinsky MG. Thyroid surgery in dogs and cats. *Vet Clin Small Anim*. 2007;37:789-798.

15. Itoh T, Kojimoto A, Nibe K, *et al*. Functional thyroid gland adenoma in a dog treated with surgical excision alone. *J Vet Med Sci*. 2007;69(1):61-63.

16. Bezzola P. Thyroid carcinoma and hyperthyroidism in a dog. *Can Vet J*. 2002;43:125-126.

17. Feldman EC, Nelson RW. Canine thyroid tumors and hyperthyroidism. In: Feldman EC, Nelson RW, editors. *Canine and feline endocrinology and reproduction*, 3rd ed. St Louis: Saunders; 2004. p. 219-249.

18. Wang C, Crapo LM. The epidemiology of thyroid disease and implications for screening. *Endocrinol Metab Clin North Am*. 1997;26(1):189-218.

19. National cancer institute. Available at: http://www.cancer.gov/cancertopics/types/thyroid
20. Rosenbaum MA, McHenry CR. Contemporary management of papillary carcinoma of the thyroid gland. *Expert Rev Anticancer Ther*. 2009;9(3):317-329.
21. Maitra A, Abbas AK. The endocrine system. In: Kumar V, Abbas AK, Fausto N. *Robbins and Cotran Pathologic basis of disease, 7th ed.* Pennsylvania: Elsevier Saunders; 2005. 1525 p.
22. Turrel JM, McEntee MC, Burke BP, Page RL. Sodium iodide ^{131}I treatment of dogs with nonresectable thyroid tumors; 39 cases (1990-2003). *J Am Vet Med Assoc*. 2006;229(4):542-548.
23. Worth AJ, Zuber RM, Hocking M. Radioiodide (^{131}I) therapy for the treatment of canine thyroid carcinoma. *Aust Vet J*. 2005;83(4):208-214.
24. Enewold L, Zhu K, Ron E, *et al*. Rising thyroid cancer incidence in the United States by demographic and tumor characteristics, 1980 – 2005. *Cancer Epidemiol Biomarkers.* 2009;18(3):784-791.
25. Ries LAG, Melbert D, Krapcho M, *et al*. SEER Cancer Statistics Review, 1975 – 2005. Bethesda, MD: National Cancer Institute; 2008.
26. Ron E, Schneider AB. Thyroid cancer. In: Schottenfeld D, Fraumeni JF Jr, editors. *Cancer epidemiology and prevention, 3rd ed.* New York, NY: Oxford University Press; 2006. p. 975-994.
27. Hollowell JG, Staehling NW, Flanders WD, *et al.* Serum TSH, T(4), and thyroid antibodies in the United States population (1988 to 1994): National Health and Nutrition Examination Survey (NHANES III). *J Clin Endocrinol Metab*. 2002;87(2):489-499.
28. Morris LG, Sikora AG, Myssiorek D, DeLacure MD. The basis of racial differences in the incidence of thyroid cancer. *Ann Surg Oncol.* 2008;15(4):1169-1176.
29. Birchard SJ, Roesel OF. Neoplasia of the thyroid gland in dogs. A retrospective study of 16 cases. *J Am Anim Hosp Assoc*. 1981;17:369-72.
30. Carver JR, Kapatkin A, Patnaik AK. A comparision of medullary thyroid carcinoma and thyroid adenocarcinoma in dogs: a retrospective study of 38 cases. *Vet Surg.* 1995;24:315-319.
31. Haley PJ, Hahn FF, Muggenburg BA, Griffith WC. Thyroid neoplasms in a colony of Beagle dogs. *Vet Pathol*. 1989;26(5):438-441.
32. Gilliland FD, Hunt WC, Morris DM, Key CR. Prognostic factors for thyroid carcinoma. A population-based study of 15,698 cases from the Surveillance, Epidemiology and End Results (SEER) program 1973-1991. *Cancer.* 1997;79(3):564-573.
33. Thompson LDR, Wieneke JA, Paal E, *et al*. A clinicopathologic study of minimally invasive follicular carcinoma of the thyroid gland with a review of the english literature. *Cancer*. 2001;91:505-524.

34. Biliotti GC, Martini F, Vezzosi V, *et al.* Specific features of differentiated thyroid carcinoma in patients over 70 years of age. *J Surg Oncol*. 2006;93:194-198.
35. Hogan AR, Zhuge Y, Perez EA, *et al.* Pediatric thyroid carcinoma: incidence and outcomes in 1753 patients. *J Surg Res*. 2009;156(1):167-172.
36. Benjamin SA, Stephens LC, Hamilton BF, *et al.* Assoications between lymphocytic thyroiditis, hypothyroidism, and thyroid neoplasia in beagles. *Vet Pathol*. 1996;33(5):486-494
37. Mitchell M, Hurov LI, Troy GC. Canine thyroid carcinomas: clinical occurrence, staging by means of scintiscans, and therapy of 15 cases. *Vet Surg*. 1979;8:112-118.
38. Benjamin SA, Saunders WJ, Lee AC, *et al*. Non-neoplastic and neoplastic thyroid disease in beagles irradiated during prenatal and postnatal development. *Radiation Research*. 1997;147:422-430.
39. Shore RE. Issues and epidemiological evidence regarding radiation-induced thyroid cancer. *Radiat Res*. 1992;131:98-111.
40. Robbins J, Schneider AB. Thyroid cancer following exposure to radioactive iodine. *Rev Endocr Metab Disord*. 2000;1:197-203.
41. Thompson DE, Mabuchi K, Ron E, *et al*. Cancer incidence in atomic bomb survivors. Part II; Solid tumors, 1958-1987. *Radiat Res*. 1994;137:S17-S67.
42. Ron E, Lubin JH, Shore RE. Thyroid cancer after exposure to external radiation: a pooled analysis of seven studies. *Radiation Research*. 1995;141:259-277.
43. Soh EY, Sobhi SA, Wong MG, *et al.* Thyroid-stimulating hormone promotes the secretion of vascular endothelial growth factor in thyroid cancer cell lines. *Surgery*. 1996;120(6):944-947.
44. Di Pasquale M, Rothstein JL, Palazzo JP. Pathologic features of Hashimoto's-associated papillary thyroid carcinomas. *Hum Pathol*. 2001;32:24-30.
45. Bradly DP, Reddy V, Prinz RA, Gattuso P. Incidental papillary carcinoma in patients treated surgically for benign thyroid diseases. *Surgery*. 2009;146(6):1099-1104.
46. Okayasu I, Fujiwara M, Hara Y, *et al.* Association of chronic lymphocytic thyroiditis and thyroid papillary carcinoma; A study of surgical cases among Japanese, and White and African Americans. *Cancer*. 1995;76:2312-2318.
47. Ott RA, McCall AR, McHenry C, *et al.* The incidence of thyroid carcinoma in Hashimoto's thyroiditis. *Am Surg*. 1987;53(8):442-445.
48. Matesa-Anić D, Matesa N, Dabelić N, Kusić Z. Coexistence of papillary carcinoma and Hashimoto's thyroiditis. *Acta Clin Croat*. 2009;48(1):9-12.
49. Capen CC. Tumors of the endocrine glands. In: Meuten DJ (ed). *Tumors in Domestic Animals*, 4th ed. Iowa State Press, Blackwell Publishing Company. 2002. p. 607-696.
50. Schlumberger MJ. Papillary and follicular thyroid carcinoma. *N Engl J Med*. 1998;338(5):297-306.

51. Grebe SK, Hay ID. Follicular thyroid cancer. *Endocrinol Metab Clin North Am.* 1995;24(4):761-801.
52. Kloos RT. Papillary thyroid cancer: medical management and follow-up. *Curr Treat Options Oncol.* 2005;6(4):323-338.
53. Passler C, Prager G, Scheuba C, *et al.* Follicular variant of papillary thyroid carcinoma. A long-term follow-up. *Arch Surg.* 2003;138:1362-1366.
54. Schmid KW, Farid NR. How to define follicular thyroid carcinoma? *Virchows Arch.* 2006;448(4):385-393.
55. Patnaik AK, Lieberman PH. Gross, histologic, cytochemical, and immunocytochemical study of medullary thyroid carcinoma in sixteen dogs. *Vet Pathol*. 1991;28(3):223-233.
56. Ramos-Vara JA, Miller MA, Johnson GC, Pace LW. Immunohistochemical detection of thyroid transcription factor-1, thyroglobulin, and calcitonin in canine normal, hyperplastic, and neoplastic thyroid gland. *Vet Pathol.* 2002;39(4):480-487.
57. Lee J-J, Larsson C, Lui W-O, *et al.* A dog with familial medullary thyroid cancer. *International Journal of Oncology*. 2006;29:1173-1182.
58. Holm R, Sobrinho-Simoes M, Nesland JM, *et al*. Medullary carcinoma of the thyroid gland: an immunocytochemical study. *Ultrastruct Pathol.* 1985;8:25-41.
59. Holm R, Farrants GW, Nesland JM, *et al.* Ultrastructural and electron immunohistochemical features of medullary thyroid carcinoma. *Virchows Arch A Pathol Anat Histopathol.* 1989;414:375-384.
60. You YN, Lakhani V, Wells SA Jr, Moley JF. Medullary thyroid cancer. *Surg Oncol Clin N Am.* 2006;15(3):639-660.
61. Barber LG. Thyroid tumors in dogs and cats. *Vet Clin North Am Small Anim Pract.* 2007;37(4):755-773.
62. Liptak JM. Canine thyroid carcinoma. *Clin Tech Small Anim Pract*. 2007;22(2):75-81.
63. D'Avanzo A, Treseler P, Ituarte PHG, *et al.* Follicular thyroid carcinoma: histology and prognosis. *Cancer*. 2004;100:1123-1129.
64. Miles KG, Lattimer JC, Jergens AE, Krause GF. A retrospective evaluation of the radiographic evidence of pulmonary metastatic disease on initial presentation in the dog. *Vet Radiol.* 1990;31(2):79-82.
65. Théon AP, Marks SL, Feldman ES, Griffey S. Prognostic factors and patterns of treatment failure in dogs with unresectable differentiated thyroid carcinomas treated with megavoltage irradiation. *J Am Vet Med Assoc*. 2000;216(11):1775-1779.
66. Tuohy J, Worley D, Withrow SJ. Outcomes of bilateral thyroidectomies for simultaneous discrete bilateral mobile canine thyroid carcinoma at a single institution. *Vet Surg*. 2010;39:E57.
67. Almes KM, Heaney AM, Andrews GA. Intracardiac ectopic thyroid carcinosarcoma in a dog. *Vet Pathol*. 2008;45:500-504.

68. Bracha S, Caron I, Holmberg DL, *et al*. Ectopic thyroid carcinoma causing right ventricular outflow tract obstruction in a dog. *J Am Anim Hosp Assoc*. 2009;45:138-141.
69. Liptak JM, Kamstock DA, Dernell WS, *et al.* Cranial mediastinal carcinomas in nine dogs. *Vet Comp Oncol*. 2008;6(1):19-30.
70. Lantz GC, Salisbury SK. Surgical excision of ectopic thyroid carcinoma involving the base of the tongue in dogs: three cases (1980 – 1987). *J Am Vet Med Assoc*. 1989;195(11):1606-1608.
71. Bailey DB, Page RL. Tumors of the endocrine system. In: Withrow SJ, Vail DM. *Withrow and MacEwen's small animal clinical oncology* 4th ed. St. Louis: Saunders; 2007. p. 591-596.
72. Nelson RW, Couto CG. *Small animal internal medicine* 4th ed. St Louis: Mosby Elsevier; 2009. p. 758-762.
73. LeJeune A, Boston S, Hayes GM, Foster RA. Evaluation of prognostic factors in thyroid carcinoma in dogs: a retrospective study (1999-2009). *Vet Surg*. 2010;39:E31.
74. Klein MK, Powers BE, Withrow SJ, *et al.* Treatment of thyroid carcinoma in dogs by surgical resection alone: 20 cases (1981-1989). *J Am Vet Med Assoc*. 1995;206(7):1007-1009.
75. Fossum TW. Surgery of the endocrine system. In: Fossum TW, editor. *Small animal surgery*, 2nd ed. St Louis: Mosby; 2002. p. 527-529.
76. Tamura S, Tamura Y, Suzuoka N, *et al.* Multiple metastases of thyroid cancer in the cranium and pituitary gland in two dogs. *J Small Anim Pract*. 2007;48:237-239.
77. Owen LN. TNM classification of tumours in domestic animals. Geneva, *World Health Organization*, 1980.
78. Wisner ER, Nyland TG. Ultrasonagraphy of the thyroid and parathyroid glands. *Vet Clin North Am Small Anim Pract.* 1998;28:973-991.
79. Feeney DA, Anderson KL. Nuclear imaging and radiation therapy in canine and feline thyroid disease. *Vet Clin Small Anim*. 2007;37:799-821.
80. Marks SL, Koblik PD, Hornof WJ, Feldman EC. 99mTc-pertechnetate imaging of thyroid tumors in dogs: 29 cases (1980-1992). *J Am Vet Med Assoc*. 1994;204(5):756-760.
81. Waters CB, Scott-Moncrieff JCR. Cancer of endocrine origin. In: Morrison WB, ed. *Cancer in dogs and cats: medical and surgical management*, 2nd ed. Jackson: Teton New Media; 2002. p. 573-580.
82. Thompson EJ, Stirtzinger T, Lumsden JH, Little PB. Fine needle aspiration cytology in the diagnosis of canine thyroid carcinoma. *Can Vet J*. 1980;21(6):186-188.
83. Yeh MW, Demircan O, Ituarte P, Clark OH. False-negative fine-needle aspiration cytology results delay treatment and adversely affect outcome in patients with thyroid carcinoma. *Thyroid*. 2004;14(3):207-215.

84. Verburg FA, MäderW, Luster M, Reiners C. Histology does not influence prognosis in differentiated thyroid carcinoma when accounting for age, tumour diameter, invasive growth and metastases. *Eur J Endocrinol*. 2009;160:619-624.
85. Cooper DS, Doherty GM, Haugen BR, *et al.* Management guidelines for patients with thyroid nodules and differentiated thyroid cancer. *Thyroid*. 2006;16(2):109-142.
86. Nix P, Nicolaides A, Coatesworth AP. Thyroid cancer review 2: management of differentiated thyroid cancers. *Int J Clin Pract*. 2005;59(12):1459-1463.
87. Miccoli P, Pinchera A, Materazzi G, *et al.* Surgical treatment of low- and intermediate-risk papillary thyroid cancer with minimally invasive video-assisted thyroidectomy. *J Clin Endocrinol Metab.* 2009;94(5):1618-1622.
88. Pack L, Roberts RE, Dawson SD, Dookwah HD. Definitive radiation therapy for infiltrative thyroid carcinoma in dogs. *Vet Radiol Ultrasound*. 2001;42(5):471-474.
89. Ford D, Giridharan S, McConkey C, *et al.* External beam radiotherapy in the management of differentiated thyroid cancer. *Clin Oncol (R Coll Radiol).* 2003;15(6):337-341.
90. Fassnacht M, Kreissl MC, Weismann D, Allolio B. New targets and therapeutic approaches for endocrine malignancies. *Pharmacol Ther*. 2009;123:117-141.
91. O'Doherty MJ, Coakley AJ. Drug therapy alternatives in the treatment of thyroid cancer. *Drugs*. 1998;55(6):801-812.
92. Schlumberger M, Challeton C, De Vathaire R, *et al*. Radioactive iodine treatment and external radiotherapy for lung and bone metastases from thyroid carcinoma. *J Nucl Med*. 1996;37(4):598-605.
93. Fineman LS, Hamilton TA, de Gortari A, Bonney P. Cisplatin chemotherapy for treatment of thyroid carcinoma in dogs: 13 cases. *J Am Anim Hosp Assoc*. 1998;34:109-112.
94. Matuszczyk A, Petersenn S, Bockisch A, *et al.* Chemotherapy with doxorubicin in progressive medullary and thyroid carcinoma of the follicular epithelium. *Horm Metab Res*. 2008;40:210-213
95. Scherübl H, Raue F, Ziegler R. Combination chemotherapy of advanced medullary and differentiated thyroid cancer. Phase II study. *J Cancer Res Clin Oncol*. 1990;116(1):21-23.
96. Deitz KD, Anderson ML, Wilke VL. Cyclooxygenase-2 expression in canine thyroid tumors. *Submitted to Veterinary Pathology.*
97. Ito Y, Yoshida H, Nakano K, *et al.* Cyclooxygenase-2 expression in thyroid neoplasms. *Histopathology*. 2003;42(5):492-497.
98. Quidville V, Segond N, Pidoux E, *et al.* Tumor growth inhibition by indomethacin in a mouse model of human medullary thyroid cancer: implication of cyclooxygenases and 15-hydroxyprostaglandin dehydrogenase. *Endocrinology*. 2004;145:2561-2571.
99. Devilee P, VanLeeuwen IS, Voesten A, *et al*. The canine p53 gene is subject to somatic mutations in thyroid carcinoma. *Anticancer Res*. 1994;14:2039-2046.

100. Verschueren CP, Rutteman GR, Vos JH, *et al.* Thyrotrophin receptors in normal and neoplastic (primary and metastatic) canine thyroid tissue. *J Endocrinol*. 1992;132:461-468.
101. Kondo T, Ezzat S, Asa SL. Pathogenetic mechanisms in thyroid follicular-cell neoplasia. *Nat Rev Cancer*. 2006;6:292-306.
102. Castro P, Eknaes M, Teixeira MR, *et al*. Adenomas and follicular carcinomas of the thyroid display two major patterns of chromosomal changes. *J Pathol*. 2005;206(3):305-311.
103. Airaksinen MS, Saarma M. The GDNF family: signaling, biological functions and therapeutic value. *Nat Rev Neurosci*. 2002;3(5):383-394.
104. Marx SJ. Molecular genetics of multiple endocrine neoplasia types 1 and 2. *Nat Rev Cancer*. 2005;5:367-375.
105. Tallini G, Asa SL. RET oncogene activation in papillary thyroid carcinoma. *Adv Anat Pathol.* 2001;8:345-354.
106. Namba H, Nakashima M, Hayashi T, *et al.* Clinical implication of hot spot BRAF mutation, V599E, in papillary thyroid cancers. *J Clin Endocrinol Metab*. 2003;88(9):4393-4397.
107. Boelaert K, McCabe CJ, Tannahill LA, *et al*. Pituitary tumor transforming gene and fibroblast growth factor-2 expression: potential prognostic indicators in differentiated thyroid cancer. *J Clin Endocrinol Metab*. 2003;88(5):2341-2347.
108. Morikawa Y, Ishihara Y, Tohya K, *et al.* Expression of the fibroblast growth factor receptor-1 in human normal tissues and tumors determined by a new monoclonal antibody. *Arch Pathol Lab Med*. 1996;120(5):490-496.
109. St Bernard R, Zheng L, Liu W, *et al.* Fibroblast growth factor receptors as molecular targets in thyroid carcinoma. *Endocrinology*. 2005;146(3):1145-1153.
110. Ruco LP, Ranalli T, Marzullo A, *et al.* Expression of Met protein in thyroid tumors. *J Pathol*. 1996;180(3):266-270.
111. Schiff BA, McMurphy AB, Jasser SA, *et al*. Epidermal growth factor receptor (EGFR) is overexpressed in anaplastic thyroid cancer, and the EGFR inhibitor gefitinib inhibits the growth of anaplastic thyroid cancer. *Clin Cancer Res*. 2004;10(24):8594-8602.
112. Soh EY, Duh QY, Sobhi SA, *et al.* Vascular endothelial growth factor expression is higher in differentiated thyroid cancer than in normal or benign thyroid. *J Clin Endocrinol Metab*. 1997;82(11):3741-3747.
113. Donghi R, Longoni A, Pilotti S, *et al.* Gene p53 mutations are restricted to poorly differentiated and undifferentiated carcinomas of the thyroid gland. *J Clin Invest*. 1993;91(4):1753-1760.
114. Fagin JA, Matsuo K, Karmakar A, *et al*. High prevalence of mutations of the p53 gene in poorly differentiated human thyroid carcinomas. *J Clin Invest*. 1993;91(1):179-184.
115. Spambalg d, Sharifi N, Elisei R, *et al*. Structural studies of the thyrotropin receptor and Gs alpha in human thyroid cancers: low prevalence of mutations

predicts infrequent involvement in malignant transformation. *J Clin Endocrinol Metab*. 1996;81(11):3898-3901.

116. Alizadeh AA, Ross DT, Perou CM, *et al.* Towards a novel classification of human malignancies based on gene expression patterns. *J Pathol*. 2001;195:41-52.

117. Barden CB, Shister KW, Zhu B, *et al.* Classification of follicular thyroid tumors by molecular signature: results of gene profiling. *Clin Cancer Res*. 2003;9:1792-1800.

118. Trovato M, Villari D, Bartolone L, *et al.* Expression of the hepatocyte growth factor and c-met in normal thyroid, non-neoplastic, and neoplastic nodules. *Thyroid*. 1998;8(2):125-131.

119. Chevillard s, Ugolin N, Vielh P, *et al.* Gene expression profiling of differentiated thyroid neoplasms: diagnostic and clinical implications. *Clin Cancer Res*. 2004;10:6586-6597.

120. Weber F, Shen L, Aldred MA, *et al.* Genetic classification of benign and malignant thyroid follicular neoplasia based on a three-gene combination. *J Clin Endocrinol Metab*. 2005;90:2512-2521.

121. Zhao J, Leonard C, Gemsenjäger E, *et al.* Differentiation of human follicular thyroid adenomas from carcinomas by gene expression profiling. *Oncol Rep*. 2008;19(2):329-337.

122. Wang Z, Chamberlain JS, Tapscott SJ, Storb R. Gene therapy in large animal models of muscular dystrophy. *ILAR J*. 2009;50(2):187-198.

123. Uva P, Aurisicchio L, Watters J, *et al.* Comparative expression pathway analysis of human and canine mammary tumors. *BMC Genomics*. 2009:10:135

124. Capen CC. Overview of structural and functional lesions in endocrine organs of animals. *Toxicol Pathol*. 2001;29(1):8-33.

125. Knostman KAB, Jhiang SM, Capen CC. Genetic alterations in thyroid cancer: the role of mouse models. *Vet Pathol*. 2007;44:1-14.

126. Kaneshige M, Kaneshige K, Zhu X, *et al.* Mice with a targeted mutation in the thyroid hormone beta receptor gene exhibit impaired growth and resistance to thyroid hormone. *Proc Natl Acad Sci USA*. 2000;97(24):13209-13214.

127. Paoloni M, Khanna C. Translation of new cancer treatments from pet dogs to humans. *Nat Rev Cancer*. 2008;8:147-156.

128. Hoffman MM, Birney E. Estimating the neutral rate of nucleotide substitution using introns. *Mol Biol Evol*. 2007;24(2):522-531.

129. Kent MS, Griffey SM, Verstraete FJ, *et al.* Computer-assisted image analysis of neovascularization in thyroid neoplasms from dogs. *American Journal of Veterinary Research* 2002; 63(3): 363-369.

130. Shibru D, Chung KW, Kebebew E. Recent developments in the clinical application of thyroid cancer biomarkers. *Current Opinion in Oncology*. 2008; 20(1): 13-8.

131. Wang KX, Denhardt DT. "Osteopontin: role in immune regulation and stress responses". *Cytokine Growth Factor Rev*. 2008;19(5-6):333-345.

132. Choi ST, Kim JH, Kang EJ, *et al.* Osteopontin might be involved in bone remodeling rather than in inflammation in ankylosing spondylitis. *Rheumatology.* 2008;47(12):1775-1779.
133. Reinholt FP, Hultenby K, Oldberg A, Heinegard D. Osteopontin – a possible anchor of osteoclasts to bone. *Proceedings of the National Aacademy of Sciences of the United States of America* 1990; 87(12): 4473-4475.
134. Denhardt DT, Noda M, O'Regan AW, Pavlin D, Berman JS. Osteopontin as a means to cope with environmental insults: regulation of inflammation, tissue remodeling, and cell survival. The *Journal of Clinical Investigation* 2001; 107(9): 1055-1061.
135. Guarino V, Faviana P, Salvatore G, *et al*. Osteopontin is overexpressed in human papillary thyroid carcinomas and enhanced thyroid carcinoma cell invasiveness. *J Clin Endocrinol Metab.* 2005;90(9):5270-5278.
136. Shibuya M, Claesson-Welsh L. Signal transduction by VEGF receptors in regulation of angiogenesis and lymphangiogenesis. *Exp Cell Res*. 2006;312:549-560.
137. Veikkola T, Alitalo K. VEGFs, receptors and angiogenesis. *Semin Cancer Biol*. 1999;9:211-220.
138. Witmer AN, Dai J, Weich HA, *et al*. Expressio of vascular endothelial growth factor receptors 1, 2, and 3 in quiescent endothelia. *J Histochem Cytochem*. 2002;50(6):767-777.
139. Mi Z, Guo H, Russell MB, *et al.* RNA aptamer blockade of osteopontin inhibits growth and metastasis of MDA-MB231 breast cancer cells. *Molecular Therapy* 2009; 17(1): 153-161.
140. Bramwell VHC, Doig GS, Tuck AB, *et al*. Serial plasma osteopontin levels have prognostic value in metastatic breast cancer. *Clin Cancer Res*. 2006;12(11):3337-3343.
141. Weber GF, Lett GS and Haubein NC. Osteopontin is a marker for cancer aggressiveness and patient survival. *British Journal of Cancer* 2010; 103: 861-869.
142. Xu WW, Carter CJ. Parallel multiplicity and error discovery rate (EDR) in microarray experiments. *BMC Bioinformatics*. 2010;11:465
143. Benjamini Y and Hochberg Y. Controlling the false discovery rate: a practical and powerful approach to multiple testing. *Journal. Royal Statistical Society Series B* 1995; 57(1): 289-300.
144. Peters IR, Peeters D, Helps CR, Day MJ. Development and application of multiple internal reference (housekeeper) gene assays for accurate normalization of canine gene expression studies. *Veterinary Immunol Immunopathol* 2007; 117(1-2): 55-66.
145. Pfaffl MW. In: Bustin SA (ed): *A–Z of Quantitative PCR*. California: IUL Biotechnology Series, International University Line, 2004: 87-120.

146. Chakraborty G, Jain S and Kundu GC. Osteopontin promotes vascular endothelial growth factor-dependent breast tumor growth and angiogenesis via autocrine and paracrine mechanisms. *Cancer Research* 2008; 68(1): 152-161.
147. Solberg TD, Nearman J, Mullins J, Li S and Baranowska-Kortylewicz J. Correlation between tumor growth delay and expression of cancer and host VEGF, VEGFR2, and osteopontin in response to radiotherapy. *International Journal of Radiation Oncology, Biology, Physics*. 2008; 72(3): 918-926.
148. Coppola D, Szabo M, Boulware D, *et al*. Correlation of osteopontin protein expression and pathological stage across a wide variety of tumor histologies. *Clin Cancer Res* 2004; 10(1Pt1): 184-190.
149. Ramaiah SK, Rittling S. Pathophysiological role of osteopontin in hepatic inflammation, toxicity, and cancer. *Toxicological Sciences* 2008; 103(1): 4-13.
150. Zhang X, Tsukamoto T, Mizoshita T, Ban H, Suzuki H, Toyoda T and Tatematsu M . Expression of osteopontin and CDX2: indications of phenotypes and prognosis in advanced gastric cancer. *Oncology Reports* 2009; 21(3): 609-613.
151. Sodek J, Ganss B, McKee MD. Osteopontin. *Crit Rev Oral Biol Med*. 2000;11:279-303.
152. Briese J, Cheng S, Ezzat S, *et al*. Osteopontin (OPN) expression in thyroid carcinoma. *Anticancer Res*. 2010;30(5):1681-1688.
153. Kim JH, Skates SJ, Uede T, *et al*. Osteopontin as a potential diagnostic biomarker for ovarian cancer. *JAMA*. 2002;287(13):1671-1679.
154. Singhal H, Bautista DS, Tonkin KS *et al*. Elevated plasma osteopontin in metastatic breast cancer associated with increased tumor burden and decreased survival. *Clin Cancer Res*. 1997;3:605-611.
155. Koopmann J, Fedarko NS, Jain A, *et al.* Evaluation of osteopontin as biomarker for pancreatic adenocarcinoma. *Cancer Epidemiol Biomarkers Prev*. 2004;13(3):487-491.
156. Hotte SJ, Winquist EW, Stitt L, *et al*. Plasma osteopontin: associations with survival and metastasis to bone in men with hormone-refractory prostate carcinoma. *Cancer*. 2002;95(3):506-512.
157. Hu Z, Lin D, Yuan J, *et al*. Overexpression of osteopontin is associated with more aggressive phenotypes in human non-small cell lung cancer. *Clin Cancer Res*. 2005;11(13):4646-4652.
158. Standal T, Hjorth-Hansen H, Rasmussen T, *et al*. Osteopontin is an adhesive factor for myeloma cells and is found in increased levels in plasma from patients with multiple myeloma. *Haematologica*. 2004;89(2):174-182.
159. Metivier KS, Deitz K, Xu WW, *et al*. Differential expression of osteopontin in follicular thyroid carcinomas compared to normal thyroid tissues in dogs. Submitted to Vet Comp Oncol.
160. Sun Y, Fang S, Dong H, *et al*. Correlation between osteopontin messenger RNA expression and microcalcification shown on sonography in papillary thyroid carcinoma. *J Ultrasound Med*. 2011;30(6):765-771.

161. Dai J, Peng L, Fan K, *et al*. Osteopontin induces angiogenesis through activation of PI3K/AKT and ERK1/2 in endothelial cells. *Oncogene*. 2009;28(38):3412-3422.
162. Davies MM, Jonas SK, Kaur S, Allen-Mersh TG. Plasma vascular endothelial but not fibroblast growth factor levels correlate with colorectal liver metastasis vascularity and volume. *Br J Cancer*. 2000;82(5):1004-1008.
163. Hyodo I, Doi T, Endo H, *et al*. Clinical significance of plasma vascular endothelial growth factor in gastrointestinal cancer. *Eur J Cancer*. 1998;34(13):2041-2045.
164. Jantus-Lewintre E, Sanmartin E, Sirera R, *et al*. Combined VEGF-A and VEGFR-2 concentrations in plasma: Diagnostic and prognostic implications in patients with advanced NSCLSC. *Lung Cancer*. 2011;Epub ahead of print.
165. Jinno K, Tanimizu M, Hyodo I, *et al*. Circulating vascular endothelial growth factor (VEGF) is a possible tumor marker for metastasis in human hepatolcellular carcinoma. *J Gastroenterol*. 1998;33(3):376-382.
166. Nakae M, Iwamoto I, Fujino T, *et al*. Preoperative plasma osteopontin level as a biomarker complementary to carbohydrate antigen 125 in predicting ovarian cancer. *J Obstet Gynaecol Res*. 2006;32(3):309-314.
167. Pezzilli R, Fabbri D, Corsi MM, *et al*. Plasma concentrations of angiogenic factors and angiogenetic inhibitors in patients with ductal pancreatic neoplasms. A pilot study. *Clin Chem Lab Med*. 2011;49(6):1047-1051.
168. Yoshikawa T, Tsuburaya A, Kobayashi O, *et al*. Plasma concentrations of VEGF and bFGF in patients with gastric carcinoma. *Cancer Lett*. 2000;153(1-2):7-12.
169. Fedarko NS, Jain A, Karadag A, *et al*. Elevated serum bone sialoprotein and osteopontin in colon, breast, prostate, and lung cancer. *Clin Cancer Res*. 2001;7:4060-4066.
170. Creaney J, Yeoman D, Musk AW, *et al*. Plasma versus serum levels of osteopontin and mesothelin in patients with malignant mesothelioma-Which is best? *Lung Cancer*. 2011;Epub ahead of print.
171. Cristaudo A, Foddis R, Bonotti A, *et al*. Comparison between plasma and serum osteopontin levels: usefulness in diagnosis of epithelial malignant pleural mesothelioma. *Int J Biol Markers*. 2010;25(3):164-170.

APPENDIX A

MICROARRAY ANALYSIS – DIFFERENTIALLY EXPRESSED GENES

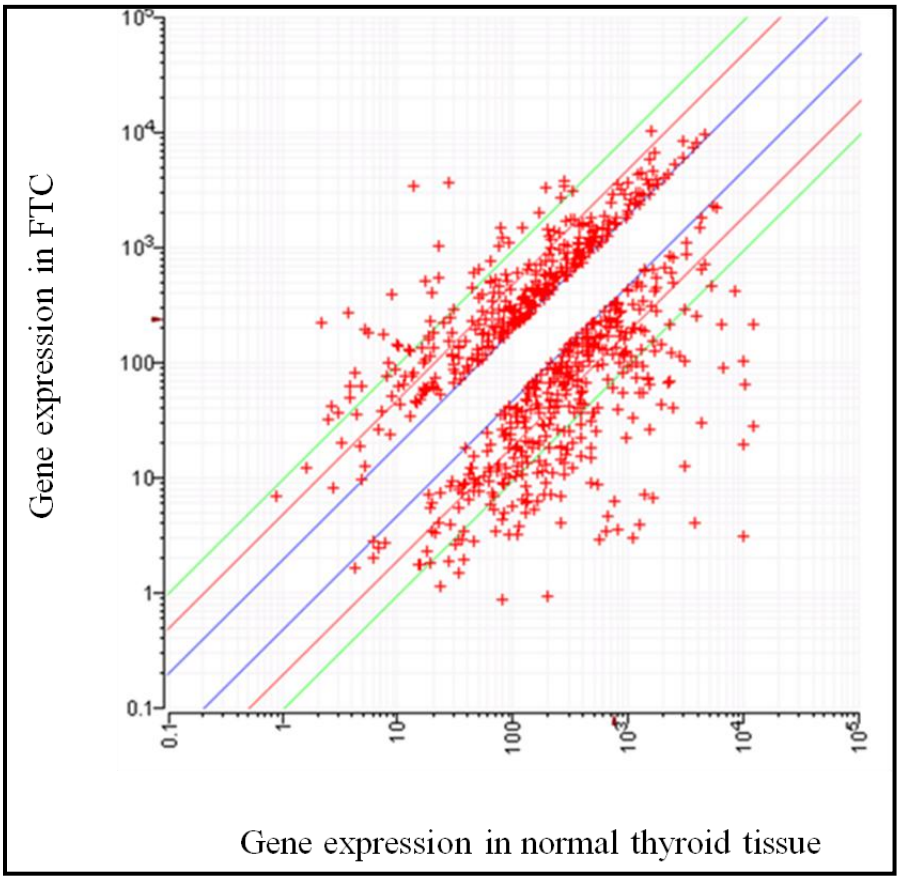

Figure A-1 Log-log plot showing distribution of differentially expressed transcripts between follicular thyroid carcinoma and normal thyroid tissue (microarray analysis)

The data points on the log-log plot represent differentially expressed transcripts. Points located within and above the upper three lines represent transcripts that are up-regulated in FTC compared to normal thyroid tissue; and points located within and below the lower three lines represent transcripts that are down-regulated in FTC compared to normal thyroid tissue. Transcripts between the blue and red lines have fold differences between 2.0 and 4.9; transcripts between the red and green lines have fold differences

between 5.0 and 9.9; and transcripts above and below the green lines have fold differences greater than or equal to 10. There are no points between the two blue lines since transcripts with fold differences less than 2.0 were not considered differentially expressed.

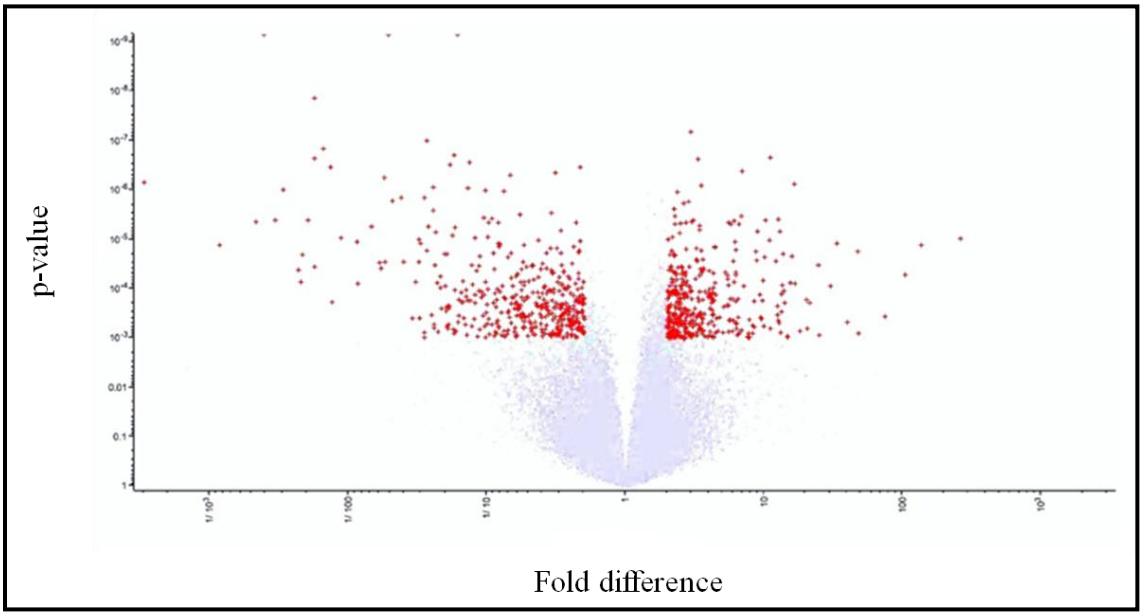

Figure A-2. Volcano plot representing differentially expressed transcripts between follicular thyroid carcinoma and normal thyroid tissue (microarray analysis)

Data points on the volcano plot represent all transcripts that were evaluated by microarray analysis with their corresponding fold differences and p-values. Gray-colored points were not significantly different between FTC and normal thyroid tissue; red-colored points were significantly different ($p < 0.001$).

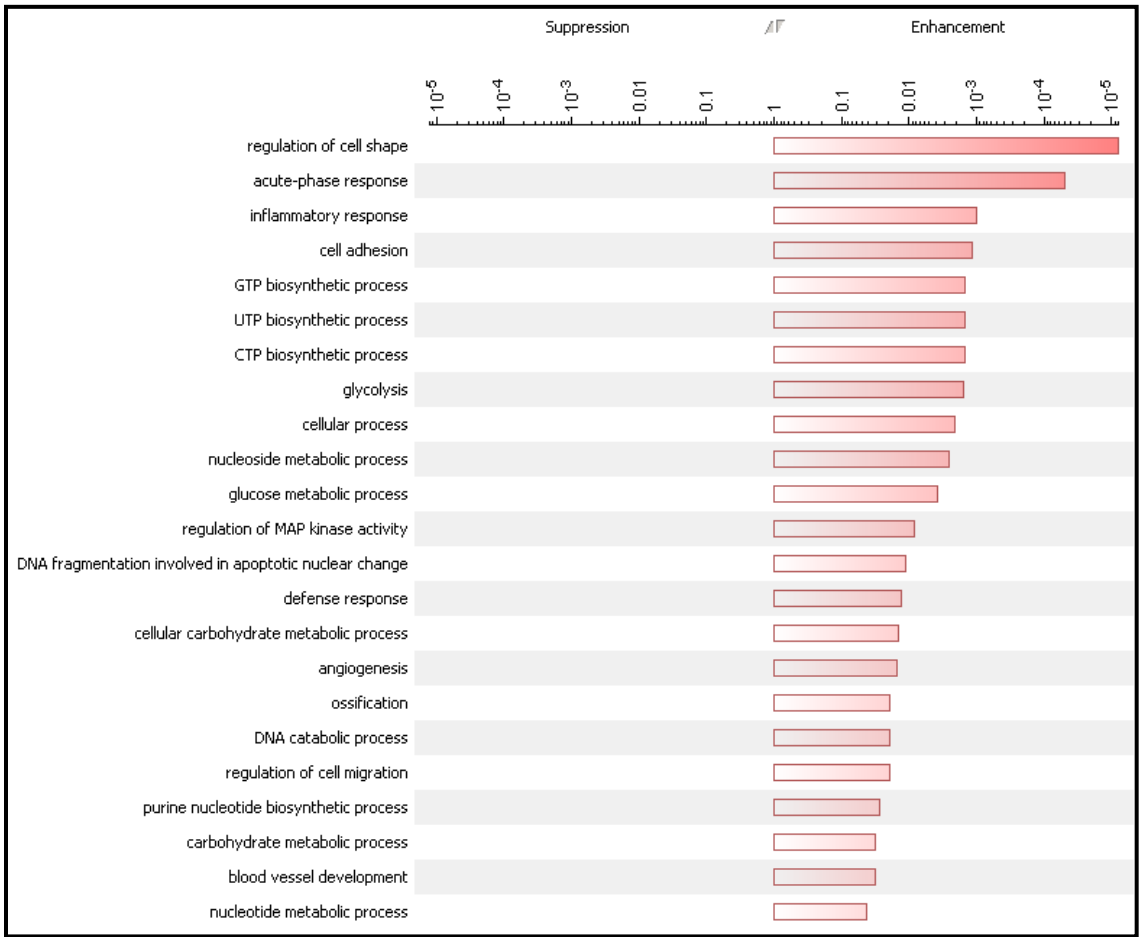

Figure A-3. Gene ontology biological processes significantly up-regulated in follicular thyroid carcinoma compared to normal thyroid tissue (microarray analysis)

Table A-1 Complete list of genes that were up-regulated in follicular thyroid carcinoma compared to normal thyroid tissue (microarray analysis)

Transcript ID	Gene Symbol	Gene Title	Fold	p-value	EDR	BH Q-Value
CfaAffx.7926.1	ABP1	amiloride binding protein 1 (amine oxidase (copper-containing))	9.73	0.0001	0.0000	0.0113
Cfa.10633.1	ACOT8	acyl-CoA thioesterase 8	2.45	0.0002	0.0001	0.0163
CfaAffx.26498.1	ACP5	acid phosphatase 5, tartrate resistant	20.50	0.0007	0.0000	0.0310
Cfa.18293.1	ACP5	acid phosphatase 5, tartrate resistant	13.14	0.0008	0.0001	0.0340
CfaAffx.30252.1	ADAMTSL2	ADAMTS-like 2	13.34	0.0001	0.0001	0.0148
CfaAffx.20932.1	AIDA	axin interactor, dorsalization associated	2.21	0.0001	0.0001	0.0141
Cfa.7165.1	AK1	adenylate kinase 1	5.86	0.0002	0.0000	0.0161
CfaAffx.6803.1	AMD1	adenosylmethionine decarboxylase 1	2.84	0.0000	0.0000	0.0020
CfaAffx.17331.1	AMZ2	archaelysin family metallopeptidase 2	2.54	0.0001	0.0000	0.0097
CfaAffx.12208.1	ANAPC10	anaphase promoting complex subunit 10	3.05	0.0003	0.0027	0.0224
Cfa.9973.1	AQP5	aquaporin 5	12.40	0.0003	0.0000	0.0230
CfaAffx.2390.1	ATAD2	ATPase family, AAA domain containing 2	2.13	0.0008	0.0202	0.0348
CfaAffx.16764.1	ATP6V1A	ATPase, H+ transporting, lysosomal 70kDa, V1 subunit A	2.92	0.0004	0.0006	0.0232
CfaAffx.19856.1	B4GALT3	UDP-Gal:betaGlcNAc beta 1,4- galactosyltransferase, polypeptide 3	2.17	0.0007	0.0035	0.0325
CfaAffx.17020.1	BAI2	brain-specific angiogenesis inhibitor 2	5.52	0.0000	0.0000	0.0030
Cfa.651.1	BCAR3	breast cancer anti-estrogen resistance 3	3.61	0.0007	0.0009	0.0326
CfaAffx.30818.1	BCAR3	breast cancer anti-estrogen resistance 3	3.03	0.0008	0.0023	0.0348
CfaAffx.14359.1	BHMT	betaine-homocysteine S-methyltransferase	8.49	0.0002	0.0003	0.0170
Cfa.20792.1	BLOC1S2	biogenesis of lysosomal organelles complex-1, subunit 2	2.78	0.0000	0.0000	0.0056
CfaAffx.13990.1	BMP2K	BMP2 inducible kinase	2.17	0.0006	0.0045	0.0302

Table A-1 cont'd Complete list of genes that were up-regulated in follicular thyroid carcinoma compared to normal thyroid tissue (microarray analysis)

Transcript ID	Gene Symbol	Gene Title	Fold	p-value	EDR	BH Q-Value
Cfa.7711.2	BMP2K	BMP2 inducible kinase	2.07	0.0001	0.0001	0.0154
CfaAffx.14101.1	BUB1B	budding uninhibited by benzimidazoles 1 homolog beta (yeast)	3.69	0.0003	0.0024	0.0226
CfaAffx.15371.1	CBLB	Cas-Br-M (murine) ecotropic retroviral transforming sequence b	3.59	0.0000	0.0000	0.0077
Cfa.15815.1	CCL3	chemokine (C-C motif) ligand 3	2.62	0.0003	0.0014	0.0216
Cfa.16248.1	CCND1	cyclin D1	2.60	0.0001	0.0000	0.0116
Cfa.1824.1	CCT5	chaperonin containing TCP1, subunit 5 (epsilon)	2.54	0.0001	0.0000	0.0126
Cfa.180.1	CD40	CD40 molecule, TNF receptor superfamily member 5	11.09	0.0007	0.0010	0.0310
Cfa.21050.1	CD6	CD6 molecule	6.27	0.0006	0.0135	0.0306
CfaAffx.22581.1	CDCA3	cell division cycle associated 3	16.48	0.0000	0.0000	0.0015
Cfa.20663.1	CDK1	cyclin-dependent kinase 1	9.24	0.0001	0.0000	0.0148
CfaAffx.15807.1	CDK18	cyclin-dependent kinase 18	6.03	0.0000	0.0000	0.0030
CfaAffx.12430.1	CENPH	centromere protein H	12.61	0.0004	0.0014	0.0255
CfaAffx.24199.1	CEP170	centrosomal protein 170kDa	2.67	0.0004	0.0020	0.0255
Cfa.10143.1	CEP170	centrosomal protein 170kDa	2.47	0.0001	0.0000	0.0126
CfaAffx.24202.1	CEP170	centrosomal protein 170kDa	2.24	0.0003	0.0025	0.0225
Cfa.18878.1	CHADL	chondroadherin-like	6.81	0.0002	0.0000	0.0169
CfaAffx.2550.1	CHADL	chondroadherin-like	3.59	0.0000	0.0000	0.0092
Cfa.5198.1	CHCHD1	coiled-coil-helix-coiled-coil-helix domain containing 1	2.68	0.0006	0.0008	0.0298
CfaAffx.16068.1	CHI3L1	chitinase 3-like 1 (cartilage glycoprotein-39)	47.55	0.0008	0.0000	0.0346
CfaAffx.7350.1	CHORDC1	cysteine and histidine-rich domain (CHORD)-containing 1	2.88	0.0001	0.0000	0.0126

Table A-1 cont'd Complete list of genes that were up-regulated in follicular thyroid carcinoma compared to normal thyroid tissue (microarray analysis)

Transcript ID	Gene Symbol	Gene Title	Fold	p-value	EDR	BH Q-Value
Cfa.17691.1	CHORDC1	cysteine and histidine-rich domain (CHORD)-containing 1	2.32	0.0001	0.0000	0.0111
CfaAffx.9164.1	CHRDL2	chordin-like 2	39.50	0.0005	0.0000	0.0266
CfaAffx.9810.1	CKAP2	cytoskeleton associated protein 2	2.86	0.0008	0.0090	0.0347
CfaAffx.17101.1	COL16A1	collagen, type XVI, alpha 1	12.17	0.0000	0.0000	0.0081
CfaAffx.25614.1	CRABP2	cellular retinoic acid binding protein 2	14.03	0.0002	0.0001	0.0175
CfaAffx.22652.1	CRLF1	cytokine receptor-like factor 1	15.31	0.0001	0.0000	0.0119
Cfa.8149.1	CRLF1	cytokine receptor-like factor 1	3.39	0.0007	0.0020	0.0316
CfaAffx.3170.1	CSF2RB	colony stimulating factor 2 receptor, beta	3.37	0.0006	0.0069	0.0290
CfaAffx.10092.1	CSNK1D	casein kinase 1, delta	2.21	0.0007	0.0027	0.0332
Cfa.20724.1	CTSA	cathepsin A	2.28	0.0001	0.0000	0.0148
CfaAffx.15405.1	CTSA	cathepsin A	2.23	0.0005	0.0003	0.0277
Cfa.21450.1	CTSB	cathepsin B	3.62	0.0000	0.0000	0.0091
Cfa.4159.1	CTSB	cathepsin B	2.23	0.0003	0.0001	0.0230
CfaAffx.21741.1	CTSH	cathepsin H	3.96	0.0001	0.0000	0.0146
Cfa.2521.1	CTSH	cathepsin H	3.72	0.0001	0.0000	0.0141
CfaAffx.8579.1	CXCR4	chemokine (C-X-C motif) receptor 4	6.09	0.0001	0.0000	0.0116
CfaAffx.5204.1	CYCS	cytochrome c, somatic	2.48	0.0002	0.0000	0.0161
Cfa.379.1	CYCS	cytochrome c, somatic	2.24	0.0001	0.0000	0.0139
Cfa.16735.1	CYHR1	cysteine/histidine-rich 1	2.36	0.0001	0.0001	0.0143
CfaAffx.26047.1	DAPK2	death-associated protein kinase 2	6.00	0.0000	0.0000	0.0080

Table A-1 cont'd Complete list of genes that were up-regulated in follicular thyroid carcinoma compared to normal thyroid tissue (microarray analysis)

Transcript ID	Gene Symbol	Gene Title	Fold	p-value	EDR	BH Q-Value
Cfa.6728.1	DCAF7	DDB1 and CUL4 associated factor 7	5.58	0.0005	0.0007	0.0257
CfaAffx.21648.1	DDT	D-dopachrome tautomerase	2.17	0.0000	0.0000	0.0046
CfaAffx.23135.1	DLGAP5	discs, large (Drosophila) homolog-associated protein 5	2.19	0.0009	0.0262	0.0364
Cfa.17880.1	DNAJB9	DnaJ (Hsp40) homolog, subfamily B, member 9	2.06	0.0005	0.0003	0.0270
Cfa.1926.1	DNM1L	dynamin 1-like	2.00	0.0006	0.0050	0.0299
Cfa.11380.1	DOLK	dolichol kinase	2.71	0.0000	0.0000	0.0096
Cfa.5643.1	DOLK	dolichol kinase	2.03	0.0010	0.0112	0.0373
Cfa.19507.1	DPH5	DPH5 homolog (S. cerevisiae)	3.44	0.0006	0.0016	0.0302
CfaAffx.30605.1	DPH5	DPH5 homolog (S. cerevisiae)	2.61	0.0005	0.0020	0.0271
Cfa.1802.1	DPM1	dolichyl-phosphate mannosyltransferase polypeptide 1	2.44	0.0002	0.0001	0.0158
Cfa.1317.1	EIF4G3	eukaryotic translation initiation factor 4 gamma, 3	2.01	0.0002	0.0002	0.0162
CfaAffx.14438.1	ENTPD4	ectonucleoside triphosphate diphosphohydrolase 4	2.88	0.0001	0.0001	0.0109
Cfa.8841.1	FBL	fibrillarin	2.26	0.0000	0.0000	0.0030
CfaAffx.21653.1	FKBP3	FK506 binding protein 3, 25kDa	2.46	0.0004	0.0008	0.0232
Cfa.11247.1	FKBP3	FK506 binding protein 3, 25kDa	2.25	0.0003	0.0002	0.0222
Cfa.3707.3	FN1	fibronectin 1	5.94	0.0004	0.0001	0.0256
CfaAffx.9617.1	FOLR2	folate receptor 2 (fetal)	2.47	0.0009	0.0010	0.0354
Cfa.11362.1	FOLR2	folate receptor 2 (fetal)	2.03	0.0009	0.0008	0.0364
Cfa.12090.1	FOXM1	forkhead box M1	5.53	0.0001	0.0000	0.0125

Table A-1 cont'd Complete list of genes that were up-regulated in follicular thyroid carcinoma compared to normal thyroid tissue (microarray analysis)

Transcript ID	Gene Symbol	Gene Title	Fold	p-value	EDR	BH Q-Value
Cfa.12987.1	FTH1	ferritin, heavy polypeptide 1	2.04	0.0003	0.0001	0.0220
Cfa.16196.1	G3BP1	GTPase activating protein (SH3 domain) binding protein 1	2.32	0.0001	0.0000	0.0096
CfaAffx.3746.1	GABRA2	gamma-aminobutyric acid (GABA) A receptor, alpha 2	7.61	0.0010	0.0007	0.0366
Cfa.18790.1	GALM	galactose mutarotase (aldose 1-epimerase)	3.01	0.0003	0.0004	0.0225
Cfa.16332.1	GAPDH	glyceraldehyde-3-phosphate dehydrogenase	5.40	0.0002	0.0001	0.0186
CfaAffx.8103.1	GAPDH	glyceraldehyde-3-phosphate dehydrogenase	2.58	0.0001	0.0001	0.0148
CfaAffx.22564.1	GAPDH	glyceraldehyde-3-phosphate dehydrogenase	2.38	0.0001	0.0000	0.0143
CfaAffx.26731.1	GAPDH	glyceraldehyde-3-phosphate dehydrogenase	2.22	0.0000	0.0000	0.0065
CfaAffx.23015.1	GAPDH	glyceraldehyde-3-phosphate dehydrogenase	2.19	0.0000	0.0000	0.0065
CfaAffx.15531.1	GDAP2	ganglioside induced differentiation associated protein 2	2.33	0.0007	0.0040	0.0331
Cfa.21522.1	GPRC5C	G protein-coupled receptor, family C, group 5, member C	3.61	0.0004	0.0002	0.0249
Cfa.20631.1	GPRC5C	G protein-coupled receptor, family C, group 5, member C	2.43	0.0005	0.0003	0.0270
Cfa.18146.1	HEATR3	HEAT repeat containing 3	3.46	0.0000	0.0000	0.0092
CfaAffx.15624.1	HEATR3	HEAT repeat containing 3	2.55	0.0001	0.0000	0.0109
CfaAffx.12909.1	HELLS	helicase, lymphoid-specific	3.57	0.0008	0.0136	0.0347
CfaAffx.332.1	HEXIM1	hexamethylene bis-acetamide inducible 1	4.51	0.0004	0.0007	0.0244
Cfa.441.1	HSD17B12	hydroxysteroid (17-beta) dehydrogenase 12	2.63	0.0010	0.0012	0.0373
Cfa.273.6	HSPA8	heat shock 70kDa protein 8	2.95	0.0000	0.0000	0.0006
Cfa.13016.1	HSPA9	heat shock 70kDa protein 9 (mortalin)	2.16	0.0003	0.0004	0.0226
Cfa.9260.1	HSPD1	heat shock 60kDa protein 1 (chaperonin)	2.09	0.0001	0.0000	0.0126

Table A-1 cont'd Complete list of genes that were up-regulated in follicular thyroid carcinoma compared to normal thyroid tissue (microarray analysis)

Transcript ID	Gene Symbol	Gene Title	Fold	p-value	EDR	BH Q-Value
CfaAffx.10792.1	HSPH1	heat shock 105kDa/110kDa protein 1	10.83	0.0000	0.0000	0.0049
Cfa.2783.1	HSPH1	heat shock 105kDa/110kDa protein 1	6.53	0.0000	0.0000	0.0031
Cfa.18131.1	HSPH1	heat shock 105kDa/110kDa protein 1	5.46	0.0001	0.0000	0.0109
CfaAffx.11449.1	ID1	inhibitor of DNA binding 1	4.64	0.0007	0.0001	0.0332
Cfa.15185.1	IDE	insulin-degrading enzyme	2.40	0.0006	0.0033	0.0293
CfaAffx.13362.1	IFT81	intraflagellar transport 81 homolog (Chlamydomonas)	2.49	0.0004	0.0039	0.0250
Cfa.3496.1	IL1RN	interleukin 1 receptor antagonist	9.34	0.0004	0.0002	0.0238
CfaAffx.28191.1	ITGA2	integrin, alpha 2 (CD49B, alpha 2 subunit of VLA-2 receptor)	3.31	0.0002	0.0001	0.0159
Cfa.17104.1	JKAMP	JNK1/MAPK8-associated membrane protein	2.67	0.0001	0.0000	0.0099
Cfa.564.1	KDELC1	KDEL (Lys-Asp-Glu-Leu) containing 1	2.05	0.0008	0.0057	0.0344
Cfa.19724.1	KLHL5	kelch-like 5 (Drosophila)	2.49	0.0002	0.0001	0.0173
CfaAffx.28475.1	KSR1	kinase suppressor of ras 1	2.01	0.0001	0.0002	0.0140
Cfa.19749.1	L2HGDH	L-2-hydroxyglutarate dehydrogenase	2.34	0.0007	0.0069	0.0332
Cfa.14417.1	LCN15	lipocalin 15	2.86	0.0008	0.0052	0.0341
CfaAffx.12739.1	LDHA	lactate dehydrogenase A	2.34	0.0004	0.0058	0.0244
CfaAffx.4027.1	LDHA	lactate dehydrogenase A	2.04	0.0003	0.0009	0.0214
CfaAffx.27663.1	LINGO1	leucine rich repeat and Ig domain containing 1	3.58	0.0002	0.0005	0.0163
CfaAffx.28045.1	LRRC8E	leucine rich repeat containing 8 family, member E	6.80	0.0000	0.0000	0.0030
CfaAffx.15764.1	LZTS1	leucine zipper, putative tumor suppressor 1	3.27	0.0007	0.0186	0.0332
Cfa.12114.1	MAGEB5	melanoma antigen family B, 5	7.81	0.0004	0.0053	0.0251

Table A-1 cont'd Complete list of genes that were up-regulated in follicular thyroid carcinoma compared to normal thyroid tissue (microarray analysis)

Transcript ID	Gene Symbol	Gene Title	Fold	p-value	EDR	BH Q-Value
CfaAffx.27961.1	MARK3	MAP/microtubule affinity-regulating kinase 3	4.24	0.0001	0.0001	0.0143
Cfa.1597.1	MGAT2	mannosyl (alpha-1,6-)-glycoprotein beta-1,2-N-acetylGALT	2.00	0.0003	0.0001	0.0201
Cfa.21528.1	MICALL1	MICAL-like 1	6.19	0.0001	0.0000	0.0097
CfaAffx.1775.1	MIOX	myo-inositol oxygenase	12.89	0.0000	0.0000	0.0038
CfaAffx.4313.1	MITD1	MIT, microtubule interacting and transport, domain containing 1	2.71	0.0000	0.0000	0.0059
Cfa.13593.1	MITD1	MIT, microtubule interacting and transport, domain containing 1	2.24	0.0009	0.0238	0.0362
CfaAffx.29494.1	MMP25	matrix metallopeptidase 25	3.56	0.0000	0.0000	0.0096
CfaAffx.22252.1	MPP3	membrane protein, palmitoylated 3	2.97	0.0004	0.0014	0.0255
Cfa.6025.1	MPST	mercaptopyruvate sulfurtransferase	2.65	0.0001	0.0003	0.0148
Cfa.15925.1	MRPL13	mitochondrial ribosomal protein L13	2.32	0.0001	0.0002	0.0144
Cfa.10749.1	MRPS6	mitochondrial ribosomal protein S6	2.08	0.0006	0.0003	0.0291
Cfa.8132.1	NCAPD3	non-SMC condensin II complex, subunit D3	4.04	0.0007	0.0061	0.0332
Cfa.360.2	NCEH1	neutral cholesterol ester hydrolase 1	2.24	0.0000	0.0000	0.0096
CfaAffx.27681.1	NCOR1	nuclear receptor co-repressor 1	2.11	0.0000	0.0000	0.0090
CfaAffx.26929.1	NDUFAB1	NADH dehydrogenase (ubiquinone) 1, alpha/beta subcomplex, 1	2.23	0.0000	0.0000	0.0026
Cfa.10920.1	NDUFAB1	NADH dehydrogenase (ubiquinone) 1, alpha/beta subcomplex, 1	2.10	0.0000	0.0000	0.0065
CfaAffx.15897.1	NFKB2	nuclear factor of kappa light polypeptide gene enhancer in B-cells 2	2.97	0.0001	0.0001	0.0139
Cfa.2659.1	NFS1	NFS1 nitrogen fixation 1 homolog (S. cerevisiae)	2.33	0.0005	0.0004	0.0258
CfaAffx.13200.1	NFS1	NFS1 nitrogen fixation 1 homolog (S. cerevisiae)	2.26	0.0009	0.0016	0.0352
Cfa.11321.1	NIT1	nitrilase 1	2.04	0.0001	0.0001	0.0143

Table A-1 cont'd Complete list of genes that were up-regulated in follicular thyroid carcinoma compared to normal thyroid tissue (microarray analysis)

Transcript ID	Gene Symbol	Gene Title	Fold	p-value	EDR	BH Q-Value
Cfa.15094.1	NME1	non-metastatic cells 1, protein (NM23A)	2.49	0.0002	0.0001	0.0183
CfaAffx.26479.1	NME2	non-metastatic cells 2, protein (NM23B)	2.26	0.0005	0.0012	0.0270
Cfa.15233.1	NOL9	nucleolar protein 9	6.51	0.0008	0.0054	0.0344
CfaAffx.23573.1	NPTX2	neuronal pentraxin II	4.27	0.0002	0.0000	0.0167
Cfa.11383.1	NUDCD2	NudC domain containing 2	2.78	0.0001	0.0001	0.0154
CfaAffx.26317.1	NUDCD2	NudC domain containing 2	2.36	0.0005	0.0023	0.0275
Cfa.4886.1	OCA2	oculocutaneous albinism II	8.20	0.0008	0.0004	0.0346
CfaAffx.22481.1	P4HA1	prolyl 4-hydroxylase, alpha polypeptide I	3.22	0.0000	0.0000	0.0077
Cfa.21239.1	P4HA1	prolyl 4-hydroxylase, alpha polypeptide I	3.15	0.0003	0.0002	0.0198
CfaAffx.22494.1	P4HA1	prolyl 4-hydroxylase, alpha polypeptide I	2.64	0.0003	0.0001	0.0197
Cfa.21541.1	PARP1	poly (ADP-ribose) polymerase 1	2.74	0.0003	0.0003	0.0225
CfaAffx.24694.1	PARP1	poly (ADP-ribose) polymerase 1	2.53	0.0000	0.0000	0.0090
CfaAffx.10024.1	PCNA	proliferating cell nuclear antigen	3.42	0.0001	0.0000	0.0099
Cfa.525.1	PCNA	proliferating cell nuclear antigen	2.87	0.0000	0.0000	0.0089
CfaAffx.25948.1	PDK2	pyruvate dehydrogenase kinase, isozyme 2	3.30	0.0000	0.0000	0.0009
Cfa.17829.1	PDK2	pyruvate dehydrogenase kinase, isozyme 2	2.72	0.0000	0.0000	0.0030
Cfa.10684.2	PFKP	phosphofructokinase, platelet	3.50	0.0000	0.0000	0.0015
Cfa.10684.1	PFKP	phosphofructokinase, platelet	2.89	0.0001	0.0000	0.0128
CfaAffx.14307.1	PGAM1	phosphoglycerate mutase 1 (brain)	2.88	0.0005	0.0001	0.0274
Cfa.1362.1	PGAM1	phosphoglycerate mutase 1 (brain)	2.12	0.0002	0.0000	0.0181

Table A-1 cont'd Complete list of genes that were up-regulated in follicular thyroid carcinoma compared to normal thyroid tissue (microarray analysis)

Transcript ID	Gene Symbol	Gene Title	Fold	p-value	EDR	BH Q-Value
CfaAffx.25994.1	PGF	placental growth factor	10.03	0.0000	0.0000	0.0070
Cfa.6094.1	PIP4K2A	phosphatidylinositol-5-phosphate 4-kinase, type II, alpha	2.71	0.0007	0.0024	0.0332
Cfa.11446.1	PIP5K1B	phosphatidylinositol-4-phosphate 5-kinase, type I, beta	6.22	0.0002	0.0000	0.0170
CfaAffx.3808.1	PIP5K1B	phosphatidylinositol-4-phosphate 5-kinase, type I, beta	4.24	0.0003	0.0001	0.0204
Cfa.14230.1	PMEPA1	prostate transmembrane protein, androgen induced 1	6.50	0.0002	0.0001	0.0161
CfaAffx.18740.1	PMEPA1	prostate transmembrane protein, androgen induced 1	2.71	0.0009	0.0085	0.0355
CfaAffx.13745.1	PPID	peptidylprolyl isomerase D	2.61	0.0010	0.0047	0.0369
CfaAffx.10943.1	PPP1R3B	protein phosphatase 1, regulatory (inhibitor) subunit 3B	2.43	0.0009	0.0143	0.0358
Cfa.19761.1	PPP3CB	protein phosphatase 3, catalytic subunit, beta isozyme	2.75	0.0001	0.0000	0.0114
CfaAffx.25175.1	PRELID1	PRELI domain containing 1	2.27	0.0003	0.0001	0.0197
CfaAffx.25672.1	PRSS53	protease, serine, 53	24.44	0.0000	0.0000	0.0088
Cfa.19384.1	PTRH1	peptidyl-tRNA hydrolase 1 homolog (S. cerevisiae)	2.32	0.0007	0.0015	0.0332
Cfa.6938.1	RHCG	Rh family, C glycoprotein	2.78	0.0008	0.0184	0.0344
CfaAffx.14592.1	RHOBTB2	Rho-related BTB domain containing 2	4.40	0.0001	0.0000	0.0117
Cfa.20490.1	RIPK2	receptor-interacting serine-threonine kinase 2	4.22	0.0001	0.0000	0.0143
CfaAffx.14149.1	RIPK2	receptor-interacting serine-threonine kinase 2	2.16	0.0005	0.0012	0.0258
CfaAffx.26110.1	RNF222	ring finger protein 222	2.41	0.0002	0.0021	0.0195
CfaAffx.29253.1	ROGDI	rogdi homolog (Drosophila)	5.68	0.0004	0.0003	0.0250
Cfa.15992.1	ROGDI	rogdi homolog (Drosophila)	2.73	0.0003	0.0001	0.0198
Cfa.13912.1	RRM2	ribonucleotide reductase M2	20.09	0.0002	0.0000	0.0163

Table A-1 cont'd Complete list of genes that were up-regulated in follicular thyroid carcinoma compared to normal thyroid tissue (microarray analysis)

Transcript ID	Gene Symbol	Gene Title	Fold	p-value	EDR	BH Q-Value
Cfa.11836.1	RRP12	ribosomal RNA processing 12 homolog (S. cerevisiae)	2.97	0.0009	0.0018	0.0364
Cfa.9009.1	SACS	spastic ataxia of Charlevoix-Saguenay (sacsin)	4.16	0.0002	0.0002	0.0161
Cfa.7349.1	SAPS1	SAPS domain family, member 1	2.44	0.0004	0.0013	0.0238
CfaAffx.1846.1	SBF1	SET binding factor 1	5.49	0.0002	0.0000	0.0186
Cfa.18352.1	SBF1	SET binding factor 1	2.90	0.0001	0.0001	0.0142
CfaAffx.11400.1	SBSN	suprabasin	103.50	0.0001	0.0000	0.0099
CfaAffx.24215.1	SDCCAG8	serologically defined colon cancer antigen 8	3.39	0.0006	0.0052	0.0307
CfaAffx.24213.1	SDCCAG8	serologically defined colon cancer antigen 8	3.29	0.0004	0.0017	0.0234
CfaAffx.7692.1	SDK2	sidekick homolog 2 (chicken)	2.14	0.0001	0.0006	0.0116
CfaAffx.21471.1	SERPINE1	serpin peptidase inhibitor, clade E, member 1	6.40	0.0009	0.0008	0.0352
Cfa.109.1	SERPINE1	serpin peptidase inhibitor, clade E, member 1	5.11	0.0002	0.0001	0.0192
CfaAffx.16900.1	SLC12A7	solute carrier family 12, member 7	7.72	0.0008	0.0001	0.0344
CfaAffx.21748.1	SLC12A9	solute carrier family 12, member 9	2.02	0.0009	0.0097	0.0352
CfaAffx.10063.1	SLC16A3	solute carrier family 16, member 3	9.54	0.0004	0.0003	0.0248
CfaAffx.14394.1	SLC25A37	solute carrier family 25, member 37	2.92	0.0005	0.0005	0.0273
Cfa.7803.1	SLC25A37	solute carrier family 25, member 37	2.01	0.0006	0.0012	0.0304
CfaAffx.16640.1	SLC2A10	solute carrier family 2, member 10	3.05	0.0005	0.0032	0.0257
Cfa.7132.1	SLC2A9	solute carrier family 2, member 9	21.31	0.0002	0.0000	0.0176
CfaAffx.2845.1	SLC35B4	solute carrier family 35, member B4	2.30	0.0001	0.0000	0.0126
CfaAffx.22615.1	SLC35F2	solute carrier family 35, member F2	3.44	0.0003	0.0003	0.0228

Table A-1 cont'd Complete list of genes that were up-regulated in follicular thyroid carcinoma compared to normal thyroid tissue (microarray analysis)

Transcript ID	Gene Symbol	Gene Title	Fold	p-value	EDR	BH Q-Value
Cfa.7157.1	SLC38A3	solute carrier family 38, member 3	3.24	0.0004	0.0005	0.0240
Cfa.13147.1	SLC38A3	solute carrier family 38, member 3	3.01	0.0006	0.0029	0.0293
CfaAffx.29293.1	SLC43A2	solute carrier family 43, member 2	2.11	0.0001	0.0001	0.0143
CfaAffx.6570.1	SLC7A11	solute carrier family 7, member 11	13.43	0.0001	0.0000	0.0126
CfaAffx.30456.1	SLC7A5	solute carrier family 7, member 5	2.05	0.0005	0.0020	0.0271
CfaAffx.14205.1	SLIT1	slit homolog 1 (Drosophila)	30.11	0.0001	0.0000	0.0126
Cfa.15406.1	SMC5	structural maintenance of chromosomes 5	4.10	0.0001	0.0008	0.0156
CfaAffx.30097.1	SNAPC4	small nuclear RNA activating complex, polypeptide 4	2.25	0.0000	0.0000	0.0067
Cfa.18423.1	SNCG	synuclein, gamma (breast cancer-specific protein 1)	6.90	0.0000	0.0000	0.0011
CfaAffx.15042.1	SPP1	secreted phosphoprotein 1 (osteopontin)	134.70	0.0000	0.0000	0.0054
CfaAffx.21963.1	SSFA2	sperm specific antigen 2	2.49	0.0002	0.0002	0.0195
CfaAffx.21959.1	SSFA2	sperm specific antigen 2	2.16	0.0008	0.0010	0.0335
CfaAffx.30768.1	ST6GALNAC4	ST6 (alpha-N-acetyl-neuraminyl-2,3-beta-galactosyl-1,3)	2.63	0.0000	0.0000	0.0021
Cfa.21091.1	ST6GALNAC6	ST6 (alpha-N-acetyl-neuraminyl-2,3-beta-galactosyl-1,3)	10.21	0.0000	0.0000	0.0030
Cfa.20852.1	STIP1	stress-induced-phosphoprotein 1	2.21	0.0004	0.0004	0.0236
Cfa.10099.1	SUGT1	SGT1, suppressor of G2 allele of SKP1 (S. cerevisiae)	2.11	0.0000	0.0000	0.0089
Cfa.10593.1	SYNCRIP	synaptotagmin binding, cytoplasmic RNA interacting protein	2.51	0.0005	0.0010	0.0271
CfaAffx.27773.1	SYT17	synaptotagmin XVII	4.26	0.0001	0.0000	0.0131
CfaAffx.18841.1	TAF5L	TAF5-like, p300/CBP-associated factor-associated factor	2.53	0.0005	0.0471	0.0280
Cfa.19077.1	TAGLN2	transgelin 2	2.36	0.0002	0.0001	0.0169

Table A-1 cont'd Complete list of genes that were up-regulated in follicular thyroid carcinoma compared to normal thyroid tissue (microarray analysis)

Transcript ID	Gene Symbol	Gene Title	Fold	p-value	EDR	BH Q-Value
Cfa.10819.1	TBC1D8	TBC1 domain family, member 8 (with GRAM domain)	2.03	0.0002	0.0001	0.0186
CfaAffx.27744.1	TCOF1	Treacher Collins-Franceschetti syndrome 1	8.93	0.0000	0.0000	0.0038
CfaAffx.11201.1	TMEM132B	transmembrane protein 132B	6.46	0.0004	0.0006	0.0239
CfaAffx.11204.1	TMEM132B	transmembrane protein 132B	2.78	0.0008	0.0051	0.0347
CfaAffx.4052.1	TMEM165	transmembrane protein 165	3.00	0.0002	0.0000	0.0161
CfaAffx.25713.1	TMEM88	transmembrane protein 88	4.27	0.0009	0.0204	0.0365
Cfa.18946.1	TOP2A	topoisomerase (DNA) II alpha 170kDa	6.19	0.0000	0.0000	0.0061
CfaAffx.30583.1	TOR1A	torsin family 1, member A (torsin A)	2.33	0.0005	0.0010	0.0271
Cfa.14202.1	TP53RK	TP53 regulating kinase	8.40	0.0005	0.0001	0.0275
CfaAffx.16606.1	TP53RK	TP53 regulating kinase	4.31	0.0002	0.0000	0.0168
CfaAffx.21539.1	TSPAN15	tetraspanin 15	4.48	0.0001	0.0000	0.0148
Cfa.21314.1	TSPAN17	tetraspanin 17	2.69	0.0010	0.0046	0.0371
CfaAffx.25460.1	TSPAN17	tetraspanin 17	2.44	0.0000	0.0000	0.0039
CfaAffx.5815.1	TTC15	tetratricopeptide repeat domain 15	2.00	0.0004	0.0008	0.0252
CfaAffx.22940.1	TUBG2	tubulin, gamma 2	2.64	0.0002	0.0002	0.0161
CfaAffx.19102.1	UBE2D1	ubiquitin-conjugating enzyme E2D 1 (UBC4/5 homolog, yeast)	2.36	0.0002	0.0001	0.0175
Cfa.18209.1	UBE2D1	ubiquitin-conjugating enzyme E2D 1 (UBC4/5 homolog, yeast)	2.10	0.0001	0.0002	0.0143
Cfa.11552.1	UBE2V1	ubiquitin-conjugating enzyme E2 variant 1	2.21	0.0001	0.0000	0.0116
CfaAffx.27040.1	UBFD1	ubiquitin family domain containing 1	3.28	0.0009	0.0148	0.0352
Cfa.10244.1	UMPS	uridine monophosphate synthetase	2.36	0.0003	0.0003	0.0229

Table A-1 cont'd Complete list of genes that were up-regulated in follicular thyroid carcinoma compared to normal thyroid tissue (microarray analysis)

Transcript ID	Gene Symbol	Gene Title	Fold	p-value	EDR	BH Q-Value
Cfa.11226.1	UTP6	UTP6, small subunit (SSU) processome, homolog (yeast)	3.24	0.0000	0.0000	0.0059
Cfa.3581.1	VEGFA	vascular endothelial growth factor A	2.25	0.0007	0.0030	0.0332
Cfa.11912.1	WDR77	WD repeat domain 77	2.27	0.0002	0.0001	0.0187
Cfa.17944.1	WRB	tryptophan rich basic protein	2.83	0.0003	0.0002	0.0204
Cfa.11168.1	WRB	tryptophan rich basic protein	2.73	0.0006	0.0008	0.0302
Cfa.15085.1	YWHAG	tryptophan 5-monooxygenase activation protein	2.63	0.0008	0.0023	0.0334
Cfa.5462.1	ZFAND2A	zinc finger, AN1-type domain 2A	4.00	0.0001	0.0000	0.0153
CfaAffx.16809.1	ZMYND8	zinc finger, MYND-type containing 8	3.28	0.0008	0.0013	0.0334

Table A-2 Complete list of genes that were down-regulated in follicular thyroid carcinoma compared to normal thyroid tissue (microarray analysis)

Transcript ID	Gene Symbol	Gene Title	Fold	p-value	EDR	BH Q-Value
Cfa.10297.1	AARSD1	alanyl-tRNA synthetase domain containing 1	2.24	0.0002	0.0002	0.0161
Cfa.14659.1	AARSD1	alanyl-tRNA synthetase domain containing 1	2.18	0.0001	0.0001	0.0156
Cfa.4754.1	ABCA6	ATP-binding cassette, sub-family A, member 6	6.14	0.0001	0.0000	0.0116
Cfa.19.1	ABCB1	ATP-binding cassette, sub-family B, member 1	8.59	0.0008	0.0012	0.0344
CfaAffx.14161.1	ABCC8	ATP-binding cassette, sub-family C, member 8	2.59	0.0006	0.0065	0.0289
Cfa.1897.1	ACSL3	acyl-CoA synthetase long-chain family member 3	3.82	0.0004	0.0001	0.0236
CfaAffx.24825.1	ACSL3	acyl-CoA synthetase long-chain family member 3	3.42	0.0003	0.0001	0.0222
CfaAffx.18712.1	ADAMTSL4	ADAMTS-like 4	5.20	0.0002	0.0003	0.0158
CfaAffx.22813.1	ADD1	adducin 1 (alpha)	2.21	0.0005	0.0017	0.0270
Cfa.8413.2	AGPHD1	aminoglycoside phosphotransferase domain containing 1	2.56	0.0003	0.0006	0.0215
Cfa.20409.1	AIF1L	allograft inflammatory factor 1-like	5.02	0.0001	0.0000	0.0114
Cfa.20201.1	AKAP12	A kinase (PRKA) anchor protein 12	11.92	0.0000	0.0000	0.0094
Cfa.227.1	AKAP12	A kinase (PRKA) anchor protein 12	3.33	0.0002	0.0001	0.0197
Cfa.7424.1	AMPD3	adenosine monophosphate deaminase 3	2.49	0.0005	0.0269	0.0270
CfaAffx.10145.1	ANKRD10	ankyrin repeat domain 10	2.14	0.0000	0.0000	0.0049
Cfa.442.1	ANKRD10	ankyrin repeat domain 10	2.01	0.0002	0.0005	0.0179
Cfa.14527.1	ANKRD55	ankyrin repeat domain 55	3.60	0.0001	0.0002	0.0137
CfaAffx.13980.1	ANXA3	annexin A3	5.45	0.0006	0.0005	0.0296
Cfa.21549.1	AQP3	aquaporin 3 (Gill blood group)	8.84	0.0001	0.0001	0.0143
CfaAffx.3685.1	AQP7	aquaporin 7	5.69	0.0004	0.0013	0.0244

Table A-2 cont'd Complete list of genes that were down-regulated in follicular thyroid carcinoma compared to normal thyroid tissue (microarray analysis)

Transcript ID	Gene Symbol	Gene Title	Fold	p-value	EDR	BH Q-Value
CfaAffx.17465.1	ARFGEF2	ADP-ribosylation factor guanine nucleotide-exchange factor 2	8.91	0.0009	0.0011	0.0358
CfaAffx.25281.1	ARL5C	ADP-ribosylation factor-like 5C	6.17	0.0004	0.0037	0.0234
Cfa.6733.1	ASB9	ankyrin repeat and SOCS box-containing 9	4.14	0.0002	0.0001	0.0194
CfaAffx.11843.1	ASCL1	achaete-scute complex homolog 1 (Drosophila)	19.35	0.0002	0.0002	0.0187
Cfa.4590.1	ASPN	asporin	3.04	0.0004	0.0012	0.0251
CfaAffx.30635.1	ATMIN	ATM interactor	2.09	0.0002	0.0001	0.0161
Cfa.8203.1	BARD1	BRCA1 associated RING domain 1	2.24	0.0003	0.0006	0.0212
CfaAffx.22033.1	BARD1	BRCA1 associated RING domain 1	2.23	0.0003	0.0010	0.0224
Cfa.8704.1	BEND5	BEN domain containing 5	2.84	0.0010	0.0079	0.0369
CfaAffx.21522.1	C1QL1	complement component 1, q subcomponent-like 1	11.33	0.0007	0.0034	0.0313
CfaAffx.28437.1	C7	complement component 7	3.90	0.0002	0.0001	0.0165
CfaAffx.5173.1	C9orf5	chromosome 9 open reading frame 5	2.48	0.0004	0.0005	0.0244
CfaAffx.28464.1	CACHD1	cache domain containing 1	24.27	0.0006	0.0002	0.0304
Cfa.18422.1	CALB1	calbindin 1, 28kDa	215.50	0.0000	0.0000	0.0065
CfaAffx.14235.1	CALB1	calbindin 1, 28kDa	58.25	0.0000	0.0000	0.0090
Cfa.3806.1	CALCA	calcitonin/calcitonin-related polypeptide, alpha	112.20	0.0000	0.0000	0.0049
CfaAffx.13524.1	CALCB	calcitonin-related polypeptide beta	410.40	0.0000	0.0000	0.0000
CfaAffx.13254.1	CAMKK2	calcium/calmodulin-dependent protein kinase kinase 2, beta	2.01	0.0002	0.0004	0.0160
Cfa.9156.1	CAMTA1	calmodulin binding transcription activator 1	2.35	0.0005	0.0051	0.0273
CfaAffx.18360.1	CASR	calcium-sensing receptor	177.40	0.0000	0.0000	0.0009

Table A-2 cont'd Complete list of genes that were down-regulated in follicular thyroid carcinoma compared to normal thyroid tissue (microarray analysis)

Transcript ID	Gene Symbol	Gene Title	Fold	p-value	EDR	BH Q-Value
CfaAffx.18453.1	CASR	calcium-sensing receptor	176.90	0.0000	0.0000	0.0002
CfaAffx.18421.1	CASR	calcium-sensing receptor	10.26	0.0000	0.0000	0.0016
Cfa.14452.1	CFH	complement factor H	28.28	0.0008	0.0012	0.0340
CfaAffx.9952.1	CHGB	chromogranin B (secretogranin 1)	231.30	0.0000	0.0000	0.0092
Cfa.20395.1	CHGB	chromogranin B (secretogranin 1)	177.80	0.0000	0.0000	0.0089
Cfa.4096.1	CHML	choroideremia-like (Rab escort protein 2)	2.42	0.0005	0.0006	0.0257
CfaAffx.22427.1	CLDN5	claudin 5	7.39	0.0002	0.0000	0.0161
Cfa.949.1	CLGN	calmegin	13.85	0.0000	0.0000	0.0016
CfaAffx.6486.1	CLGN	calmegin	5.56	0.0003	0.0008	0.0222
CfaAffx.30203.1	CLSTN1	calsyntenin 1	2.19	0.0000	0.0000	0.0096
CfaAffx.22780.1	CLTCL1	clathrin, heavy chain-like 1	2.68	0.0006	0.0024	0.0286
CfaAffx.1773.1	CNKSR3	CNKSR family member 3	2.02	0.0008	0.0047	0.0343
CfaAffx.15512.1	CNTN1	contactin 1	6.24	0.0002	0.0001	0.0173
Cfa.3828.1	cOR2L18	cOR2L18 olfactory receptor family 2 subfamily L-like	2.64	0.0008	0.1802	0.0346
CfaAffx.13996.1	CPE	carboxypeptidase E	27.39	0.0000	0.0000	0.0007
Cfa.1374.1	CPE	carboxypeptidase E	18.59	0.0000	0.0000	0.0010
Cfa.116.1	CRSP-2	calcitonin receptor-stimulating peptide-2	469.20	0.0000	0.0000	0.0030
CfaAffx.20589.1	DNAJC12	DnaJ (Hsp40) homolog, subfamily C, member 12	2.47	0.0009	0.0064	0.0361
CfaAffx.16492.1	DNER	delta/notch-like EGF repeat containing	4.27	0.0000	0.0000	0.0048
CfaAffx.3880.1	DOCK8	dedicator of cytokinesis 8	2.62	0.0003	0.0005	0.0216

Table A-2 cont'd Complete list of genes that were down-regulated in follicular thyroid carcinoma compared to normal thyroid tissue (microarray analysis)

Transcript ID	Gene Symbol	Gene Title	Fold	p-value	EDR	BH Q-Value
Cfa.17233.1	DOCK8	dedicator of cytokinesis 8	2.20	0.0006	0.0017	0.0299
Cfa.11170.1	DOCK8	dedicator of cytokinesis 8	2.16	0.0007	0.0003	0.0309
CfaAffx.8389.1	DPP10	dipeptidyl-peptidase 10 (non-functional)	5.69	0.0000	0.0000	0.0092
Cfa.4040.1	DPP10	dipeptidyl-peptidase 10 (non-functional)	4.94	0.0005	0.0035	0.0258
Cfa.15116.1	DPP4	dipeptidyl-peptidase 4	17.39	0.0003	0.0000	0.0197
CfaAffx.23464.1	DPT	dermatopontin	34.55	0.0004	0.0001	0.0242
Cfa.6133.1	DPT	dermatopontin	10.46	0.0006	0.0001	0.0290
CfaAffx.27518.1	DTNA	dystrobrevin, alpha	12.83	0.0001	0.0000	0.0122
CfaAffx.27506.1	DTNA	dystrobrevin, alpha	6.69	0.0000	0.0000	0.0065
CfaAffx.27521.1	DTNA	dystrobrevin, alpha	6.02	0.0003	0.0001	0.0198
CfaAffx.19491.1	ECE2	endothelin converting enzyme 2	14.72	0.0004	0.0002	0.0243
CfaAffx.27128.1	EEF2K	eukaryotic elongation factor-2 kinase	7.88	0.0009	0.0033	0.0354
Cfa.6765.1	EEFSEC	eukaryotic elongation factor, selenocysteine-tRNA-specific	3.98	0.0008	0.0045	0.0340
Cfa.3903.1	EGFR	epidermal growth factor receptor	2.43	0.0000	0.0000	0.0085
CfaAffx.16581.1	ELF3	E74-like factor 3	2.78	0.0003	0.0006	0.0222
Cfa.9231.1	ELMOD1	ELMO/CED-12 domain containing 1	25.36	0.0003	0.0000	0.0231
CfaAffx.5193.1	EPB41L4B	erythrocyte membrane protein band 4.1 like 4B	2.46	0.0006	0.0017	0.0289
CfaAffx.9991.1	FGFR1	fibroblast growth factor receptor 1	2.07	0.0003	0.0004	0.0208
Cfa.13659.3	FLOT1	Flotillin 1	4.77	0.0000	0.0000	0.0088
Cfa.12371.1	FMO2	flavin containing monooxygenase 2	28.27	0.0000	0.0000	0.0019

Table A-2 cont'd Complete list of genes that were down-regulated in follicular thyroid carcinoma compared to normal thyroid tissue (microarray analysis)

Transcript ID	Gene Symbol	Gene Title	Fold	p-value	EDR	BH Q-Value
Cfa.13382.1	FOXA2	forkhead box A2	5.75	0.0002	0.0001	0.0186
CfaAffx.13868.1	FSTL5	follistatin-like 5	8.31	0.0000	0.0000	0.0052
Cfa.13946.1	FXYD2	FXYD domain containing ion transport regulator 2	40.25	0.0000	0.0000	0.0081
CfaAffx.11553.1	FXYD3	FXYD domain containing ion transport regulator 3	24.31	0.0005	0.0002	0.0280
CfaAffx.3748.1	GABRA4	gamma-aminobutyric acid (GABA) A receptor, alpha 4	5.10	0.0009	0.0123	0.0355
CfaAffx.8446.1	GATA3	GATA binding protein 3	8.48	0.0004	0.0005	0.0255
Cfa.88.1	GCG	glucagon	54.39	0.0000	0.0000	0.0081
CfaAffx.24846.1	GDF10	growth differentiation factor 10	8.44	0.0001	0.0001	0.0136
CfaAffx.1631.1	GFPT2	glutamine-fructose-6-phosphate transaminase 2	5.44	0.0005	0.0013	0.0260
CfaAffx.10341.1	GFRA4	GDNF family receptor alpha 4	297.20	0.0000	0.0000	0.0016
CfaAffx.7334.1	GNG8	guanine nucleotide binding protein (G protein), gamma 8	4.01	0.0000	0.0000	0.0085
CfaAffx.18348.1	GPM6B	glycoprotein M6B	3.44	0.0000	0.0000	0.0092
CfaAffx.25288.1	GPR125	G protein-coupled receptor 125	3.12	0.0009	0.0020	0.0352
Cfa.14342.3	GPX3	glutathione peroxidase 3	14.96	0.0002	0.0000	0.0172
Cfa.14342.1	GPX3	glutathione peroxidase 3	9.85	0.0001	0.0000	0.0135
CfaAffx.6303.1	GREB1	growth regulation by estrogen in breast cancer 1	3.98	0.0009	0.0193	0.0359
CfaAffx.7437.1	HIF3A	hypoxia inducible factor 3, alpha subunit	2.21	0.0007	0.0050	0.0325
CfaAffx.5350.1	HOXA5	homeobox A5	2.06	0.0006	0.0079	0.0296
CfaAffx.25748.1	HOXB2	homeobox B2	6.29	0.0006	0.0049	0.0304
CfaAffx.25767.1	HOXB5	homeobox B5	2.68	0.0003	0.0147	0.0206

Table A-2 cont'd Complete list of genes that were down-regulated in follicular thyroid carcinoma compared to normal thyroid tissue (microarray analysis)

Transcript ID	Gene Symbol	Gene Title	Fold	p-value	EDR	BH Q-Value
Cfa.15630.1	HOXB7	homeobox B7	3.38	0.0000	0.0000	0.0096
CfaAffx.30577.1	HSD17B2	hydroxysteroid (17-beta) dehydrogenase 2	3.21	0.0000	0.0000	0.0011
CfaAffx.3550.1	HYAL4	hyaluronoglucosaminidase 4	8.20	0.0000	0.0000	0.0056
Cfa.16440.1	IFI35	interferon-induced protein 35	2.63	0.0002	0.0002	0.0187
CfaAffx.4464.1	IGFBPL1	insulin-like growth factor binding protein-like 1	2.68	0.0001	0.0002	0.0135
CfaAffx.15784.1	IGSF5	immunoglobulin superfamily, member 5	2.08	0.0002	0.0018	0.0179
Cfa.3136.1	IL17RB	interleukin 17 receptor B	10.55	0.0000	0.0000	0.0030
CfaAffx.15017.1	KCNE1	potassium voltage-gated channel, Isk-related family, member 1	5.47	0.0004	0.0008	0.0236
Cfa.205.1	KCNE2	potassium voltage-gated channel, Isk-related family, member 2	2.53	0.0006	0.0066	0.0291
CfaAffx.28331.1	KCNJ12	potassium inwardly-rectifying channel, subfamily J, member 12	4.33	0.0002	0.0011	0.0186
Cfa.6173.1	KLK11	kallikrein-related peptidase 11	16.15	0.0005	0.0002	0.0267
Cfa.4559.1	LGALS9	lectin, galactoside-binding, soluble, 9	2.35	0.0005	0.0009	0.0276
CfaAffx.25230.1	LGI2	leucine-rich repeat LGI family, member 2	7.86	0.0003	0.0003	0.0220
CfaAffx.11543.1	LGI4	leucine-rich repeat LGI family, member 4	3.34	0.0001	0.0003	0.0143
CfaAffx.8527.1	LMO7	LIM domain 7	31.08	0.0000	0.0000	0.0081
CfaAffx.8526.1	LMO7	LIM domain 7	21.91	0.0001	0.0000	0.0130
Cfa.19387.1	LMO7	LIM domain 7	13.41	0.0000	0.0000	0.0010
Cfa.5970.1	LMO7	LIM domain 7	6.02	0.0001	0.0000	0.0097
Cfa.17748.1	LMO7	LIM domain 7	3.41	0.0003	0.0007	0.0222
CfaAffx.30935.1	LRRC8B	leucine rich repeat containing 8 family, member B	2.90	0.0002	0.0010	0.0185

Table A-2 cont'd Complete list of genes that were down-regulated in follicular thyroid carcinoma compared to normal thyroid tissue (microarray analysis)

Transcript ID	Gene Symbol	Gene Title	Fold	p-value	EDR	BH Q-Value
CfaAffx.12229.1	LYVE1	lymphatic vessel endothelial hyaluronan receptor 1	10.01	0.0005	0.0001	0.0273
CfaAffx.12760.1	MAB21L2	mab-21-like 2 (C. elegans)	6.99	0.0003	0.0008	0.0208
CfaAffx.1126.1	MALT1	mucosa associated lymphoid tissue lymphoma translocation gene 1	2.79	0.0001	0.0001	0.0135
Cfa.2561.1	MAPK10	mitogen-activated protein kinase 10	2.13	0.0006	0.0071	0.0304
CfaAffx.9241.1	MBNL2	muscleblind-like 2 (Drosophila)	6.23	0.0001	0.0003	0.0148
CfaAffx.9237.1	MBNL2	muscleblind-like 2 (Drosophila)	5.77	0.0001	0.0000	0.0116
CfaAffx.9236.1	MBNL2	muscleblind-like 2 (Drosophila)	2.27	0.0004	0.0010	0.0241
CfaAffx.15515.1	MMRN1	multimerin 1	23.06	0.0001	0.0000	0.0117
CfaAffx.24527.1	NEDD4	neural precursor cell expressed, developmentally down-regulated 4	12.97	0.0000	0.0000	0.0087
Cfa.19510.1	NEO1	neogenin homolog 1 (chicken)	2.25	0.0003	0.0004	0.0214
CfaAffx.8815.1	NET1	neuroepithelial cell transforming gene 1	5.06	0.0001	0.0000	0.0156
Cfa.20245.1	NNAT	neuronatin	23.93	0.0000	0.0000	0.0087
CfaAffx.13891.1	NNAT	neuronatin	7.10	0.0003	0.0001	0.0220
CfaAffx.7797.1	NR2C2	nuclear receptor subfamily 2, group C, member 2	2.04	0.0002	0.0003	0.0167
Cfa.7236.1	NRXN1	neurexin 1	2.16	0.0000	0.0000	0.0061
CfaAffx.2958.1	NTRK2	neurotrophic tyrosine kinase, receptor, type 2	4.04	0.0007	0.0021	0.0316
Cfa.21602.1	OLFML3	olfactomedin-like 3	2.29	0.0000	0.0000	0.0030
CfaAffx.24222.1	OR10A11	olfactory receptor	2.87	0.0006	0.0057	0.0290
CfaAffx.9281.1	OXTR	oxytocin receptor	3.83	0.0002	0.0015	0.0177
Cfa.1484.1	PAM	peptidylglycine alpha-amidating monooxygenase	3.60	0.0008	0.0019	0.0348

Table A-2 cont'd Complete list of genes that were down-regulated in follicular thyroid carcinoma compared to normal thyroid tissue (microarray analysis)

Transcript ID	Gene Symbol	Gene Title	Fold	p-value	EDR	BH Q-Value
CfaAffx.21961.1	PAPPA2	pappalysin 2	14.22	0.0001	0.0000	0.0137
CfaAffx.249.1	PCP4	Purkinje cell protein 4	7.62	0.0007	0.0023	0.0332
CfaAffx.9213.1	PCSK2	proprotein convertase subtilisin/kexin type 2	55.55	0.0000	0.0000	0.0012
Cfa.13533.1	PCSK5	proprotein convertase subtilisin/kexin type 5	15.31	0.0002	0.0002	0.0172
Cfa.3517.1	PDE1A	phosphodiesterase 1A, calmodulin-dependent	9.88	0.0000	0.0000	0.0046
CfaAffx.9519.1	PDE2A	phosphodiesterase 2A, cGMP-stimulated	2.81	0.0003	0.0018	0.0222
Cfa.4851.1	PDE4DIP	phosphodiesterase 4D interacting protein	2.37	0.0001	0.0003	0.0153
CfaAffx.19042.1	PHACTR3	phosphatase and actin regulator 3	21.80	0.0001	0.0000	0.0103
Cfa.9569.1	PHACTR3	phosphatase and actin regulator 3	11.52	0.0001	0.0000	0.0140
CfaAffx.20627.1	PHEX	phosphate regulating endopeptidase homolog, X-linked	19.54	0.0000	0.0000	0.0065
Cfa.7899.1	PHEX	phosphate regulating endopeptidase homolog, X-linked	5.50	0.0000	0.0000	0.0081
CfaAffx.13033.1	PI15	peptidase inhibitor 15	2.21	0.0001	0.0005	0.0135
CfaAffx.27950.1	PLS3	plastin 3	3.62	0.0003	0.0001	0.0226
CfaAffx.25078.1	PNMT	phenylethanolamine N-methyltransferase	32.88	0.0001	0.0000	0.0116
Cfa.17876.1	PNPLA2	patatin-like phospholipase domain containing 2	3.90	0.0001	0.0000	0.0131
CfaAffx.15010.1	PNPLA2	patatin-like phospholipase domain containing 2	2.07	0.0002	0.0009	0.0179
CfaAffx.28974.1	PPAP2B	phosphatidic acid phosphatase type 2B	2.70	0.0003	0.0000	0.0198
Cfa.10489.1	PPAP2B	phosphatidic acid phosphatase type 2B	2.63	0.0004	0.0001	0.0247
Cfa.4105.1	PPAP2B	phosphatidic acid phosphatase type 2B	2.47	0.0005	0.0001	0.0274
CfaAffx.26993.1	PPP4R4	protein phosphatase 4, regulatory subunit 4	8.98	0.0002	0.0001	0.0175

Table A-2 cont'd Complete list of genes that were down-regulated in follicular thyroid carcinoma compared to normal thyroid tissue (microarray analysis)

Transcript ID	Gene Symbol	Gene Title	Fold	p-value	EDR	BH Q-Value
CfaAffx.19461.1	PRKD1	protein kinase D1	3.86	0.0008	0.0021	0.0344
Cfa.12558.1	PRKD1	protein kinase D1	3.71	0.0002	0.0001	0.0186
CfaAffx.23459.1	PTPRN	protein tyrosine phosphatase, receptor type, N	5.49	0.0006	0.0118	0.0302
CfaAffx.8725.1	PTPRN2	protein tyrosine phosphatase, receptor type, N polypeptide 2	14.00	0.0009	0.0010	0.0352
Cfa.5408.1	RARRES2	retinoic acid receptor responder (tazarotene induced) 2	14.39	0.0005	0.0007	0.0280
CfaAffx.12898.1	RASSF10	Ras association domain family (N-terminal) member 10	27.22	0.0000	0.0000	0.0061
CfaAffx.5492.1	RASSF6	Ras association domain family member 6	9.31	0.0000	0.0000	0.0030
CfaAffx.26877.1	RBBP6	retinoblastoma binding protein 6	2.49	0.0005	0.0018	0.0272
CfaAffx.26633.1	RGL3	ral guanine nucleotide dissociation stimulator-like 3	3.38	0.0008	0.0016	0.0334
Cfa.10103.1	RHOG	Ras homolog gene family, member G (rho G)	3.04	0.0009	0.0197	0.0352
CfaAffx.9942.1	RRM1	ribonucleotide reductase M1	2.08	0.0001	0.0001	0.0148
CfaAffx.5849.1	RSPO1	R-spondin homolog (Xenopus laevis)	5.81	0.0003	0.0021	0.0229
Cfa.14613.1	RSPO3	R-spondin 3 homolog (Xenopus laevis)	17.72	0.0000	0.0000	0.0042
Cfa.155.1	RTN1	reticulon 1	8.67	0.0002	0.0001	0.0190
CfaAffx.13702.1	RXFP1	relaxin/insulin-like family peptide receptor 1	8.34	0.0000	0.0000	0.0030
CfaAffx.13260.1	SCARA5	scavenger receptor class A, member 5 (putative)	18.93	0.0005	0.0003	0.0278
Cfa.21158.1	SCARA5	scavenger receptor class A, member 5 (putative)	6.41	0.0003	0.0002	0.0197
Cfa.21112.1	SCARA5	scavenger receptor class A, member 5 (putative)	3.72	0.0000	0.0000	0.0090
CfaAffx.893.1	SCG2	secretogranin II	135.50	0.0000	0.0000	0.0010
Cfa.11197.1	SCG3	secretogranin III	28.47	0.0010	0.0000	0.0369

Table A-2 cont'd Complete list of genes that were down-regulated in follicular thyroid carcinoma compared to normal thyroid tissue (microarray analysis)

Transcript ID	Gene Symbol	Gene Title	Fold	p-value	EDR	BH Q-Value
CfaAffx.13062.1	SCG5	secretogranin V (7B2 protein)	222.50	0.0001	0.0000	0.0116
Cfa.10794.1	SCG5	secretogranin V (7B2 protein)	68.71	0.0000	0.0000	0.0033
CfaAffx.10585.1	SCGB1C1	secretoglobin, family 1C, member 1	114.30	0.0000	0.0000	0.0046
Cfa.16459.1	SCGB1C1	secretoglobin, family 1C, member 1	22.71	0.0008	0.0001	0.0334
CfaAffx.16503.1	SCGN	secretagogin, EF-hand calcium binding protein	132.10	0.0002	0.0000	0.0173
Cfa.18398.1	SCGN	secretagogin, EF-hand calcium binding protein	6.18	0.0001	0.0000	0.0103
CfaAffx.25993.1	SEZ6L2	seizure related 6 homolog (mouse)-like 2	10.26	0.0010	0.0011	0.0369
CfaAffx.3255.1	SH3GL2	SH3-domain GRB2-like 2	2.16	0.0002	0.0002	0.0168
CfaAffx.21915.1	SIK2	salt-inducible kinase 2	2.45	0.0007	0.2364	0.0314
Cfa.15044.1	SLC15A2	solute carrier family 15, member 2	7.13	0.0007	0.0004	0.0326
CfaAffx.15889.1	SLC18A1	solute carrier family 18, member 1	197.00	0.0000	0.0000	0.0030
CfaAffx.15891.1	SLC18A1	solute carrier family 18, member 1	16.00	0.0004	0.0001	0.0234
Cfa.18351.1	SLC20A2	solute carrier family 20, member 2	3.80	0.0002	0.0002	0.0195
CfaAffx.8995.1	SLC24A3	solute carrier family 24, member 3	2.12	0.0007	0.0042	0.0332
Cfa.14551.1	SLC27A5	solute carrier family 27, member 5	2.61	0.0001	0.0000	0.0103
Cfa.6122.1	SLC30A3	solute carrier family 30, member 3	30.95	0.0004	0.0000	0.0243
CfaAffx.8189.1	SLC30A3	solute carrier family 30, member 3	6.75	0.0002	0.0000	0.0179
CfaAffx.16375.1	SLC37A1	solute carrier family 37, member 1	2.58	0.0001	0.0000	0.0126
CfaAffx.16711.1	SLC39A8	solute carrier family 39, member 8	11.40	0.0000	0.0000	0.0069
Cfa.12906.1	SLC39A8	solute carrier family 39, member 8	8.61	0.0002	0.0000	0.0165

Table A-2 cont'd Complete list of genes that were down-regulated in follicular thyroid carcinoma compared to normal thyroid tissue (microarray analysis)

Transcript ID	Gene Symbol	Gene Title	Fold	p-value	EDR	BH Q-Value
Cfa.1207.1	SNAP25	synaptosomal-associated protein, 25kDa	337.30	0.0000	0.0000	0.0030
CfaAffx.15497.1	SNCA	synuclein, alpha (non A4 component of amyloid precursor)	10.38	0.0001	0.0000	0.0116
CfaAffx.1776.1	SNX31	sorting nexin 31	6.59	0.0001	0.0000	0.0126
CfaAffx.5019.1	SPTBN1	spectrin, beta, non-erythrocytic 1	2.26	0.0006	0.0011	0.0308
Cfa.3860.1	SST	somatostatin	23.54	0.0000	0.0000	0.0038
CfaAffx.15692.1	ST14	suppression of tumorigenicity 14 (colon carcinoma)	5.40	0.0001	0.0000	0.0116
Cfa.9133.1	ST8SIA3	ST8 alpha-N-acetyl-neuraminide alpha-2,8-sialyltransferase 3	9.65	0.0009	0.0032	0.0352
CfaAffx.16970.1	SYNM	synemin, intermediate filament protein	4.11	0.0000	0.0000	0.0092
CfaAffx.27070.1	SYT4	synaptotagmin IV	3.05	0.0008	0.0116	0.0346
CfaAffx.15603.1	TAOK3	TAO kinase 3	3.69	0.0002	0.0001	0.0175
CfaAffx.22377.1	TBX1	T-box 1	20.49	0.0000	0.0000	0.0065
Cfa.18308.1	TGFBR3	transforming growth factor, beta receptor III	7.14	0.0000	0.0000	0.0070
CfaAffx.30901.1	TGFBR3	transforming growth factor, beta receptor III	5.68	0.0001	0.0000	0.0157
Cfa.11048.1	TLE1	transducin-like enhancer of split 1 homolog, Drosophila)	3.24	0.0004	0.0004	0.0236
CfaAffx.23567.1	TMEM130	transmembrane protein 130	8.21	0.0006	0.0022	0.0296
Cfa.18172.1	TMEM130	transmembrane protein 130	5.87	0.0003	0.0003	0.0198
CfaAffx.27269.1	TMEM159	transmembrane protein 159	2.93	0.0007	0.0081	0.0320
Cfa.11292.1	TMOD1	tropomodulin 1	3.14	0.0006	0.0015	0.0307
Cfa.15388.1	TMOD1	tropomodulin 1	2.90	0.0000	0.0000	0.0087
Cfa.2726.1	TNMD	tenomodulin	31.19	0.0000	0.0000	0.0048

Table A-2 cont'd Complete list of genes that were down-regulated in follicular thyroid carcinoma compared to normal thyroid tissue (microarray analysis)

Transcript ID	Gene Symbol	Gene Title	Fold	p-value	EDR	BH Q-Value
CfaAffx.24599.1	TNRC18	trinucleotide repeat containing 18	2.31	0.0009	0.0342	0.0361
CfaAffx.31179.1	TPPP3	tubulin polymerization-promoting protein family member 3	9.08	0.0000	0.0000	0.0065
Cfa.11737.1	TPPP3	tubulin polymerization-promoting protein family member 3	2.99	0.0002	0.0000	0.0183
CfaAffx.2422.1	TRDN	triadin	8.12	0.0001	0.0005	0.0142
Cfa.3748.1	TRIB2	tribbles homolog 2 (Drosophila)	4.62	0.0001	0.0000	0.0109
CfaAffx.6393.1	TRIB2	tribbles homolog 2 (Drosophila)	3.17	0.0000	0.0000	0.0059
Cfa.18232.1	TRMT11	tRNA methyltransferase 11 homolog (S. cerevisiae)	2.71	0.0002	0.0002	0.0176
CfaAffx.7398.1	TSPAN1	tetraspanin 1	6.48	0.0001	0.0001	0.0156
Cfa.12808.1	TUT1	terminal uridylyl transferase 1, U6 snRNA-specific	2.97	0.0002	0.0039	0.0194
Cfa.15947.1	USP13	ubiquitin specific peptidase 13 (isopeptidase T-3)	2.94	0.0000	0.0000	0.0037
CfaAffx.14042.1	VEPH1	ventricular zone expressed PH domain homolog 1 (zebrafish)	26.54	0.0000	0.0000	0.0033
CfaAffx.8282.1	VILL	villin-like	6.35	0.0008	0.0044	0.0337
CfaAffx.8283.1	VILL	villin-like	5.28	0.0004	0.0043	0.0238
Cfa.15076.2	VTN	vitronectin	10.99	0.0005	0.0012	0.0280
CfaAffx.17618.1	VWA2	von Willebrand factor A domain containing 2	11.80	0.0009	0.0052	0.0362
CfaAffx.30659.1	WWOX	WW domain containing oxidoreductase	2.14	0.0000	0.0000	0.0010
Cfa.2535.1	ZFP106	zinc finger protein 106 homolog (mouse)	2.01	0.0004	0.0155	0.0244
Cfa.6903.1	ZFYVE1	zinc finger, FYVE domain containing 1	3.52	0.0000	0.0000	0.0059
CfaAffx.1121.1	ZNF532	zinc finger protein 532	3.05	0.0007	0.0011	0.0316
Cfa.11754.1	ZNF532	zinc finger protein 532	2.33	0.0002	0.0000	0.0170
Cfa.3546.2	ZONAB	Y-box protein ZONAB-A	2.94	0.0003	0.0001	0.0198
CfaAffx.21932.1	ZSCAN4	zinc finger and SCAN domain containing 4	5.01	0.0004	0.0001	0.0232

APPENDIX B

DESCRIPTIVE ANALYSIS OF PCR CASES

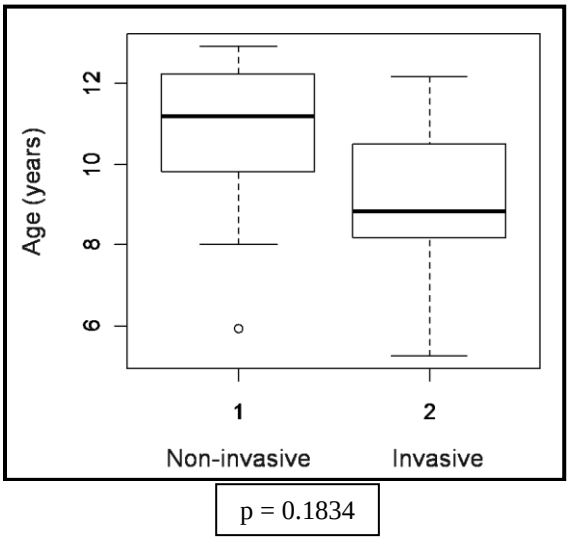

Figure B-1 Comparison of age at presentation for dogs with non-invasive and invasive follicular thyroid carcinoma

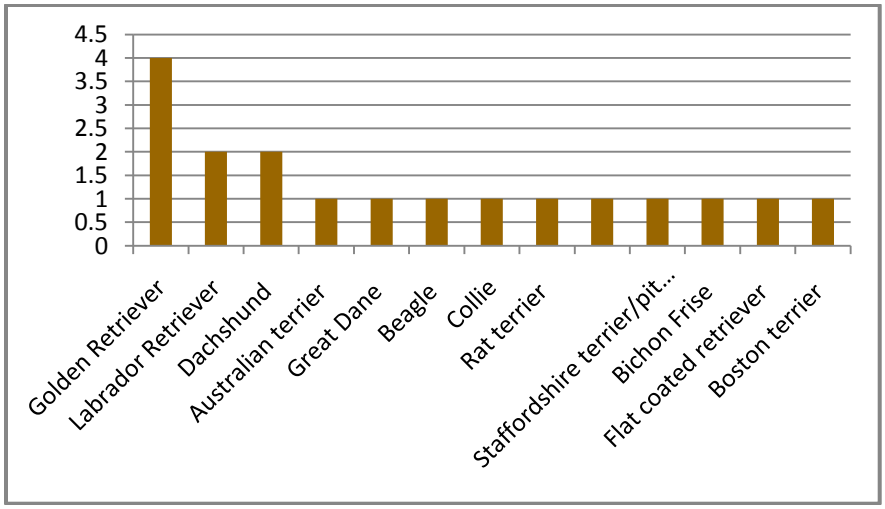

Figure B-2 Breeds represented among eighteen follicular thyroid carcinoma cases recruited for gene and protein expression studies

Table B-1 Demographic description of dogs recruited for the gene and protein expression studies

Non-invasive follicular thyroid carcinoma		
Breed	**Gender**	**Age (yrs)**
Labrador Retriever	Intact male	9.83
Golden Retriever	Neutered male	12.25
Australian Terrier	Spayed female	5.92
Great Dane	Neutered male	8.00
Rat terrier	Spayed female	12.92
Golden Retriever	Spayed female	12.33
Staffordshire terrier / pitbull	Spayed female	11.17
Boston terrier	Neutered male	11.42
Dachshund (L hair)	Spayed female	10.17
Invasive follicular thyroid carcinoma		
Breed	**Gender**	**Age (yrs)**
Labrador Retriever	Neutered male	6.50
Golden Retriever	Neutered male	10.50
Beagle	Spayed female	5.25
Collie	Neutered male	10.08
Golden Retriever	Spayed female	8.17
German Short Hair Pointer	Spayed female	12.17
Bichon Frise	Neutered male	8.17
Flat coated retriever	Neutered male	8.83
Dachshund	Spayed female	11.08
Healthy controls		
Breed	**Gender**	**Age (yrs)**
Beagle	Spayed female	2.00
Beagle	Intact male	2.00
Border collie	Spayed female	2.00
Beagle	Intact female	2.00
Hound X	Intact female	1.75
Hound X	Intact female	1.42
Hound X	Intact female	1.08
Hound X	Intact male	1.33
Hound X	Intact male	0.17

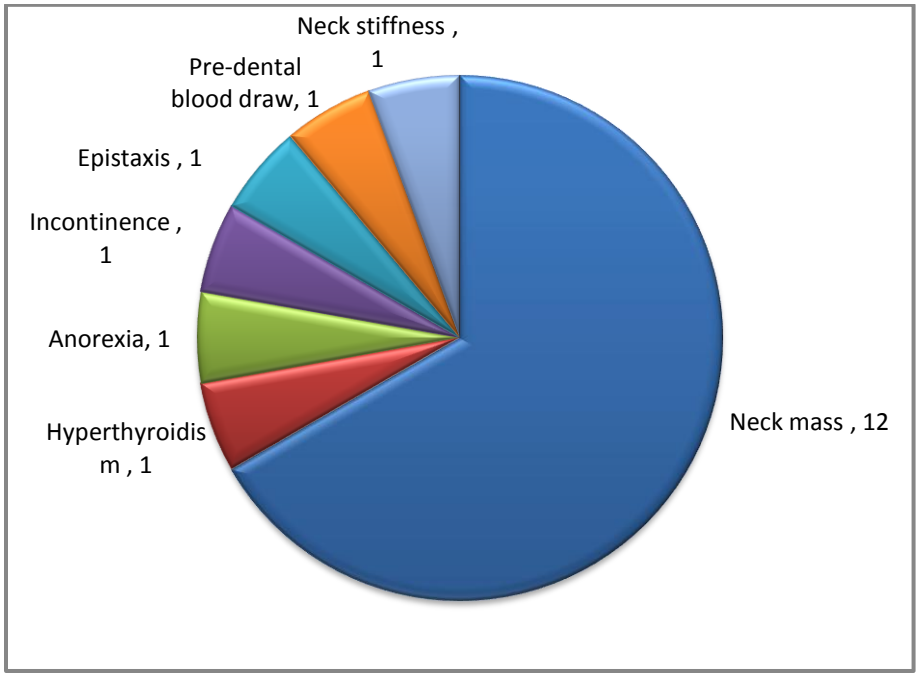

Figure B-3 Primary presenting complaint of follicular thyroid carcinoma cases recruited for gene and protein expression studies